Final Report
2014 Uinta Basin Winter Ozone Study

Prepared for:
Brock LeBaron
Utah Division of Air Quality
195 North 1950 West
Salt Lake City, UT 84114

Edited by:
Till Stoeckenius
ENVIRON International Corporation
773 San Marin Drive, Suite 2115
Novato, California, 94998
www.environcorp.com
P-415-899-0700
F-415-899-0707

February 2015

ENVIRON

This page left intentionally blank

CONTENTS

TABLES

FIGURES

This page left intentionally blank

EXECUTIVE SUMMARY

Background

The Uinta Basin is a rural area of northeastern Utah where the majority of the state's oil and gas production occurs. Ozone concentrations in excess of the current national air quality standard have been measured in the Basin during the winter. These high ozone levels are only observed in the Basin during winter inversion periods when the ground is covered by snow and stagnant, 'cold pool' conditions are present; ozone levels outside of these periods have remained below the air quality standard and conditions resulting in exceedances of the standard do not occur every year.

A multi-phased study (the Uinta Basin Winter Ozone Study, UBWOS) was initiated in the first quarter of 2012 to identify the emissions sources and the unique photochemical processes that cause elevated winter ozone concentrations, and to identify the most effective strategies to reduce winter ozone. UBWOS 2012 included measurements of ozone and ozone precursor concentrations and meteorological conditions throughout the Basin. Meteorological conditions during UBWOS 2012 were not conducive to ozone formation due to a lack of snow cover; no exceedances of the 8-hour average 75 parts per billion (ppb) National Ambient Air Quality Standard (NAAQS) were observed during UBWOS 2012. Key findings from UBWOS 2012 are described in a summary report (Final Report: 2012 Uinta Basin Winter Ozone and Air Quality Study; available at http://www.deq.utah.gov/locations/U/uintahbasin/ozone/docs/2014/03Mar/ubos_2011-12_final_report.pdf.

UBWOS 2013 took place between January and March 2013. In contrast to UBWOS 2012, conditions during UBWOS 2013 were favorable to ozone formation and numerous exceedances of the NAAQS were observed. Results from UBWOS 2013, in combination with those from UBWOS 2012, provide a wealth of information about the meteorological conditions and atmospheric chemistry associated with winter ozone episodes in the Uinta Basin. Key findings from UBWOS 2013 are described in a summary report (Final Report: 2013 Uinta Basin Winter Ozone Study; available at http://www.deq.utah.gov/locations/U/uintahbasin/ozone/strategies/studies/UBOS-2013.htm).

Results from UBWOS 2012 and UBWOS 2013 suggested that additional measurements were needed to address key remaining areas of uncertainty, foremost among which was the need to better understand the role of nitrous acid (HONO) in promoting ozone formation during the winter episodes. A more limited field campaign was undertaken during January – February 2014 to address this need. Several periods of elevated ozone associated with snow cover and strong temperature inversions were captured by the UBWOS 2014 measurements and significant additional information about the atmospheric chemical conditions during winter ozone episodes was obtained.

Findings

Key findings from UBWOS 2014 are summarized below:

Air Quality and Meteorological Conditions during UBWOS 2014

- Conditions favorable for ozone formation occurred at times during the December 2013 – March 2014 winter ozone season. Eight-hour average ozone concentrations exceeded the level of EPA's ambient air quality standard (75 ppb) at twelve out of 18 monitored locations within the Uinta Basin; Ouray experienced the most exceedance days (17).
- The most severe high ozone episodes of the winter occurred in December: the maximum 8-hour average concentration of the season (104 ppb) was recorded at Horsepool on 16 December and concentrations in excess of 75 ppb were observed at several locations within the Basin during mid and late December. Additional episodes occurred in January and early February. As in previous years, the episodes were associated with snow cover and strong inversions. Lack of snow cover precluded the occurrence of any episodes after early February.
- While ozone episodes captured by the intensive field study measurements during January and February were shorter and peak ozone concentrations were lower than episodes during the 2013 field study, conditions were nevertheless representative of typical winter ozone events.

Ozone Formation Mechanisms

- Results from UBWOS 2013 showed that the primary chemical drivers of winter ozone formation in the Uinta Basin differ greatly from summer ozone formation in urban areas but were inconclusive regarding the relative importance of HONO. Measurements made during UBWOS 2014 confirmed the unique nature of winter ozone formation mechanisms and helped clarify the role of HONO. Comparisons of five different HONO measurement techniques and HONO measurements made over a wider range of elevations within the polluted atmospheric boundary layer showed that HONO does <u>not</u> appear to be a major source of radical species driving ozone formation during the winter episodes. Instead, results from the 2014 measurements confirmed that formaldehyde and other aldehydes are the dominant radical sources. These compounds are both directly released from various emission sources and form in the atmosphere from directly emitted volatile organic compounds (VOCs) such as those emitted from oil and natural gas exploration and production activities. Aromatic VOCs (including toluene and xylene), while less abundant than other VOC species in the Basin, were also found to be particularly important sources of radicals.
- New "box model" simulations of ozone formation chemistry based on data collected at the Horsepool study site confirm earlier analyses indicating that ozone formation at this location is sensitive to VOC reductions, i.e. VOC reductions would result in ozone reductions. These results also suggest that NOx reductions, either by themselves or in conjunction with VOC reductions, would lead to ozone reductions at Horsepool. While providing an important reference point, these box model results do not take into

account spatial variations in emissions and the mixing of emissions from different sources (among other factors) and thus do not provide an assessment of the expected impact of basin-wide VOC or NOx emission reductions on ozone levels sufficiently robust to allow formulation of a comprehensive regulatory control strategy. Nevertheless, this result provides support for on-going VOC reduction measures and is an important contribution to the overall "weight of evidence" guiding control strategy design.

Results from the past three winter UBWOS field campaigns have provided valuable information for the development of improved emission inventories and model simulations of winter episodes, thereby contributing to the scientific foundations needed to develop an effective air quality management plan for the Basin:

- Several different government and university groups are continuing to develop and evaluate inventories of pollutant emissions in the Basin. Discrepancies between current emission estimates and observed pollutant concentrations have been noted and are being further investigated by these groups. The Utah Division of Air Quality is working with the Western Energy Alliance to update the inventory of emissions from oil and gas operations in the Basin. Recently enacted federal reporting and permitting regulations are also expected to generate data contributing to future improvements in the inventory. Research efforts are underway at Utah State University to better quantify emissions of formaldehyde (an important ozone precursor).

- Full scale three-dimensional computer model simulations of winter ozone episodes are under development by the Utah Division of Air Quality, EPA, BLM, University of Utah, Utah State University and NOAA. A number of areas in which model improvements are needed have been identified and work is continuing. The State of Utah has also committed $300,000 towards development of improved emissions data and models for evaluation of winter ozone control strategies.

Recommendations

UBWOS participants developed several recommendations based on the results of UBWOS 2014:

- Additional measurements are needed to compare radical sources in the western basin (where oil production dominates) with those that have been collected at Horsepool during UBWOS 2012 – 2014 (where natural gas production dominates) so as to better characterize the influence of oil production sources on ozone episodes.
- UBWOS results have shown that current emission inventories contain biases which need to be corrected. Current emission measurement and other emission inventory improvement activities are high priority and should be continued with emphasis on close collaboration between the groups involved in these efforts.
- Meteorological and air quality modeling results obtained to date are promising but additional model development and application work is needed to support emission reduction efforts.

This important work was made possible by funding and in-kind support from the following: Uintah Impact Mitigation Special Service District (UIMSSD), Western Energy Alliance, Questar Energy Products, Bureau of Land Management (BLM), National Oceanic and Atmospheric Administration (NOAA), Environmental Protection Agency (EPA), Environment Canada, and Utah Department of Environmental Quality (UDEQ). UBWOS 2014 field study measurements were conducted by researchers from the National Oceanic and Atmospheric Administration (NOAA), Utah State University (USU), University of Utah (UU), University of California Los Angeles (UCLA), University of Toronto, Environment Canada, University of Houston, University of Calgary, and University of Washington (UW). Emission inventory development and atmospheric modeling work is on-going and is being conducted by several groups, including Utah Department of Environmental Quality (UDEQ), University of Utah, Utah State University, NOAA, the U.S. Environmental Protection Agency (EPA) and the Houston Advanced Research Center.

1.0 PREFACE, CONTRIBUTORS AND ACKNOWLEDGEMENTS

1.1 Preface

The Uinta Basin Winter Ozone Study (UBWOS) began with a relatively modest measurement program during the winter of 2010-2011 followed by an intensive set of measurements during each of the following three winters focusing on the January to early March period when high ozone episodes are most common. We refer to these measurement studies here as the 2012, 2013 and 2014 winter ozone studies. A comprehensive discussion of the relevant background information and results from the UBWOS 2012 and UBWOS 2013 studies was presented in the UBWOS 2013 Synthesis Report (Stoeckenius and McNally, 2014; referred to hereafter as SR2013). A brief summary of the 2012 and 2013 results is presented here but readers are encouraged to refer to the UBWOS 2013 report for more detailed information.

1.2 Contributors

This report is a result of the contributions of a large number of dedicated scientists from federal and state government departments and agencies as well as several research universities. Primary authors are listed by section below. In most cases, a number of other UBWOS participants provided detailed and helpful comments which greatly improved the initial drafts prepared by the primary authors. Affiliations of all authors are listed in the author list at the beginning of each section.

Executive Summary: Till Stoeckenius, Brock LeBaron, Gail Tonnesen and Jim Roberts.

1.0 Preface, Contributors and Acknowledgements: Till Stoeckenius.

2.0 Synthesis of Results: Till Stoeckenius and Dennis McNally (parts of Section 2.1 contributed by Brock LeBaron).

3.0 Review of Meteorological and Air Quality Conditions, Winter 2013-2014: Seth Lyman and Howard Shorthill

4.0 Intensive Chemical Measurements at Horsepool: James M. Roberts, Patrick R. Veres, Bin Yuan, Carsten Warneke, Felix Geiger, Peter M. Edwards, Robert Wild, William Dube, Steven S. Brown, Martin Graus, Jessica Gilman, Brian Lerner, Joost A. de Gouw, Rui Li, Timothy Bates, Patricia Quinn, Abigail Koss, Shao-Meng Li, John Liggio, Hans Osthoff, Barry Lefer, James Flynn, Sergio Alvarez, Catalina Tsai, Jochen Stutz, David D. Parrish, Robert Zamora, Becky Alexander, and Maria Zatko.

5.0 Emission Inventory Development Activities: Patrick Barickman, Stuart McKeen, Ravan Ahmadov and Seth Lyman

6.0 Air Quality Modeling Studies of Winter Ozone: Gail Tonnesen, Lance Avery, Marc Mansfield, Huy Tran, Trang Tran, Ravan Ahmadov, Stuart McKeen, Peter Edwards, Erik Crosman, John Horel , Courtney Taylor

1.2.1 Acknowledgements: Funding Agencies

UBWOS 2014 was made possible by the combined contributions of several private and public sector organizations and in-kind contributions from NOAA and Environment Canada: Uintah Impact Mitigation Special Service District (UIMSSD), Western Energy Alliance, QEP Resources, Inc., Bureau of Land Management (BLM), National Oceanic and Atmospheric Administration (NOAA), Environmental Protection Agency (EPA), and Utah Department of Environmental Quality (UDEQ).

2.0 SYNTHESIS OF RESULTS

2.1 Introduction

2.1.1 Background

The Uinta Basin is an enclosed basin that lies in the northeast corner of Utah and is part of a larger area known as the Colorado Plateau. The Basin is bounded on the north by the Uinta Mountain range, on the south by the Book and Roan Cliffs, on the west by the Wasatch Range and on the east by elevated terrain separating it from the Piceance Basin in Colorado. The Green River runs through the Basin from northeast to southwest, exiting through the Book Cliffs via Desolation Canyon. The floor of the Basin is at approximately 4800 feet above sea level with significant local topography on the order of tens to hundreds of feet.

Duchesne and Uintah Counties make up essentially the entire Basin. The Uintah and Ouray Indian Reservation covers a significant portion of the Basin (Figure 2-1). EPA and the Ute Tribe have jurisdiction over air quality management on the reservations and in Indian Country.

The Basin is rural with a population of about fifty thousand people primarily located in three main towns (Duchesne, Roosevelt, and Vernal) which lie along the east-west State Highway 40 corridor. The economy of the Basin is driven by energy production from vast petroleum resources. Oil and gas development (approximately 10,000 producing wells) is widely scattered throughout the Basin (Figure 2-2) with associated drilling, processing, compression and pipeline facilities. A 500 megawatt coal fired power plant (Bonanza) operates in the Basin. There is also some agricultural production in the Basin, primarily alfalfa and corn along with other hay and grain crops.

Air quality monitoring in the Basin began in 2006 when the Utah Department of Air Quality (UDAQ) installed monitors in Vernal to measure fine particulate ($PM_{2.5}$), ozone (O_3) and oxides of nitrogen (NO_x). Data were collected from February 2006 through December 2007. Highest 8-hour ozone averages reaching 81 ppb were found in the summer. No concentrations exceeding the 0.08 ppm National Ambient Air Quality Standard (NAAQS) then in affect were recorded and no elevated ozone was noted in the winter months. Two additional special studies were conducted during the winters of 2007-08 and 2008-09, but these were focused on $PM_{2.5}$ since no elevated winter ozone values had been observed in 2006-2007.

In the spring of 2009, EPA used consent decree funding to establish two monitoring sites at Ouray and Redwash in the oil and gas production area of the Basin. These sites were instrumented to measure $PM_{2.5}$, NOx, O_3, and meteorological parameters year-round. In sharp contrast to the low ozone values found in the winter of 2006-2007, the winter of 2009-10 experienced very high ozone levels, with the highest 8-hour average of 124 ppb being measured at the Ouray site.

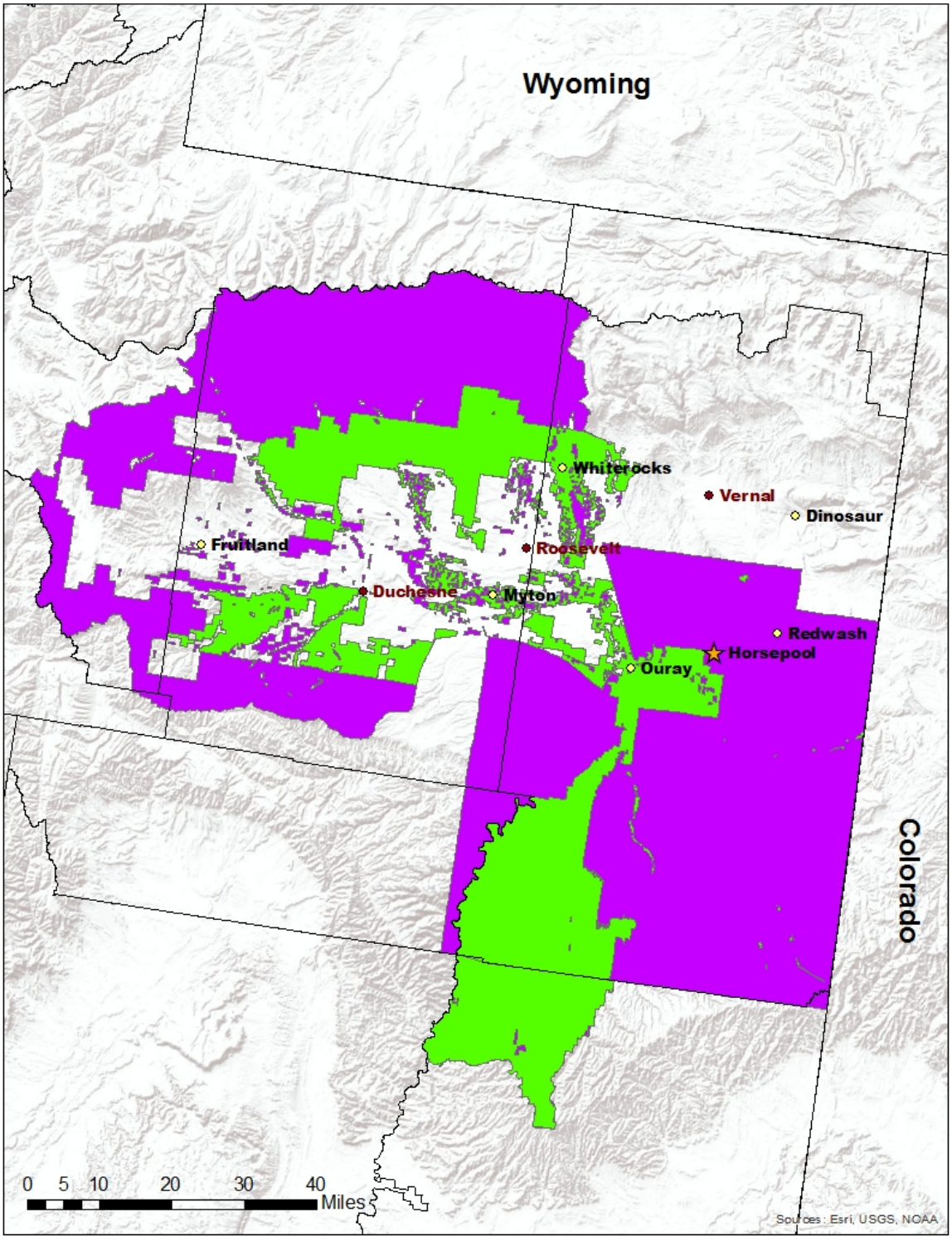

Figure 2-1. Uinta Basin and surrounding region. Green and purple areas fall under EPA and Ute tribe air jurisdiction.

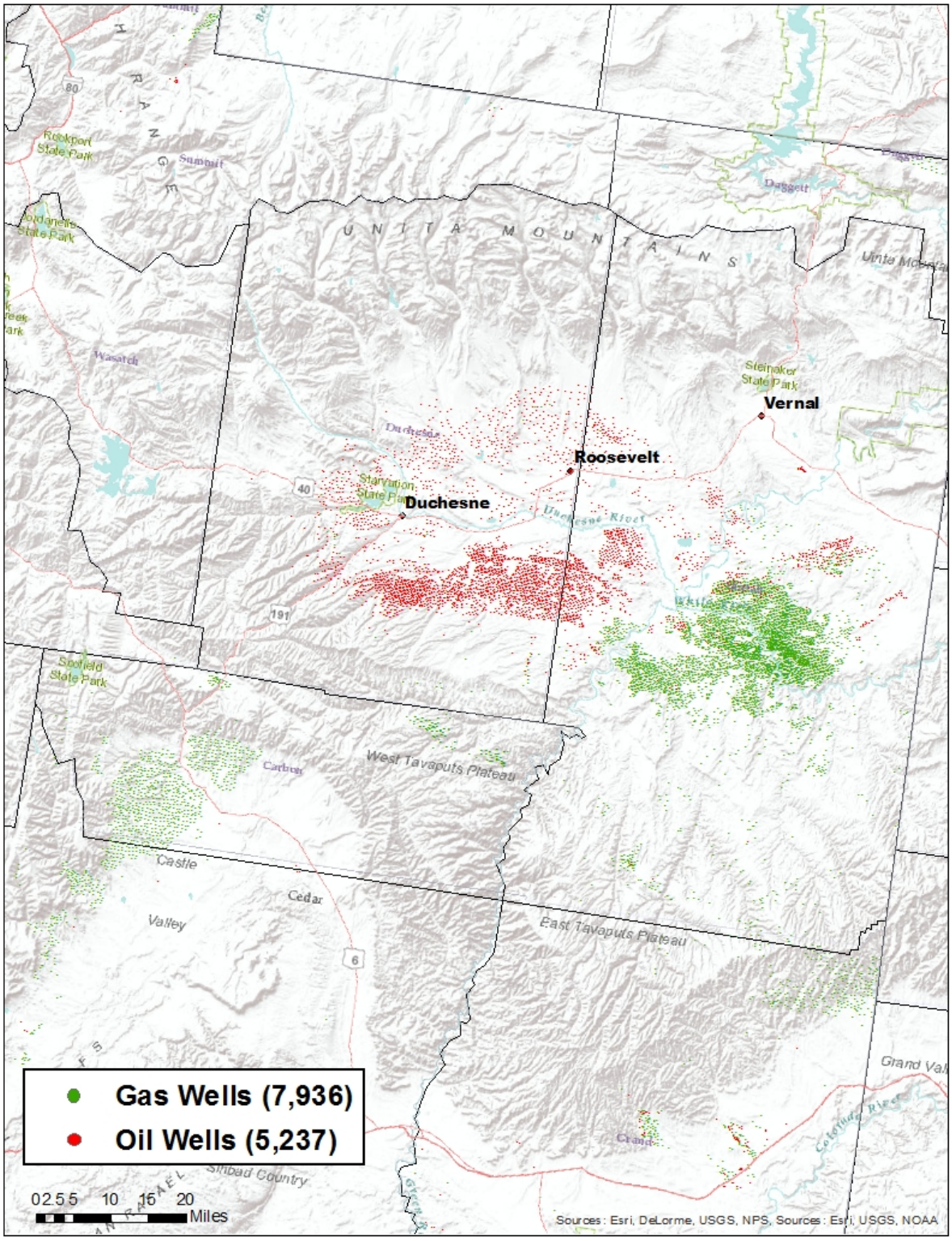

Figure 2-2. Oil and gas well sites in Utah as of 2013 (includes shut-in and producing).

Utah State University (USU) conducted a special study in the winter of 2010-11 to confirm the presence of high winter ozone concentrations and map out the spatial extent of elevated ozone levels. Results from the 2010-11 study showed that ozone values were elevated throughout the Basin, with the highest concentrations tending to occur at lower elevations in the center of the Basin. The highest 8-hour ozone value measured at Ouray was 139 ppb. The data also showed that elevated ozone correlated highly with the presence of snow-covered ground and a strong temperature inversion, and that elevated ozone values did not occur absent these conditions. A full report on results of the 2010-2011 study is available (Martin et al., 2011) and can be found at http://www.deq.utah.gov/locations/U/uintahbasin/ozone/docs/2013/02Feb/edl201011reportozonefinal.pdf.

2.1.2 2012 Uinta Basin Winter Ozone Study

A full field campaign was mounted in the winter of 2011-12 to gain a more complete understanding of factors contributing to high wintertime ozone in the Basin. This campaign was part of a multi-phase study designed to identify the emissions sources and potentially unique photochemical processes that produce elevated winter ozone concentrations and assist in determining the most effective mitigation strategies. The 2012 Uinta Basin Winter Ozone Study (UBWOS 2012) consisted of six components carried out by several research organizations, with most measurements focused on the January to early March 2012 time period. Many of the most detailed measurements were conducted at the Horsepool site located in the northern portion of the gas field in Uintah county 35 km south of Vernal. A full report (Lyman and Shorthill, 2013; referred to hereafter as the 2012 Synthesis Report or SR2012) presenting results obtained by each research group along with a synthesis of results across all groups and a unified set of key results and conclusions was prepared and made publically available via the Utah Department of Environmental Quality website http://www.deq.utah.gov/locations/U/uintahbasin/ozone/docs/2014/03Mar/ubos_2011-12_final_report.pdf.

2.1.3 2013 Uinta Basin Winter Ozone Study

Motivated by the lack of ozone-conducive conditions during UBWOS 2012, a second round of field monitoring was undertaken during January – March 2013. Recognizing the possibility that the 2012-2013 winter could also turn out to have minimal snow and no ozone episodes, UBWOS 2013 was designed to minimize upfront investment of labor and materials required to conduct an intensive measurement program unless and until such time as there was a reasonable certainty that snow cover sufficient to produce ozone conducive conditions would occur during the January – February study window. As it turned out, storms during December and early January produced a good snow pack in the Basin, and by mid-January it was obvious that conditions during UBWOS 2013 would be favorable for ozone formation, prompting the decision to proceed with the intensive measurement program. Numerous 8-hour average ozone concentrations in excess of the National Ambient Air Quality Standard (NAAQS) were subsequently observed during the study. As in the 2011-2012 study, researchers from the National Oceanic and Atmospheric Administration (NOAA) and several universities conducted extensive ground-based and airborne measurements of ozone and other key air quality and

meteorological parameters and the Horsepool site was again chosen as the location to conduct a series of intensive measurements of meteorology, ozone, ozone precursors and particulate matter. Instrumentation in 2013 differed somewhat from that used in 2012: some measurements such as the long-path differential optical absorption (DOAS) measurement of nitrous acid (HONO) and other species were not available but a new set of measurements were added to examine ozone deposition to the snow surface and chemical reactions within the snow pack which may play a role in winter ozone formation. Results from UBWOS 2013 were presented in a second study synthesis report (Stoeckenius and McNally, 2014; referred to hereafter as the 2013 Synthesis Report or SR2013) found here http://www.deq.utah.gov/locations/U/uintahbasin/ozone/strategies/studies/UBOS-2013.htm.

2.1.4 2014 Uinta Basin Winter Ozone Study

Results from UBWOS 2012 and UBWOS 2013 provided a wealth of information regarding conditions and mechanisms underlying winter ozone episodes in the Uinta Basin. A key result from these studies was the observation of apparently very high HONO measurements during the middle of the day which, if correct, would represent the major driver for ozone formation. Further analysis, however, raised questions about both the accuracy and representativeness of the HONO measurements (see SR2013 for details). This left in doubt the actual contribution of HONO to ozone formation and therefore introduced significant uncertainties into conclusions regarding the potential efficacy of emission control strategies for reducing ozone. As a result, UBWOS researchers recommended performing a follow-up study during the 2013-2014 winter focused primarily on obtaining reliable and representative HONO measurements using a variety of analytical techniques. Additional supporting measurements needed to verify and provide context for the HONO measurements were added to the research plan. Other research teams also participated in UBWOS 2014, providing measurements of reactive nitrogen chemistry at the snow/air interface, snow surface albedo, and targeted measurements of ozone precursor emissions sources.

This report provides an integrated summary of results from all of the research teams participating in UBWOS 2014. Reference is made to the two earlier synthesis reports where appropriate to provide context for the new results.[1] As has been the case in prior years, each research group participating in UBWOS 2014 prepared a final report describing in detail their individual data collection and analysis methods. These reports are included here in Sections 3 and 4. In addition, several groups have recently undertaken efforts to develop improved and updated emission inventories for the Uinta Basin as described in Section 5 and to develop model applications that provide accurate simulations of meteorology and air quality during winter episodes as described in Section 6. Several UBWOS research groups have published or are in the process of publishing their results in peer reviewed science journals, including a special issue of Atmospheric Chemistry and Physics and Atmospheric Measurement Technology

[1] The 2012 synthesis report is available at http://www.deq.utah.gov/locations/U/uintahbasin/ozone/docs/2014/03Mar/ubos_2011-12_final_report.pdf; the 2013 synthesis report is available at http://www.deq.utah.gov/locations/U/uintahbasin/ozone/strategies/studies/UBOS-2013.htm

(http://www.atmos-chem-phys-discuss.net/special_issue217.html). References to results presented in these science research papers are included here where appropriate.

2.2 Summary of Results from UBWOS 2012 and UBWOS 2013 Studies

Intensive field studies conducted during the winters of 2011-2012 and 2012-2013 provided significant insight into the conditions and ozone formation mechanisms associated with winter ozone episodes. By comparing measurements made during UBWOS 2012, when snow cover was almost completely absent and daytime ozone levels were near at background levels, with measurements made during UBWOS 2013, when snow cover was in place during most of the study period and ozone concentrations reached 142 ppb (8-hour average), UBWOS researchers were able to deduce the three key ingredients required for development of winter ozone episodes:

1. Snow cover,
2. Calm weather conditions with no storm activity and minimal cloud cover, and
3. Significant emissions of ozone precursors (VOCs and NOx) from sources near ground level.

Major findings from these studies as summarized in the 2013 Synthesis Report included:

- Ozone episodes typically occur over multi-day periods with ozone and other pollutant concentrations increasing from one day to the next and are characterized by a strong, low-level temperature inversion that traps a pool of cold, polluted air within the Basin. The top of this "cold pool" is typically found at an elevation of approximately 1650 m asl; the depth of the polluted layer varies from approximately 70 - 400 m within the Basin depending mostly on the local topography. Radiative and thermal influences of the snow cover act to keep the cold pool in place during the day under clear skies, thus providing a shallow layer in which pollutants can build up and react in sunlight to form ozone. In the absence of any snow cover, warming of the earth's surface by the sun causes too much convective mixing for a cold pool to form. This is what was observed in 2012.
- Ozone concentrations close to but just outside of the Basin as well as above the strong inversion over the basin remain in the 40 – 60 ppb range in sharp contrast to the high concentrations found within the Basin underneath the top of the inversion layer. Meteorological measurements show that the Basin is effectively isolated from its surroundings during these cold pool events and there is no evidence of transport of ozone or precursors from outside the basin contributing to the high pollution levels.
- As is the case during summer ozone episodes in major urban areas, winter ozone formation is the result of reactions of VOCs and NOx in the presence of sunlight. Although solar zenith angles are higher during the winter (i.e., the sun is lower in the sky), the highly reflective snow cover multiplies the total radiative flux by a factor of approximately 1.6 to 1.9, creating total radiative flux levels approaching values observed during summer episodes. UBWOS researchers have shown that these high solar

radiation levels are a necessary condition for creating ozone at observed concentration levels.

- VOCs in the Basin occur at much higher concentrations than those encountered during summer urban ozone episodes and the VOC species mixture is very consistent with that found in natural gas: ambient measurements show that VOC species of the types typically found in raw gas are very highly correlated with methane, indicating that releases of natural gas from venting, leaks and other fugitive sources account for the vast majority of VOCs found in the Basin. The high VOC concentrations result from significant volumes of natural gas emissions which are trapped within the shallow mixed layer underlying the strong temperature inversion.
- Oxidation of VOCs via reactions with radical species (primarily the OH radical) is a key step in ozone production. While the reactivity of VOCs varies widely, the relative contribution of individual VOC species to ozone formation depends on their abundance as well as their reactivity. Measurements made during 2012 and 2013 indicate that alkanes (including propane, iso- and n-butane and iso- and n-pentane), are much more abundant and as a result likely contribute more to ozone formation in the Basin than the more reactive but less abundant aromatic VOCs (including toluene and xylene). Nevertheless, small reductions in emissions of aromatics may be as effective as larger reductions in emissions of alkanes given the greater reactivity of aromatics. There do not appear to be large sources of other highly reactive VOCs (alkenes) in the Basin as alkene concentrations were very low relative to alkanes and aromatics.
- As with VOCs, total concentrations of reactive nitrogen (NOy which includes NOx and its reaction products) during the 2013 ozone episodes were much higher than observed in 2012, consistent with the trapping and buildup of emissions in a shallow boundary layer during the 2013 episodes. NOz (equal to NOy minus NOx) was higher in 2013, consistent with more vigorous photochemical reactions in the presence of snow. This kept NOx at levels only slightly higher than in 2012. Thus, relatively high concentrations of both ozone precursors are available to drive ozone formation under inversion conditions.
- The interplay of chemical reactions involved in winter ozone episodes is very different from summer episodes and these unique features have significant implications for the development of control strategies. Aldehydes, including formaldehyde and potentially nitrous acid (HONO) rather than ozone photolysis[2] were found to be the biggest contributors to the pool of chemical radicals responsible for ozone formation. Measurements made during UBWOS 2013 suggested that a daytime HONO source at the snow surface might be primarily responsible for the contribution of HONO to the radical pool, followed by formaldehyde. However, the magnitude of this contribution was determined to be highly uncertain due to the limited vertical extent of HONO measurements made during the 2013 study and significant concerns regarding a

[2] Ozone photolysis refers to the splitting of ozone molecules by ultraviolet solar radiation into diatomic oxygen (O_2) and an oxygen atom in an excited singlet state, usually denoted as O(1D). Some of the O(1D) atoms then combine with water vapor to form hydroxyl (OH) radicals.

potential positive bias in the HONO measurements, which were based on a single analytical method. This left a significant amount of uncertainty with regard to modeling the chemistry of ozone formation.

2.3 Synthesis of Results from UBWOS 2014

As a follow-up to the 2012 and 2013 studies described above, researchers returned to the Uinta Basin in the winter of 2013-2014 in an attempt to address remaining key uncertainties about winter ozone formation mechanisms. The primary objective of the UBWOS 2014 was resolving uncertainties about the role of HONO by obtaining high quality measurements of HONO and related species over a range of heights above the snow surface using multiple analytical methods. Additional supporting meteorological and chemical measurements were also included in the UBWOS 2014 study plan.

A synthesis of results from UBWOS 2014 is provided in the following subsections. Detailed descriptions of the data collection and analysis results from UBWOS 2014 are provided in Section 3.

2.3.1 Meteorological and Air Quality Conditions during UBWOS 2014

Meteorological and air quality conditions during the winter of 2013-2014 are described in Section 3.1. A large snowfall in early December set the stage for a series of ozone episodes which occurred off and on until the middle of February when the last of the snow melted (Figure 2-3, Figure 2-4). The close connection of ozone episodes with snow cover was consistent with findings from prior years. The presence of fresh snow and calm weather conditions in December resulted in the most severe ozone episodes of the winter during the weeks leading up to the winter solstice. In fact, the first exceedance of the 75 ppb 8-hour average level was recorded on 14 December and the highest 8-hour average concentration of the season (104 ppb) was recorded at Horsepool on 16 December. The occurrence of such high ozone concentrations in the weeks leading up to the winter solstice is remarkable given the high solar zenith angles (corresponding to the sun's position low in the sky) during this time of year. The sum of up- and downwelling UV radiation measured during the mid-December episodes was at roughly the same level as during episodes in January 2013 (see Sec. 3.1). Additional high ozone days were observed in early January 2014 and again towards the end of the month (Figure 2-3). Overall, the episodes during January-February 2014 were shorter in duration and had lower peak ozone concentrations as compared to the previous winter. Less snow cover and longer periods between snow events resulted in lower average albedo which contributed to reduced ozone formation. The lack of solid snow cover likely contributed to destabilization of the lower boundary layer and shortening of episode events from as long as 15 days during January – February 2013 to just a few days duration during January-February 2014. As in previous winters, the shorter episodes are associated with confinement of ozone concentrations in excess of 75 ppb to a smaller area in the central portion of the Basin whereas a much larger portion of the Basin was thus impacted during the longer episodes that occurred in January – February 2013. As in previous winters, the highest ozone concentrations were typically found at the lowest elevation sites.

Intensive measurements at Horsepool captured the late January ozone episodes which, while not as intense as episodes earlier in the winter or episodes during the previous winter, nevertheless exhibited the same major features and thus serve as a useful model for ozone development in the Basin.

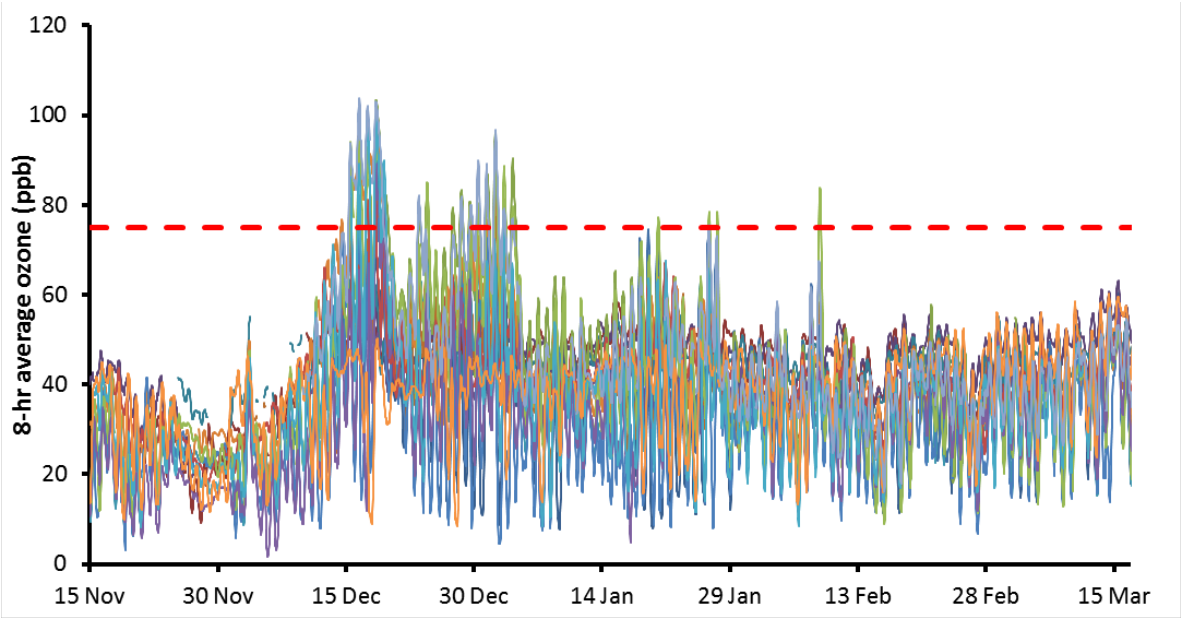

Figure 2-3. Time series of 8-hour average ozone concentrations at all monitoring sites in the Uintah Basin, winter 2013-14. Current EPA ozone standard level (75 ppb) is shown as a red dashed line.

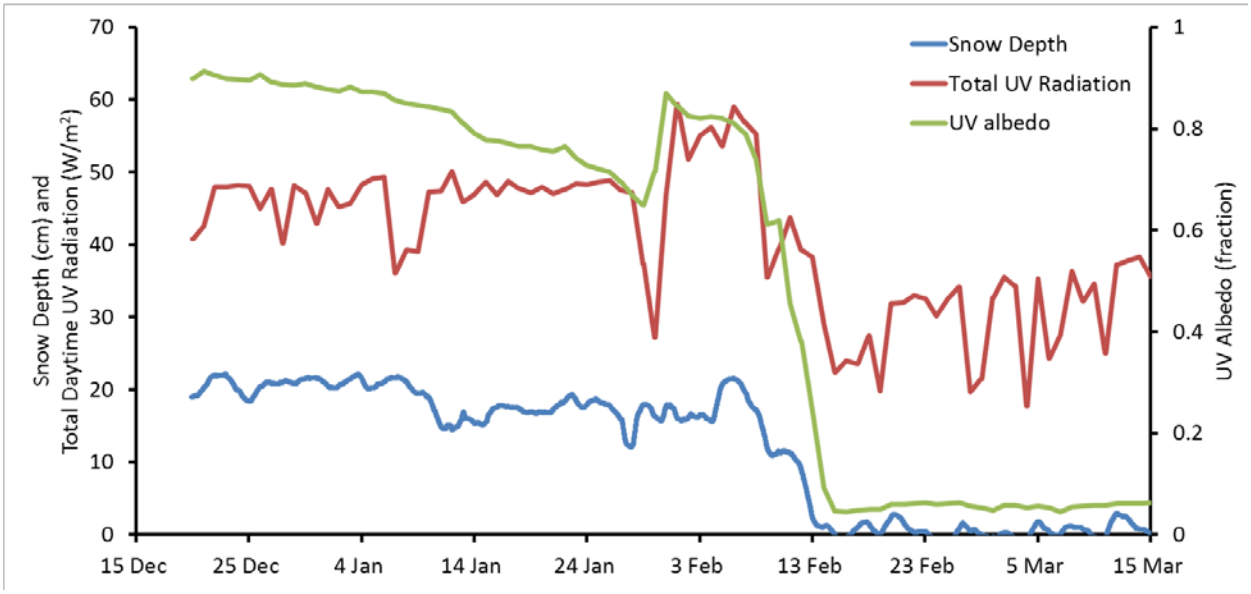

Figure 2-4. Time series of snow depth (blue line), average total (sum of upwelling and downwelling UV-A and UV-B) daytime UV radiation (red line), and the average of UV-A and UV-B albedo (green line) during winter 2013-14 at Horsepool.

2.3.2 Chemical Characteristics of UBWOS 2014 Ozone Episodes

As was the case during UBWOS 2013, detailed measurements of ozone precursors and associated photochemical reaction products were made at Horsepool during January – February 2014 with a particular emphasis on refining the contribution of HONO to ozone formation. Consistent with the reduced severity of the UBWOS 2014 episodes relative to UBWOS 2013, concentrations of most precursors and chemical indicators of photochemical activity were intermediate between the highly reactive conditions during UBWOS 2013 and the essentially non-reactive conditions during the snow free UBWOS 2012 study.

2.3.2.1 VOC/OVOC

Analyses of speciated VOC measurements at Horsepool showed that the VOC mixture and the relationship of VOCs to methane and ethane during UBWOS 2014 were very similar to what was observed in prior years. The dominant VOC constituents of raw natural gas (alkanes with between 2 and 6 carbon atoms) are very highly correlated with methane and ratios of species concentrations to propane are consistent with typical natural gas composition profiles (Figure 4-3), supporting the conclusion that VOCs at Horsepool are associated with a single dominant source type which is the release of natural gas to the atmosphere. The importance of the natural gas source to ozone formation is further illustrated by consistency across the three years of measurements in the relative contributions of different types of VOCs to total reactivity of the VOC mix with respect to hydroxyl (OH) radicals (contributions from highest to lowest are: alkanes, cycloalkanes, oxygenated VOCs (OVOCs), aromatics and alkenes; see Figure 4-8). Alkanes accounted for the bulk of OH reactivity in all three years due to their high abundance as found in natural gas despite the fact that alkane molecules are the least reactive of the four VOC types. Thus, direct emissions of natural gas are one of the key ingredients of ozone episodes in the Basin. Natural gas emissions are associated with maintenance activities (venting and blowdowns), bleeding from pneumatic devices used to control equipment at the wellsite, and equipment leaks. Gas leakages around well bore casings have also been documented (see Sec. 5.3.2) but current data are insufficient for developing an estimate of the relative contribution of such below ground leaks to total gas emissions.

Methanol concentrations in 2014 were also intermediate between the low year (2012) and the high year (2013). Methanol is important as it reacts in the atmosphere to form formaldehyde which is a significant source of radical species that drive ozone production. As in the other years, short term spikes and lack of correlation with other aldehydes such as acetaldehyde, which are formed in the atmosphere from primary (directly emitted) VOCs, indicate that most of the observed methanol is directly emitted. While plants can be an important source of methanol, this is not the case during the winter when plants are dormant. Methanol is commonly used as an antifreeze agent in oil and gas operations in the Basin so its presence at concentrations above typical background levels is not surprising. High frequency VOC monitoring data from UBWOS 2013 revealed correlations of methanol spikes with formaldehyde spikes, suggesting that methanol used in oil and gas operations contains some formaldehyde. This primary source of formaldehyde may be an important contributor to the radical pool. Measurements of the formaldehyde content of stored methanol confirm formaldehyde is present in concentrations as high as ~100 ug/mL in recovered methanol;

concentrations in methanol that had been stored for a period of months are ~10 ug/mL as compared to less than 1 ug/mL in newly delivered methanol (see Figure 5-3). This correlation of formaldehyde concentration with age of the methanol is consistent with formaldehyde formation from degradation of methanol. Formaldehyde was also found along with methanol in produced water ponds. Estimates of direct emissions of formaldehyde as a result of methanol use are not available, thus the magnitude of this potential source of a major ozone precursor is unknown. Additional study of non-combustion sources of formaldehyde in the Basin are currently underway (Sec. 5.3.1).

2.3.2.2 Odd Nitrogen

Measurements of NOx and its reaction products (NOz) during UBWOS 2014 also revealed a level of photochemical activity intermediate between the low ozone UBWOS 2012 and the more active UBWOS 2013. Relationships between NOx, NOz and ozone were consistent with results from the earlier years.

An important aspect of ozone chemistry is the potential extent to which NOx is stored in the form of N_2O_5 overnight and then photolyzes back to NO_2 the next day adding to the total NOx loading and potentially impacting the relative effectiveness of VOC vs. NOx emission controls. However, some of the N_2O_5 reacts overnight on aerosol or ground/snow surfaces to form nitric acid (HNO_3), thereby removing reactive nitrogen from the system. Calculations based on measurements during UBWOS 2012 and UBWOS 2013 indicate that N_2O_5 is primarily removed via heterogeneous reactions on aerosol surfaces as opposed to reactions on ground surfaces. In addition, N_2O_5 was removed at a greater rate during UBWOS 2013 and UBWOS 2014 (when aerosol loadings were higher) than in UBWOS 2012, thus limiting the overnight recycling of NOx. Accurate simulation of potential ozone control scenarios will require that overnight removal of N_2O_5 via heterogeneous reactions is properly accounted for.

2.3.2.3 Snow chemistry

As noted above, the major impact of snow cover is to 1) increase the total UV flux by roughly 50%, thus driving photochemical reactions which form ozone and 2) stabilize the lower boundary layer, thus promoting formation of a strong, low level inversion layer that traps ozone precursors at high concentrations in a thin layer above the surface. Snow albedo is reduced by deposition of soil dust and other particles between snowfalls. Deposition of dust can occur more rapidly when the snow cover is less extensive as was the case in 2014. Snow is also a repository for pollutant deposition with different characteristics than non-snow covered surfaces and the upper layer of snow serves as a reactor which impacts ozone photochemistry in subtle ways. Photochemical reactions have been observed in snow which contribute significantly to the chemistry of the atmospheric boundary layer in near pristine environments as found in Antarctica and Greenland (Grannas et al., 2007; Helmig et al., 2007) but the nature and relative importance of these reactions in areas such as the Uinta Basin that are much more heavily impacted by anthropogenic emissions is less clear. Snow chemistry measurements during UBWOS 2014 (Sec. 4) indicated that photochemistry in the snow was inhibited by dust and black carbon in the old snow surface at the beginning of the study period but became active after fresh snow fell between January 30 and 31. Chemical reactions in the fresh snow

caused NOy to be released to the atmosphere from the snow surface. Preliminary calculations suggest that a potentially large but short-lived "pulse" of NOy is released from the fresh snow surface during the first few hours of daylight which could help kick off ozone formation during the morning. However, additional analysis and modeling using these data will be needed to better quantify the flux of NOy and estimate the impact of snow photochemistry on ozone formation.

2.3.2.4 HONO

As noted above, the primary objective of the UBWOS 2014 measurements at Horsepool was to resolve uncertainties about the magnitude and temporal pattern of HONO sources. HONO has long been of interest to researchers studying photochemical reactions resulting in the buildup of ozone concentrations, because it has the potential to be an important source of OH radicals, which are needed to drive the reactions. Measurements of HONO in urban areas during summer have generally shown a buildup overnight culminating in an early morning peak just before sunrise (Stutz et al., 2010). HONO photolysis then provides a pool of OH radicals which helps kick off early morning ozone production before other radical sources become more important. Sources of HONO during the daytime, i.e. processes that convert NOy to HONO, will have a disproportionately large impact on the radical budget because of the rapid photolysis of HONO (Li et al., 2014; VandenBoer et al., 2014).

HONO measurements during UBWOS 2013 were made at heights ranging from 1 to 7.25 m above the snow surface using negative ion proton transfer chemical ionization mass spectrometry (NI-PT-CIMS or Acid CIMS) in which acetate ion was the reagent. This instrument employed a quadrupole mass spectrometer during the 2013 field study, which was replaced by a higher resolution time-of-flight (TOF) mass spectrometer for 2014. The TOF MS is better able to distinguish between closely related acid species. As noted in SR2013, the high mid-day HONO values obtained from the acid CIMS during UBWOS 2013 were suspected of being biased high due to interference from other species, most notably peroxynitric acid (HO_2NO_2). In addition, the 2013 measurements were made at a maximum of just 7.25 m above the snow surface and may not have been representative of HONO concentrations throughout the boundary layer given the potential ground source of HONO and the limited amount of vertical mixing. Box model simulations indicated that HONO concentrations as high as those recorded in 2013, if representative of the entire depth of the boundary layer, should have resulted in much higher ozone levels than were actually observed. Acid CIMS measurements in 2014 showed substantially lower readings than in 2013. The lower 2014 values could be due both to lower photochemical activity in 2014 and to differences in the way the instrument was set up and operated.

Four different *in situ* measurement techniques, including the acid CIMS, were used to measure HONO during UBWOS 2014 along with the long path differential optical absorption spectrometry (DOAS) technique used in UBWOS 2012. Various tests were performed to evaluate the effect of sampling height and inlet configurations. An extensive analysis of results was conducted as described in Sec. 4. Evidence of positive daytime biases in the HONO measurements from HO_2NO_2 was identified as potentially affecting all of the in situ

measurement techniques in these data, either via direct chemical interference or through HONO formation within the instrument inlet. Results obtained from the DOAS, which is not subject to such interferences, showed lower HONO concentrations. While additional research is needed, the results presented in Sec. 4 strongly suggest that daytime HONO measurements from the *in situ* methods, including the measurements made in 2013, are biased high as a result of interference from HO_2NO_2. It should be noted that this effect is particularly strong under cold winter conditions, which promote longer HO_2NO_2 lifetimes. Thus, the only reliable measurements of HONO during the UBWOS campaigns are from the DOAS. Analysis of the DOAS measurements shows that HONO concentrations during 2014 were far lower than those implied by the other methods. The 2014 DOAS HONO measurements are qualitatively similar to those obtained in 2012 with one important exception: the 2014 measurements show a small but distinct afternoon peak and concentrations during this time decrease with height implying a daytime source of HONO at the snow surface. However, the overall contribution of HONO to the radical budget and hence winter ozone formation is estimated to be very small, consistent with the preliminary conclusions based on analysis of results from the 2013 study (SR2013, Sec. 4; see also Edwards et al., 2014).

2.3.3 Emission Inventories

A reasonably comprehensive understanding of the meteorological and air quality characteristics of winter ozone episodes in the Uinta Basin has now been established based on data collected over the past three winters as part of the UBWOS. UBWOS researchers have established that VOC and NOx emission sources within the Basin, rather than transport from outside the Basin, are the root cause of the episodes. Both the scope of human activity within the Basin and analyses of the pollutant mixture within the Basin point to the conclusion that the dominant sources of ozone precursors are emissions associated with oil and gas exploration and production. Significant uncertainties remain, however, regarding the magnitudes of emissions of different pollutants from various types of oil and gas sources. Development of accurate emission inventories is a key prerequisite to preparation of conclusive air quality modeling simulations and the design of cost effective ozone reduction strategies.

Most efforts to compile emission inventories for the Uinta Basin have focused on collecting activity data such as number of wells drilled, volume of oil and gas produced, number and size of compressor stations, number of vehicle miles traveled, etc. These values are then combined with appropriate emission factors (expressed as mass of emissions released per unit of activity) obtained from published reports or emission models (such as the MOVES model for on-road mobile sources). These “bottom up” inventories provide the detailed, temporally and spatially specific emissions needed by air quality models used to develop control strategies. They are, however, subject to significant uncertainties related to inaccuracies in counting sources, estimating activity levels, and biases in emission factors. Alternatively, “top-down” estimates of emissions which avoid these difficulties can be obtained from direct measurements of average pollutant concentrations. Unfortunately, top-down inventories do not provide the detailed estimates of emissions from individual sources or temporal or spatial variations in emissions needed for dispersion modeling and emissions control policy formulation. In addition, the limited availability of ambient pollutant concentration measurements means that top-down

inventory estimates may not be fully representative of the seasonal average emissions throughout the Basin that are intended to be represented by the bottom-up inventory. Nevertheless, robust top-down inventory estimates based on sufficient amounts of accurate measurements are a key check on the accuracy of bottom-up inventories.

Existing bottom-up inventories for the Uinta Basin have been based on the "Phase III" oil and gas emissions inventory developed under sponsorship of the Western Regional Air Partnership (WRAP; http://www.wrapair.org/forums/ogwg/PhaseIII_Inventory.html) combined with data for non-O&G source categories from the National Emissions Inventory (NEI) compiled by EPA. The WRAP Phase III inventory, which was completed in 2009, was based on activity data for 2008. Emissions were also estimated for 2012 based on projected O&G development growth rates but these estimates are highly uncertain. More recently, the Bureau of Land Management conducted the Air Resource Management Strategy (ARMS) study that included an update of the WRAP Phase III inventory to 2010. In addition, the Utah Division of Air Quality (UDAQ) independently updated the WRAP Phase III inventory for 2011 as part of the state's NEI submission to EPA. Both the ARMS and NEI 2011 inventories are being used in ongoing air quality modeling studies: UDAQ and the University of Utah (UU) are modeling the January 2013 ozone episode using the UDAQ inventory updated to 2013 and researchers at the Bingham Research Center (BRC) are modeling with a version of the 2010 ARMS inventory in which the oil and gas emissions have been updated to 2013 based on trends in well counts and production data.

Efforts are currently underway to develop new inventories for the Basin, which do not rely on the WRAP Phase III inventory as a starting point. UDAQ has implemented new permitting procedures (General Approval Orders) that are expected to provide more detailed information on actual emissions than has been available to date, at least for new sources on state lands exceeding the 5 tpy *de minimus* threshold. Similarly, EPA has published a proposed rule for implementing a minor source permit program for new or modified sources in Indian Country, which is expected to help improve future inventories.

A top-down inventory for the Basin was developed by Ahmadov et al. (2015) as described in Sec. 5. Oil and gas emissions in this top-down inventory were based on the flux of methane calculated from a single instrumented aircraft flight conducted during UBWOS 2012 combined with regressions of NOy and individual VOC species against methane derived from measurements made at Horsepool during UBWOS 2012 and UBWOS 2013. Emissions from non-oil and gas point sources derived from the NEI-2005 were added to the top-down inventory. Ahmadov et al. compared the resulting top-down inventory with a bottom-up inventory based on NEI-2011 (version 1, released August 2013). On-road and off-road mobile source emissions were based on NEI-2005 in both the top-down and bottom-up inventories. Notably, emissions of methane in the bottom-up inventory were calculated by applying ratios of total organic gasses (TOG) to volatile organic compounds (VOCs) obtained from the national SPECIATE database (v 4.3) to total VOCs reported in the NEI, but profiles in SPECIATE may not be representative of TOG/VOC ratios found in the Uinta Basin. In addition, the NEI-2011 inventory is largely compiled by EPA from data provided by each state and is likely to have

significant biases, especially in early versions. These factors could have introduced significant biases into the bottom-up inventory. The top-down VOC emissions estimate developed by Ahmadov et al. was 1.8 times greater than the bottom-up estimate whereas the top-down NOx emissions estimate was less than one third the bottom-up estimate.[3] These large discrepancies between the bottom-up and top-down estimates strongly suggest that the bottom-up inventory requires significant refinement. This conclusion is further bolstered by a recent numerical analysis of aromatic VOC measurements made at Horsepool during a 7-day period at the beginning of February, 2013 by Koss et al. (2015). The Koss et al. analysis is based on a best fit of data to VOC/benzene ratios as a function of time using a simple model of reaction of aromatics with OH radical and a set of reasonable simplifying assumptions (see Sec. 5.2). The resulting independent basin-wide VOC emission rate estimate is on par with the estimate based on Karion et al.'s 2012 methane flux value used by Ahmadov et al.

In general, ozone production in the Basin is sensitive to both the concentrations of VOC and NOx and to the VOC/NOx ratio. Therefore both the absolute magnitude of VOC and NOx emissions as well as the VOC/NOx emissions ratio must be accurately determined. Results of photochemical modeling of the 29 January – 8 February 2013 episode performed by Ahmadov et al. indicate significant under estimation of ozone when the model is run using the bottom-up inventory with its relatively low VOC emissions and low VOC/NOx emissions ratio. Much better performance was achieved using the top-down inventory. This finding does not prove that the top-down inventory is more accurate than the bottom-up inventory as any number of factors, such as errors in modeled meteorological conditions or the model chemical mechanism, could be responsible for the under prediction bias noted when using the bottom-up inventory. Nevertheless, this result, together with the large discrepancies between the bottom-up VOC emissions and the top-down emissions implied by the methane flux calculated from the aircraft measurements, provides good evidence in support of the hypothesis that VOC emissions are underestimated in the bottom-up inventory used by Ahmadov et al.

Reasons for the discrepancy between bottom-up and top-down NOx emission estimates are less clear cut. In general, uncertainties in NOx inventories are relatively small and more likely to be subject to under prediction bias due to undercounting of sources as NOx emission factors are generally well characterized. While the bottom-up NOx inventory used by Ahmadov et al. may very well be in error, the top-down NOx estimate is also very uncertain as it is based on the NOy/CH_4 linear regression slope determined from observations made at a single location (Horsepool). NOy/CH_4 ratios can be expected to vary by location within the Basin depending on the relative influence of combustion sources (which release NOx and some VOCs) vs. fugitive sources of natural gas (which contain VOCs but no NOx). Estimates of NO_x emissions based on the NOy/CH_4 regression slope also relies on the assumption that NOy is conserved which is not entirely true since NOy deposition is evident from the observed buildup of nitrates in the snow over time. It is interesting to note that results from inverse modeling with a micro-scale

[3] It should be noted that the large amount of NOx emitted from the Bonanza power plant is almost the same in both the top-down and bottom-up inventories used by Ahmadov et al. and is immaterial to this comparison as results from UBWOS 2013 showed that Bonanza emissions do not play a role in winter ozone episodes (SR2013).

chemical transport model for the morning of 26 January 2013 by Olaguer and Lefer (2014) indicate that the UDAQ NOx inventory is reasonably accurate, at least for the morning of 26 January and over the 20 km x 20 km modeling domain centered near Horsepool employed in the micro-scale modeling study. Obtaining a reasonably accurate bottom-up NOx inventory for the Uinta Basin should be achievable in the near future and will be greatly facilitated by data gathered under the new rules on minor source permits noted above. In contrast, VOC emissions from oil and gas exploration and production are dominated by hard to characterize fugitive sources and bottom-up VOC inventories have long been suspected of being underestimated in other western oil and gas basins (Pétron, et al., 2012, 2014; Stoeckenius and Ma, 2009).

An on-going series of exploratory investigations of VOC emissions from non-combustion sources in the Uinta Basin have been carried out by the Bingham Research Center (BRC). Investigations of emissions from produced water evaporation ponds were described in SR2013; analyses of formaldehyde and other aldehyde contamination of liquid methanol – which would be expected to contribute to total primary formaldehyde emissions associated with methanol use – and emissions of VOCs from the soil surface near wellheads were conducted by researchers at the BRC over the past year as described in Sec. 5. Formaldehyde contamination in methanol samples was found to correlate with age of the methanol sample, ranging from near zero in newly delivered methanol to more than 100 µg/mL in recovered methanol. This confirms that methanol use is a source of primary formaldehyde but additional data are needed to relate these findings to actual emission rates. BRC is currently working to develop a formaldehyde emissions inventory for the Basin which includes emissions from methanol use and other non-combustion sources.

BRC researchers also conducted some limited measurements of methane and non-methane hydrocarbon emissions from soil surfaces near wellheads using a dome shaped flux chamber placed on top of the soil (Figure 5-6). Measurements were conducted in the Uinta, Moab and Clay basins in Utah. Emission rates on the order of 1,000 mg/m^2 per hour were measured within 60 cm of a gas wellhead in Utah but the emissions fell off very rapidly with distance from the wellhead, dropping by a factor of nearly a million at a distance of 5 m. These results suggest gas leaks from well casings are contributing to hydrocarbon emissions in at least some locations but the limited data currently available are insufficient to provide a quantitative estimate of basin-wide soil emissions. Soil hydrocarbon emissions to the atmosphere were found to correlate with soil-gas measurements, i.e., measurements of gasses in the soil pore spaces. This finding is potentially useful as soil-gas measurements are more commonly collected than the surface flux chamber measurements.

Work on development of hydrocarbon emission estimates from non-combustion sources in the Uinta Basin is on-going: further results of measurements of evaporative pond emissions along

with measurements of emissions from land farms[4] are expected to be completed by BRC in 2015. In addition, UDAQ has funded USU to measure emissions from other non-combustion sources possibly including flowback ponds and other fracking-related sources, glycol dehydrators, three-phase separators, and storage tanks.

2.3.4 Meteorological and Air Quality Modeling

Several groups are actively engaged in the development of model applications to winter episodes in the Basin as detailed in Sec. 6. This work is still in its early stages and is contributing to a quantitative understanding of the interplay of factors underlying the winter episodes. In addition to providing useful diagnostic information, modeling systems (which consist of input data, model parameter settings and model codes for simulating meteorology and air quality) that are capable of faithfully simulating winter episode conditions are needed for the development of cost-effective emission control strategies and to quantify the air quality impacts of proposed new oil and gas developments in the Basin.

Models most commonly used to simulate ozone air quality in the U.S. include the WRF meteorological model and the CMAQ and CAMx photochemical grid models for simulating air quality conditions. CMAQ and CAMx use as input results from WRF to calculate the effects of meteorology on air quality. Alternatively, it is possible to use a "coupled" model such as WRF-Chem for simulating both meteorology and air quality simultaneously thus making it possible to account for the more subtle influence of air quality conditions on meteorology (e.g., the effects of aerosols on solar radiation). Development of modeling systems for the Uinta Basin winter ozone episodes is being actively pursued by several groups (Table 2-1). Summaries of these model applications are described in Sec. 6.

Table 2-1. Current modeling activities for Uinta Basin winter ozone episodes.

Organization	Model(s)	Winter period(s)	Published Reference
BLM (ARMS)	WRF, CMAQ, CAMx	2010-2011	AECOM, 2014
EPA	WRF, CMAQ	2010-2011, 2011-2012, 2012-2013	Unpublished (see Sec. 6)
USU	WRF, CMAQ, CAMx	2012-2013	Unpublished (see Sec. 6)
UU, UDAQ	WRF, CMAQ	2012-2013	Neeman et al. (2014)
NOAA	WRF-Chem	2011-2012, 2012-2013	Ahmadov et al. (2015)
NOAA	DSMACC Box Model	2012-2013	Edwards et al. (2014)

At this stage, researchers from each organization are comparing model predictions with available observations and gaining additional insight into mechanisms and factors controlling winter ozone formation by evaluating the sensitivity of predictions to key parameters such as precursor emission rates, surface albedo, rate at which ozone is deposited on the surface, etc. Results obtained to date confirm the central importance of snow cover and associated high

[4] Land farming refers to the process of treating drilling muds and other oily waste by spreading these materials out over a field and using various methods to promote biodegradation off the hydrocarbons by soil microorganisms (http://web.ead.anl.gov/dwm/techdesc/land/).

albedo as well as the sensitivity of ozone production to estimated levels of VOC and NOx emissions and VOC composition, especially with respect to the small but important fraction of VOCs accounted for by highly reactive aromatics and aldehydes.

2.3.4.1 Box Modeling

Because the models described above are complex and require significant computer time to run, researchers at NOAA are also applying "box" models that simply assume the atmosphere below the temperature inversion can be represented by a box within which the air is well mixed. Transport and mixing in the model were represented by a simple first-order parameterization occurring only during daytime, greatly reducing the computational burden. With box models, it is possible to focus on the effects of key variables reduced to a single dimension such as the amounts of incoming and reflected solar radiation, temperature, and atmospheric composition and chemistry, while rapidly obtaining results for many different combinations of model inputs. The reduced computational burden also makes it possible to use more complete chemical mechanisms in box models. Carter and Seinfeld (2012) and Nopmongcol et al. (2008) have described box modeling studies of winter ozone episodes in the Upper Green River.

A box model with a detailed chemical mechanism (the Dynamically Simple Model of Atmospheric Chemical Complexity or DSMACC) was applied to the Uinta Basin by Edwards et al. (2014) using data collected during UBWOS 2013 to directly or indirectly specify or "constrain" the model inputs. Results obtained by Edwards et al. clearly demonstrate the signature features of winter ozone episodes in the Basin and show what makes these winter episodes different from summer ozone episodes in large urban areas:

- A highly reflective snow surface which provides a total flux of UV radiation closer to that found in urban summer episodes and promotes formation of a shallow mixed layer in which pollutants are highly concentrated;
- High concentrations of VOCs dominated by alkanes associated with natural gas which oxidize to form carbonyls which in turn are photolyzed by the strong UV radiation to produce most of the radical species that drive ozone formation (in contrast to summer urban episodes where other sources of radicals are dominant);
- Low NOx concentrations relative to the high VOC levels result in a very efficient ozone formation, i.e., the ozone formation efficiency of each NOx molecule is optimized.

With regard to the last point, model results presented by Edwards et al. suggest that winter ozone is in the "NOx sensitive" regime in which even small NOx reductions will result in ozone reductions. VOC reductions are also calculated to result in ozone reductions although the marginal sensitivity to VOC under conditions observed in 2013 is small. While the above results contribute significantly to our understanding of winter ozone formation in the Basin, it is important to keep in mind that they are based on the specific conditions observed at Horsepool during 2013. This is particularly important with respect to drawing conclusions regarding the relative effectiveness of VOC and NOx controls. Emissions from sources associated with natural gas exploration and production dominate at Horsepool. Conditions, and therefore the sensitivity of ozone to changes in emissions, in other parts of the Basin are different as

demonstrated for example by the speciated VOC data collected at various locations within the Basin - including in areas dominated by oil production - during UBWOS 2013 (see SR2013). Validated photochemical grid models capable of replicated all of the key aspects of observed episode conditions in the Basin are needed to evaluate the effectiveness of alternative emission control strategies. Significant progress towards this goal has been made over the past year as described in the following sections.

2.3.4.2 Meteorological Modeling

Simulating the extremely stable meteorological conditions characterizing the cold pool events associated with winter ozone episodes is challenging due to the strong influence of very small-scale features (Holstag et al., 2013). Accurate modeling of snow cover remains a key challenge as spatial variations in snow cover can exert a significant influence on vertical stability, winds and temperature. Current high resolution WRF simulations specifically configured for winter conditions appear to capture the basic features of the cold pool but biases in predictions of surface temperature (too warm) and wind speeds (to windy) are still evident. These biases reflect deficiencies in the model's ability to replicate the extreme low level stability associated with cold pools.

NOAA's 4 km horizontal resolution simulations for 2013 reproduced the broad features of cold pool events, including the strong inversion and shallow boundary layer, but were not able to replicate the observed spatial and temporal variations in the boundary layer structure which strongly influence pollutant concentrations. These simulations were performed in an experimental mode for research purposes that did not include the assimilation of observations. Assimilation of observations is a commonly used technique to improve the accuracy of simulated meteorological fields intended for use in dispersion modeling.

Recent higher resolution (1.33 km) WRF simulations of February 2013 episodes conducted by UU with improved initialization of snow cover as developed by UU and methods of assimilating wind and temperature observations as used in the BLM study were successful in improving the representation of snow cover and reducing the temperature bias (Neeman et al., 2014). Sensitivity tests and diagnostic analyses performed by Neeman et al. indicate that simulation of cloud microphysics (the characterization of cloud water properties and interaction of cloud water and ice particles with the surrounding environment), exert a significant influence on the structure of the boundary layer during cold pool events. Additional model development work is needed to improve WRF cloud parameterizations under these conditions.

2.3.4.3 Photochemical Modeling

The recent improvements in WRF simulations of cold pool events described above open the door to development of reasonably accurate simulations of air quality associated with these events. The BLM, NOAA and UU/UDAQ modeling groups have been able to simulate significant ozone production under episode conditions. Large under prediction biases were seen in EPA's results and at least some if not most of this bias appears to be associated with inaccuracies in the emission inventories used to drive the models. Results from the BLM group are better but still show significant (as much as 40 ppb) under prediction bias for the daily peak ozone at the

height of both the mid-January and late February – early March 2011 episodes and do not capture the timing of the afternoon peak well (the predicted peak occurs too early in the day). Predicted overnight ozone minimums at Ouray are in the 20 – 30 ppb range during the episode and to not increase from day to day whereas observed levels do not fall below 40 ppb after the first episode day and increase from one day to the next. This means that even though the model is predicting morning ozone increases roughly consistent with observations, the resulting mid-day peaks fall far short of observed values.

USU's simulations used an inventory for 2013 derived from the BLM/ARMS bottom-up inventory. Similar to the BLM results for 2011, daily peak ozone predictions for the January 2013 episode showed a severe under prediction bias which appears to be at least partly due to predictions of overnight minimum ozone levels of around 20 ppb throughout the episode whereas observations show overnight minimum ozone which increase from day-to-day reaching ~ 60 ppb around 22-23 January (Figure 2-5). When an alternative VOC speciation profile with more formaldehyde was used in the model, the amount of ozone production during the morning more closely matched observed values but the severe overnight under prediction remains and afternoon peaks were still as much as ~ 50 ppb short of the observed peak values at the height of the episode (Figure 2-5).

UDAQ used UU's WRF simulations with the UDAQ inventory described in Sec. 5 to conduct CMAQ simulations of the 1- 7 February 2013 episode (see Neeman et al., 2014 and additional results presented in Sec. 6.4.4). Their results for this "base case" simulation show characteristics similar to that of the BLM and USU results described above: both daily mean ozone and the amplitude of the diurnal ozone cycle are uniformly under predicted at Roosevelt (which is somewhat removed from the major emission source regions). Where the emissions density is high (in this case at Horsepool), daily ozone peaks are under predicted despite reasonably large simulated morning ozone increases. The under prediction of ozone peaks is due to severe under prediction during the overnight low ozone periods and under prediction of the observed day-over-day ozone increases. A potentially important feature of the CMAQ results at Horsepool noted by Neeman et al. is that the predicted depth of the layer with ozone concentrations above 75 ppb at Horsepool is greater than observed. This suggests potential problems with the WRF simulated vertical structure of the boundary layer that may be contributing to the ozone under prediction.

Sensitivity simulations performed by UDAQ showed that using the top-down inventory developed by Ahmadov et al., 2015 instead of the bottom-up inventory, significantly reduced the degree of under prediction of afternoon ozone maxima (with greater improvement at Horsepool than at Ouray) and closely matched the observed overnight ozone minima (Figure 2-6, top row). The observed day-over-day ozone buildup at Horsepool was also seen in the model predictions when using the top-down inventory. Reduced NOx emissions in the top-down inventory was also found to eliminate the large over prediction of NOx concentrations at Horsepool when using the top-down inventory (based on simulations conducted by the UDAQ – see Ch. 6, Fig. 6-7) but the model was found to under predict NOy (see Ch. 6, Fig. 6-8). This suggests that there remain significant biases in the nitrate budget in the UDAQ simulation that

are not resolved by the reduction in NOx emissions. On the other hand, augmentation of the bottom-up inventory with a hypothetical constant source of formaldehyde sufficient to produce predicted formaldehyde concentrations roughly similar to observed levels at Horsepool also resulted in a significant reduction of the base-case ozone under prediction bias at both Horsepool and Ouray (Figure 2-6, bottom row). In this case, slightly better results were obtained at Ouray as compared to Horsepool. These results suggest that uncertainties in both emissions of highly reactive VOCs such as formaldehyde as well as in the overall magnitude of VOC emissions are potentially contributing to ozone prediction errors at comparable levels.[5] Additional analysis is needed to understand the implications of these results and guide improvements in emission inventories, as ambient formaldehyde and NOx concentrations represent the net result of a series of chemical reaction cycles and are therefore sensitive not just to emission rates but also to a variety of factors effecting the overall balance of chemical reaction rates.

WRF-Chem simulations conducted by NOAA (Ahmadov et al., 2015) are described in Sec. 5 with respect to information they provide regarding biases in the bottom-up emission inventory. Afternoon maximum predicted ozone at Horsepool for the late January – early February 2013 ozone episode using the top-down inventory in which VOC emissions are doubled and NOx emissions are reduced by 75% matched observed values more closely than in the base case simulations prepared by BLM, USU and UDAQ utilizing the bottom-up inventory. Nevertheless, overnight minimum concentrations were still widely under estimated. Ahmadov et al. indicate that the nighttime under prediction was associated with over estimation of the strength of katabatic winds (nighttime drainage flow), which brought relatively clean air from higher elevations west to the Horsepool site in the WRF-Chem simulation. It is useful to note that UDAQ's simulation using the top-down inventory was able to reproduce the overnight ozone minima reasonably well as shown in the top row of Figure 2-6.

Based on the modeling results summarized above, it appears that the current suite of photochemical grid models are able to generate ozone concentrations that match observed values at Horsepool and Ouray reasonably well when available bottom-up emission inventories are modified by increasing VOCs and reducing NOx to better reflect observed VOC and NOx concentrations. However, the validity of postulated increases in alkane and aromatic VOC emissions as compared to increases in emissions of formaldehyde and the appropriate combination of these VOC increases with reductions in the NOx inventory are not yet well established. Remaining uncertainties in emissions need to be reduced before the models can be used to understand the relative contributions of emitted pollutants to ozone formation. As noted above, the box modeling performed by Edwards et al. (2014), which is heavily constrained by the extensive observations collected at Horsepool in 2013, was able to capture all of the key features of the multi-day ozone episode time series fairly well, including the day-to-day increase in ozone. However, these box model results are specific to conditions at

[5] This conclusion is consistent with findings from the NOAA modeling study (Ahmadov et al., 2015) which found that emission of the more reactive aromatic VOCs contribute to elevated ozone concentrations nearly as much as emissions of the less reactive but much more abundant alkane species.

Horsepool during a single episode and cannot be used to develop or demonstrate the efficacy of an optimal emission reduction strategy for the whole Basin. In addition, they do not provide any information on relative rates of emissions from different sources of ozone precursors.

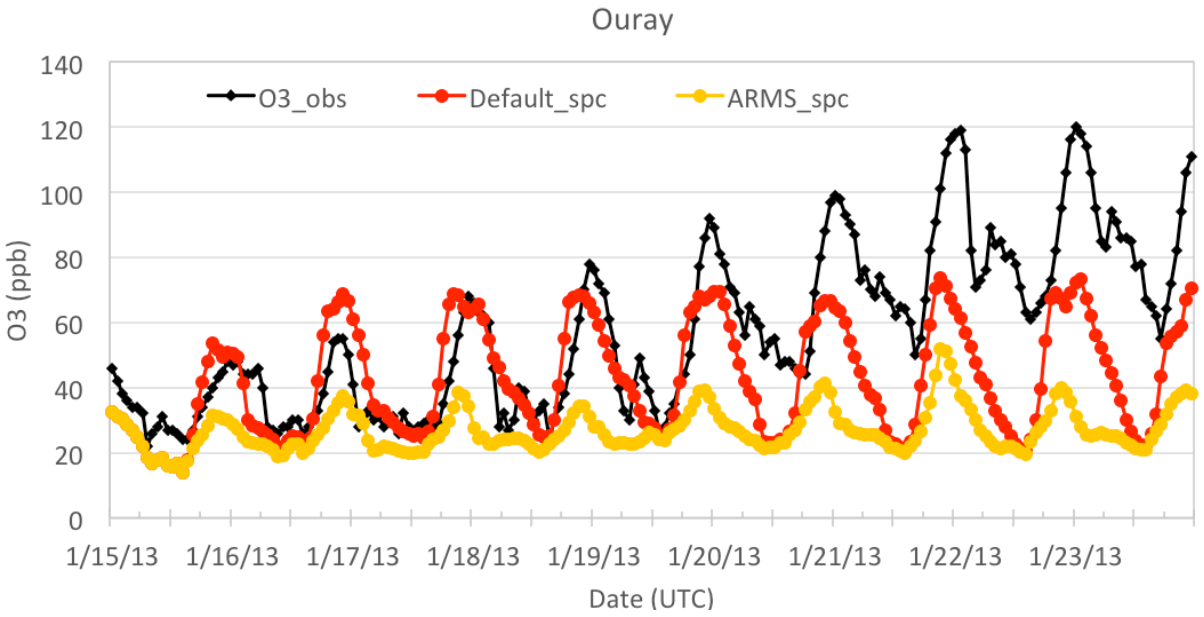

Figure 2-5. Temporal evolution of near-surface simulated (ARMS in yellow, REF in red) and observed (black) ozone concentration at Ouray from USU CAMx modeling (see Sec. 6).

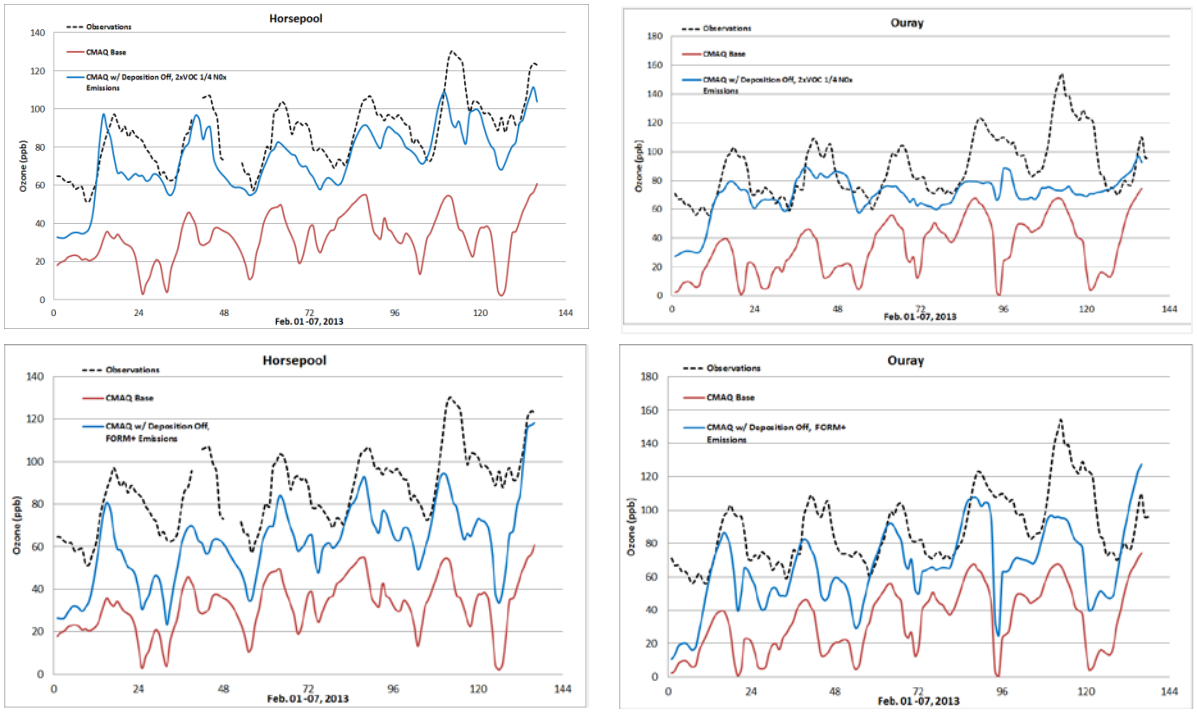

Figure 2-6. Observed (black dashed) and predicted ozone (ppb) time series at Horsepool (left) and Ouray (right) for UDAQ CMAQ Base case simulation using UDAQ bottom-up inventory (red in all panels), CMAQ using top-down inventory (blue in top row), and CMAQ using UDAQ inventory with additional formaldehyde source (blue in bottom row).

2.3.5 Recommendations

With completion of the third year of intensive measurements in the Uinta Basin, our understanding of the chemistry and meteorology of winter ozone episodes is now reasonably complete although additional research is needed to support development of accurate emission inventories and valid predictive models. On-going support is also needed to maintain long-term monitoring in the Basin. Recent work in emission inventory development and meteorological and air quality modeling of winter episode events has yielded important insights and derived additional value from the data that has been collected, e.g., the discrepancy between bottom-up VOC emissions estimates and top-down estimates derived from observations. Knowledge gaps remain in two main areas:

1. Lack of detailed measurements at locations other than Horsepool, in particular at locations in the western portion of the Basin where oil rather than gas production dominates.
2. Uncertainties in ozone precursor emission inventories.

VOC measurements made in the oil fields in western Basin locations during UBWOS 2012 and 2013 and by aircraft during UBWOS 2013 indicate a higher alkane/aromatic ratio and lower methane levels as compared to Horsepool. In contrast, mobile van VOC measurements made

during UBWOS 2012 indicated that oil well emissions were enhanced in heavier VOC species relative to gas well emissions, particularly in regard to aromatics. These results are not necessarily inconsistent given potential differences in exposures to different source types within the oil field but they do show that the VOC mixture and potentially VOC/NOx ratios are different in the oil field. Given this, there is concern that calculations of ozone sensitivity to VOC and NOx reductions based on Horsepool data may not apply at other locations within the Basin. Additional measurements are needed to compare radical sources in the western basin with those that have been collected at Horsepool and to provide data for model validation in the western Basin.

Results from current inventory development and modeling work described in this report point to the need for improvements in bottom-up inventories, particularly for VOC emissions although further development and evaluation of the NOx inventory is also needed as described above. The largest factor contributing to uncertainties in VOC emissions are lack of data on direct emissions of natural gas. This is a very difficult problem that is currently the focus of several research programs, including the NOAA SONGNEX study scheduled to begin in March 2015, which will provide additional top-down estimates for comparison with improved bottom-up inventories. Additional activity data and emission factor development is needed to quantify emissions from non-combustion primary formaldehyde sources such as methanol use, given the demonstrated sensitivity of ozone production to formaldehyde. Verification or development of VOC speciation profiles for different source types are also needed.

Additional refinement of meteorological modeling is needed to further reduce surface temperature and wind prediction biases. Continued work on photochemical modeling is also needed, although results obtained thus far suggest that the primary factors responsible for modeling errors in the current suite of results are inaccuracies in emission inventories, limitations in the ability to account for spatial and temporal variations in snow cover (both with respect to the bare ground surface and coverage of low-level vegetation), and errors in simulated near-surface meteorological conditions.

2.4 References

AECOM, 2014. Utah Air Resource Management Strategy Modeling Project: Air Quality Model Performance Evaluation. AECOM, Fort Collins, February.

Ahmadov, R., S. et al., 2015. Understanding high wintertime ozone pollution events in an oil and natural gas producing region of the western US. Atmos. Chem. Phys. 15, 411-429.

Carter, W.P. and J.H. Seinfeld, 2012. Winter ozone formation and VOC incremental reactivities in the Upper Green River Basin of Wyoming. Atmospheric Env. 50 (2012) 255-266.

Edwards, P.M. et al., High winter ozone pollution from carbonyl photolysis in an oil and gas basin. Nature, 514, 351–354 (16 October 2014) doi:10.1038/nature13767.

Grannas, A.M. et al.,. An overview of snow photochemistry: evidence, mechanisms and Impacts. Atmos. Chem. Phys., 7, 4329–4373, 2007.

Helmig, D., L. Ganzeveld, T. Butler, and S.J. Oltmans, 2007. The role of ozone atmosphere-snow gas exchange on polar, boundary-layer tropospheric ozone – a review and sensitivity analysis. Atmos. Chem. Phys., 7, 15-30.

Holstag, A. A. M. et al., 2013. Stable atmospheric boundary layers and diurnal cycles: challenges for weather and climate models. Bull. Amet. Soc., V94, N11, 1691-1706.

Koss, A.R., J. de Gouw, C. Warneke, J.B. Gilman, B.M. Lerner, M. Graus, B. Yuan, P. Edwards, S. Brown, R. Wild, J.M. Roberts, T.S. Bates, P.K. Quinn, 2015, Photochemical aging of volatile organic compounds associated with oil and natural gas extraction in the Uintah Basin, UT, during a wintertime ozone formation event, Atmos. Chem. Phys. Discuss. (in press). Olaguer, E.P. and B. Lefer, 2014. Measurement and modeling of ozone impacts of oil and gas acitivites in the Uinta Basin. Final Report, 9 October.

Li, X., et al., 2014. Missing Gas-Phase Source of HONO Inferred from Zeppelin Measurements in the Troposphere. Science, V344, N6181, 292-296, 18 April.

Lyman, S. and Shorthill, H., 2013. Final Report: 2012 Uintah Basin Winter Ozone & Air Quality Study. Doc. No. CRD13-320.32, Commercialization and Regional Development, Utah State University, 1 February (http://rd.usu.edu/files/uploads/ubos_2011-12_final_report.pdf).

Martin, R., K. Moore, M. Mansfield, S. Hill, K. Harper, and H. Shorthill, 2011. Final Report: Uinta Basin Winter Ozone and Air Quality Study, December 2010 – March 2011. EDL/11-039, Energy Dynamics Lab., Utah State University Research Foundation, Bingham Research Center, Vernal, Utah, 14 June.

Neeman, E.M., E. T. Crosman, J. D. Horel, and L. Avey, 2014. Simulations of a cold-air pool associated with elevated wintertime ozone in the Uintah Basin, Utah. Atmos. Chem. Phys. Discuss., 14, 15953-16000, doi:10.5194/acpd-14-15953-2014.

Nopmongcol, O., G. Yarwood, and T. Stoeckenius, 2008 Winter Ozone Box Model Study. Novato, CA: ENVIRON International Corp., 2010.

Pétron, G., et al., 2012. Hydrocarbon emissions characterization in the Colorado Front Range: A pilot study, J. Geophys. Res., 117, D04304, doi:10.1029/2011JD016360.

Petron, G., A. et al., 2014. A new look at methane and nonmethane hydrocarbon emissions from oil and natural gas operations in the Colorado Denver-Julesburg Basin. J. of Geophys. Res., 119 (11), 6836-6852, doi: 10.1002/2013JD021272

Stoeckenius, T. and L. Ma, 2009. A Conceptual Model of Winter Ozone Episodes in Southwest Wyoming. ENVIRON International Corp., Novato, CA, 26 October.

Stoeckenius, T. and D. McNally, 2014. 2013 Uinta Basin Winter Ozone Study. Till Stoeckenius and Dennis McNally, eds., ENVIRON International Corp., Novato, CA, March.

Stutz J., Oh H.-J., Whitlow S.I., Anderson C.H., Dibb J.E., Flynn J., Rappenglück B., Lefer B. (2010): Simultaneous DOAS and Mist-Chamber IC measurements of HONO in Houston, TX, Atmos. Environ., 44, 4090-4098, doi:10.1016/j.atmosenv.2009.02.003

VandenBoer, T.C., C.J. Young, R.K. Talukdar, M.Z. Markovic, S.S. Brown, J.M. Roberts and J.G. Murphy, 2014. Nocturnal loss and daytime source of nitrous acid through reactive uptake and displacement. Nature Geoscience, doi:10.1038/NGEO2298.

3.0 REVIEW OF METEOROLOGICAL AND AIR QUALITY CONDITIONS, WINTER 2013-14

Authors
Seth Lyman, Howard Shorthill
Bingham Entrepreneurship & Energy Research Center, Utah State University, Vernal, Utah

3.1 Introduction

Ozone concentrations have been measured continuously in the Uintah Basin since summer 2009. During winter 2009-10 ozone concentrations measured at Ouray and Red Wash exceeded the Environmental Protection Agency (EPA) standard. Following the discovery of this new phenomenon, stakeholder concern led to the establishment of several additional air quality monitoring stations to support subsequent studies. Seventeen stations operated around the Uintah Basin during winter 2010-11, 30 operated during winter 2011-12, and 20 during winter 2012-13. Martin et al. (2011), Lyman and Shorthill (2013), and Stoeckenius and McNally (2014) highlight the results of these studies. This section contains an analysis of ozone, precursor, and meteorology data from air quality monitoring sites that operated around the Basin during winter 2013-14, and an analysis of variability across the four years of available ozone data. In this chapter, "winter 2013-14," "winter," "winter season," or other similar phrases refer to the period from November 15 through March 15.

3.2 Methods

3.2.1 Ozone Measurements

During winter 2013-14, ten air quality monitoring stations were operated in the Uintah Basin by Utah State University (USU), and nine were operated by other organizations. Table 3-1 contains a list of all monitoring stations, including locations, elevations, and responsible operators. Data and methods used for stations operated by other organizations were obtained from EPA's AQS database (https://ofmext.epa.gov/AQDMRS/aqdmrs.html) or from http://airnowtech.org. We utilized 2B Technology Model 205 or 202 ozone monitors at most stations, but an Ecotech Model 9810 ozone analyzer and a Thermo 49i were used at the Horsepool and Rabbit Mountain sites, respectively. We performed calibration checks at all USU stations at least every other week using NIST-traceable ozone standards. Calibration checks passed if monitors reported in the range of ±5 ppb when exposed to 0 ppb ozone, and if monitors were within ±7% deviation from expected values when exposed to higher concentrations of ozone. We only included data bracketed by successful calibration checks in the final dataset.

Table 3-1. Air quality monitoring stations, winter 2013-14. All stations monitored at least ozone and meteorology. Stations that measured VOC, NO_x, and/or $PM_{2.5}$ are indicated. NO_2* signifies NO_2 measured with a photolytic NO_2 (rather than molybdenum) converter.

Site Name	Operator	Data Holder	Lat	Long	Elev (m)	VOC	NO_x and $PM_{2.5}$
Duchesne	USU	USU	40.162	-110.401	1682	N/A	N/A
Pine Spring	USU	USU	39.580	-109.412	2186	N/A	N/A
Mtn. Home	USU	USU	40.432	-110.382	2234	N/A	N/A
Seep Ridge	USU	USU	39.754	-109.546	1975	N/A	N/A
Seven Sisters	USU	USU	39.981	-109.345	1618	N/A	N/A
Castle Peak	USU	USU	40.051	-110.020	1605	N/A	NO, NO_2
Wildhorse	USU	USU	39.861	-109.810	1740	N/A	N/A
Sand Wash	USU	USU	39.839	-109.915	1416	N/A	N/A
Rabbit Mtn.	USU	USU	39.869	-109.097	1879	N/A	NO, NO_2, $PM_{2.5}$
Dinosaur NM	NPS	AQS dbase	40.437	-109.305	1463	N/A	N/A
Red Wash	EPA/Golder	airnowtech	40.204	-109.352	1689	N/A	NO, NO2, $PM_{2.5}$
Vernal	UDAQ	airnowtech	40.453	-109.510	1606	N/A	NO, NO_2, $PM_{2.5}$
Whiterocks	Ute Tribe/STI	airnowtech	40.469	-109.930	1841	N/A	NO, NO_2
Ouray	EPA/Golder	airnowtech	40.055	-109.688	1464	N/A	NO, NO_2, $PM_{2.5}$
Roosevelt	UDAQ/USU	airnowtech	40.294	-110.009	1587	C2-C12	NO, NO_2, NO_2*, NO_y, $PM_{2.5}$
Myton	Ute Tribe/STI	airnowtech	40.195	-110.062	1550	N/A	NO, NO_2
Fruitland	UDAQ	airnowtech	40.209	-110.840	2021	N/A	NO, NO_2
Horsepool	USU	USU	40.144	-109.467	1569	C2-C12	NO, NO_2*, NO_y, $PM_{2.5}$
Rangely	NPS/BLM	AQS dbase	40.087	-108.762	1648	N/A	NO, NO_2

3.2.2 Ozone Precursor Measurements

We measured NO, true NO_2 (via a photolytic converter), and NO_y (sum of NO, NO_2, and other reactive nitrogen compounds) at Roosevelt and Horsepool with AQD/Teledyne-API and Ecotech systems, respectively, and calibrated the systems weekly with NO standards, monthly with NO_2 standards via gas phase titration, and once during the campaign with nitric acid and n-butyl nitrate permeation tubes to calibrate for NO_y (the sum of NO_x and other reactive nitrogen compounds). All sites operated by other organizations measured NO and NO_2 via a molybdenum converter-based system, a method known to bias NO_2 and NO_x results high due to NO_y interference.

We measured 57 ozone-forming nonmethane hydrocarbons (NMHC) in 30-minute and hourly samples at Horsepool and Roosevelt, respectively, during January and February. NMHC were analyzed by sample concentration on activated carbon traps, followed by desorption into automated gas chromatography-flame ionization detection systems. We calibrated these systems every week with certified gas standards. EPA C2-C12 PAMS compounds (EPA, 2003) were measured by the automated systems at Horsepool and Roosevelt.

3.2.3 Particulate Matter Measurements

We measured particulate matter with diameter smaller than 2.5 micrometers ($PM_{2.5}$) at Horsepool and Rabbit Mountain with BAM 1020 monitors. Instruments were operated according to manufacturer protocols, with leak checks, flow calibrations, and cleanings

performed at regular intervals. Particulate matter values from other sites were extracted from the EPA AQS database (https://ofmext.epa.gov/AQDMRS/aqdmrs.html).

3.2.4 Meteorological Measurements

We deployed solar radiation sensors at Horsepool (incoming and outgoing short wave, long wave, UV-A, and UV-B radiation) and at Roosevelt (incoming and outgoing shortwave radiation). We operated a suite of comprehensive, research grade meteorological instruments at Horsepool, and more cost-effective instruments (Davis VantagePro) at other sites. We also obtained shared meteorological data from the EPA AQS database and mesowest.utah.edu. We checked wind speed and direction, temperature, and humidity against a calibration standard once during the campaign. We check radiation measurements against calibration standards once every three years.

3.3 Results and Discussion

3.3.1 Ozone

In early December, a large weather event brought snow to the Uintah Basin, with accumulations heavier on the east side than on the west (Figure 3-1). Though little additional snow fell the rest of the winter, this single event was adequate to produce inversions, increase albedo, and thus help generate a number of ozone episodes (Figure 3-2). As winter matured, the snow gradually melted, eroding ground surface reflectivity and reducing the number and duration of ozone episodes. By 15 February, no snow remained and no more ozone episodes were observed.

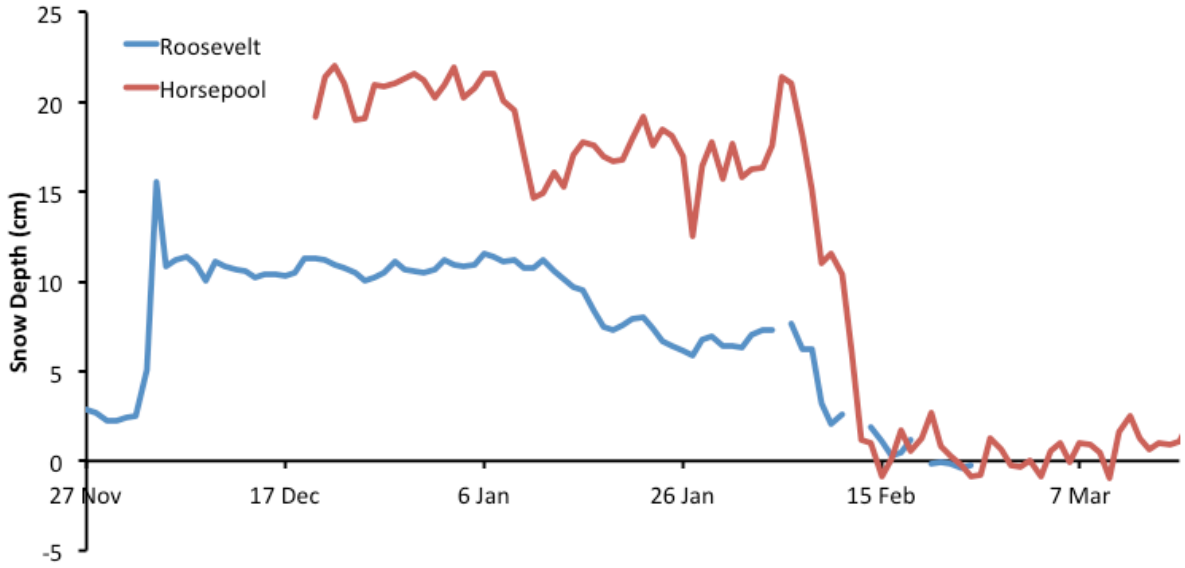

Figure 3-1. Snow depth time series at Roosevelt and Horsepool, winter 2013-14.

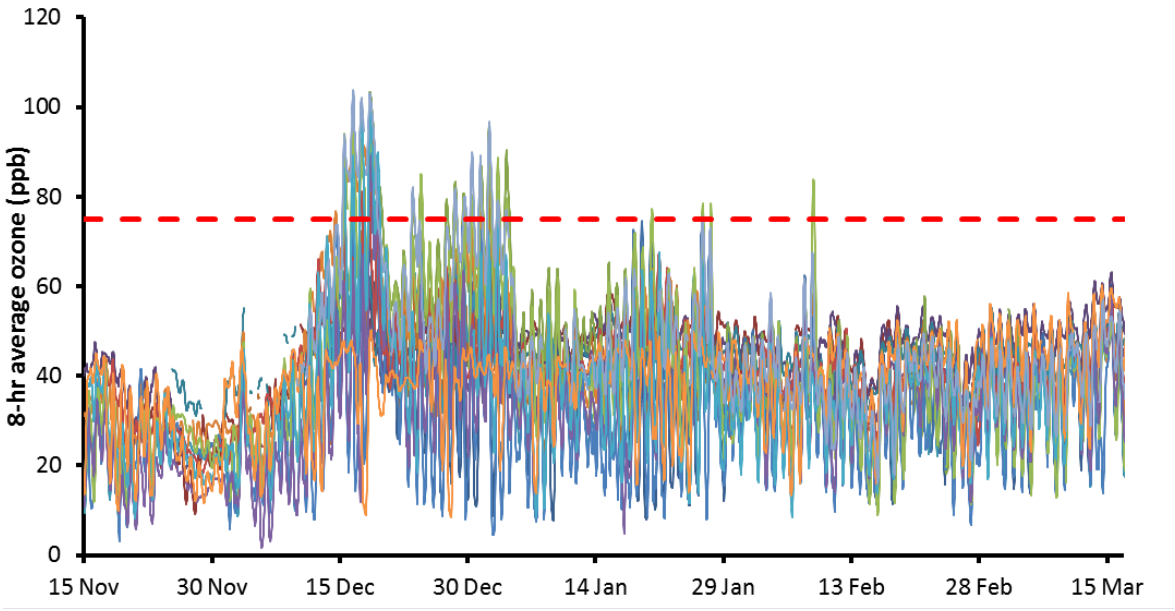

Figure 3-2. Time series of 8-hour average ozone concentrations at all monitoring sites in the Uintah Basin, winter 2013-14. Current EPA ozone standard level (75 ppb) is shown as a red dashed line.

Because the extent of snow cover and thus the average albedo of the Basin decreased as winter advanced, the highest ozone days were all observed in December, with only a few isolated exceedance days at six sites during January and February (Figure 3-2, Table 3-2). The season's first exceedance day occurred on 14 December, the earliest observed exceedance in five consecutive years of monitoring in the Uintah Basin. Previous winters likely lacked either adequate snow cover or adequate multi-day episodes with stagnant winds and high barometric pressure this early in the season. High ozone was observed during a brief episode in December 2009.

Total daytime UV radiation during mid-December 2013 was similar to UV radiation observed during winter ozone episodes in January 2013 (Figure 3-3; Stoeckenius and McNally, 2014), confirming that adequate UV radiation existed in December 2013 to facilitate production of the observed ozone. As the season matured, we observed a steady decline in UV albedo, save for a small blip on the first of February when a light snow accumulated briefly (Figure 3-3). As with winter 2012-13 (and each winter previously studied by USU), ozone production in the Uintah Basin during winter 2013-14 was dependent on snow cover.

Table 3-2. 8-hour average ozone concentrations around the Uintah Basin, winter 2013-14.

Site Name	Mean	Max	Min	Overall Daily Max*	Overall Exceedances	Jan - Mar Daily Max*	Jan - Mar Exceedances
Duchesne	37.5	77.3	7.8	63.8	1	62.3	0
Pine Spring	44.4	58.3	9.1	57.0	0	56.9	0
Mtn. Home	47.8	64.5	19.1	63.3	0	63.3	0
Seep Ridge	46.7	64.6	26.7	63.3	0	59.7	0
Seven Sisters	43.1	88.2	18.5	80.7	4	67.7	1
Castle Peak	40.6	74.7	20.1	72.2	0	72.2	0
Wildhorse	53.4	97.0	30.2	87.8	17	80.1	7
Sand Wash	47.6	103.4	14.8	90.4	10	70.1	2
Rabbit Mtn.	41.8	64.2	21.4	59.5	0	54.8	0
Dinosaur NM	38.0	91.4	6.3	80.6	5	57.5	0
Red Wash	43.4	97.9	18.6	89.0	7	62.4	0
Vernal	30.1	79.9	3.1	73.4	3	55.3	0
Whiterocks	42.5	81.3	18.3	67.3	3	62.3	0
Ouray	40.9	95.6	8.8	92.8	17	79.8	7
Roosevelt	32.6	89.3	1.6	65.5	2	58.3	0
Myton	36.1	101.0	8.1	89.3	6	67.0	1
Fruitland	38.2	60.4	8.4	58.4	0	58.4	0
Horsepool	48.5	103.8	16.3	96.8	13	75.7	3
Rangely	35.0	72.0	9.0	68.0	0	53.0	0

* Fourth highest daily maximum.

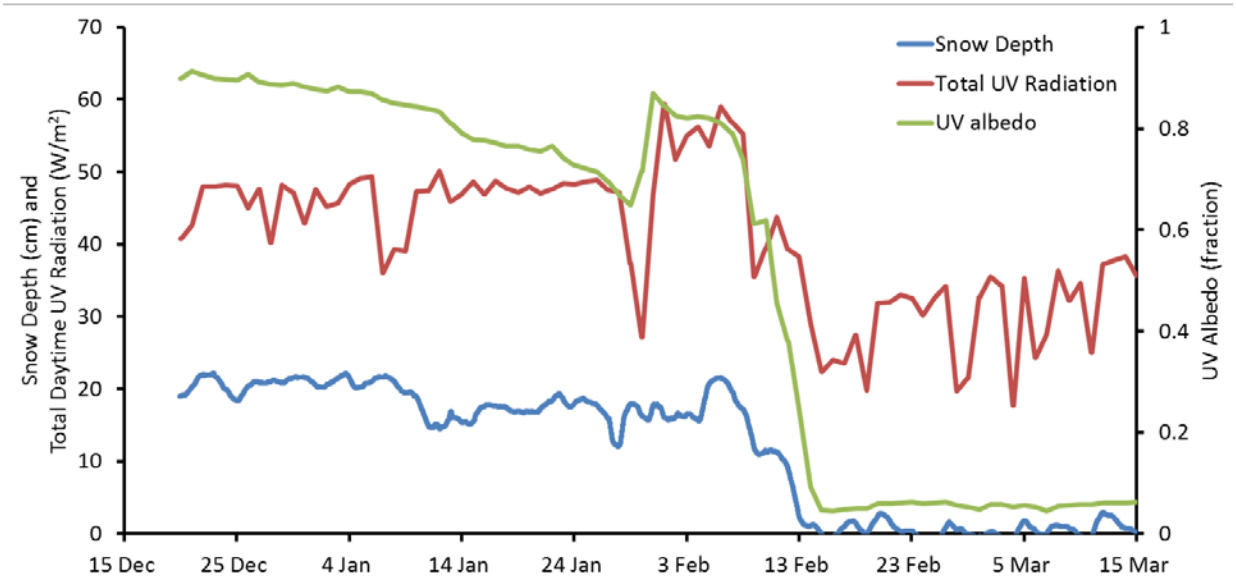

Figure 3-3. Time series of snow depth, average total daytime UV radiation (sum of upwelling and downwelling UV-A and UV-B), and average of UV-A and UV-B albedo at Horsepool, winter 2013-14.

Fewer sites exceeded the EPA standard of 75 ppb (Figure 3-4) than during winter 2012-13 (Figure 3-5), and the fourth-highest daily maximum 8-hour ozone concentrations were much lower. The previous winter's uniform snow cover and longer, more numerous inversion episodes likely account for the differences. During winter 2012-13, for example, one inversion episode lasted as long as 15 days, allowing the inversion conditions to spread across a much larger area of the Basin than had been observed in other winters.

During winter 2013-14, the longest inversion episode was nine days. This episode, which peaked on 18 December, led to a fairly broad spatial distribution of sites observing ozone exceedances (Figure 3-6). In contrast, an inversion episode that culminated on 8 February lasted only two days, and ozone above background concentrations was observed only at Ouray and Horsepool (Figure 3-7). Similarly, late-season ozone episodes during winter 2012-13 were short and confined to the center of the Basin, while early-season episodes tended to last much longer and have a broader spatial distribution (Stoeckenius and McNally, 2014).

Although the 2013-14 ozone season was from 15 December to 10 February and the 2012-13 season from 15 January to 5 March, both exhibited the same characteristics during early and late season episodes. Each observed rapidly decreasing snow cover by season's end, and it seems likely that the limited snow cover was the reason for the shorter and more spatially confined ozone episodes. As in previous years, the highest ozone was observed at sites with lowest elevation, likely because lower elevation sites experience more and longer inversion episodes (Figure 3-8).

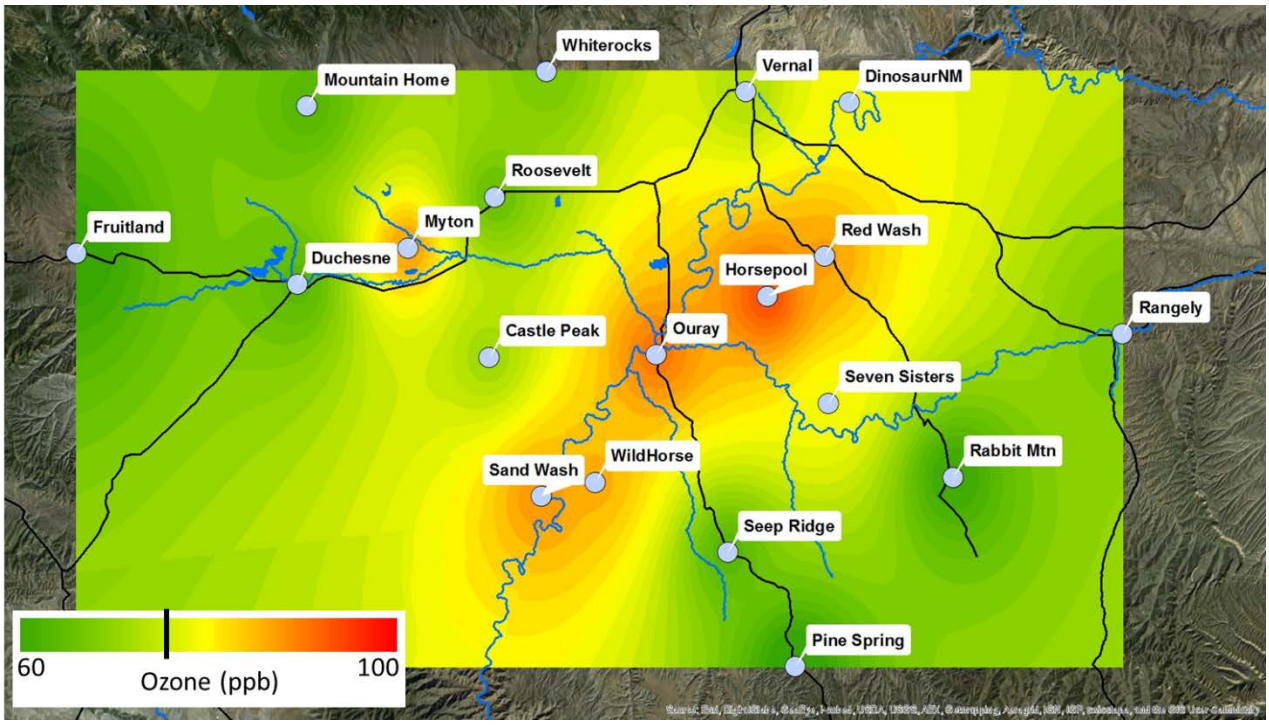

Figure 3-4. Fourth-highest daily maximum 8-hour average ozone concentrations for all sites in the Uintah Basin, winter 2013-14. The black line on the color scale indicates 75 ppb.

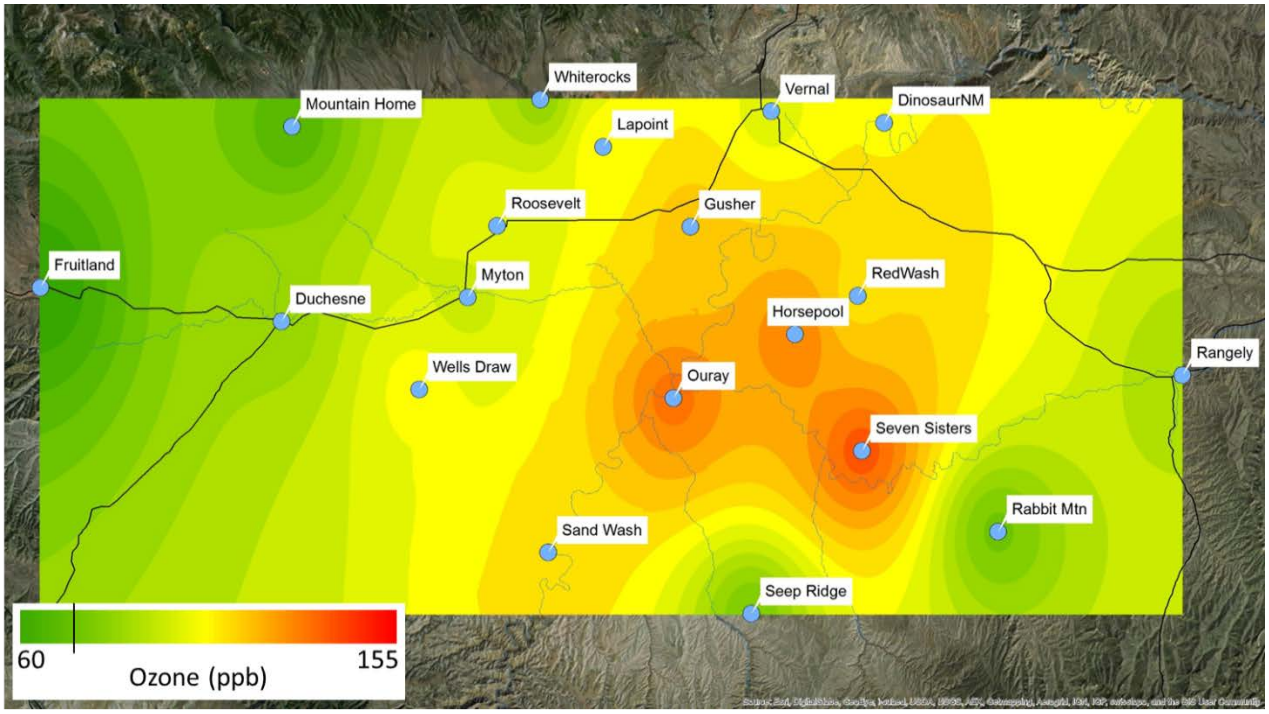

Figure 3-5. Fourth-highest daily maximum 8-hour average ozone concentrations for all sites in the Uintah Basin, winter 2012-13. The black line on the color scale indicates 75 ppb. Note change in color scale from Figure 3-4.

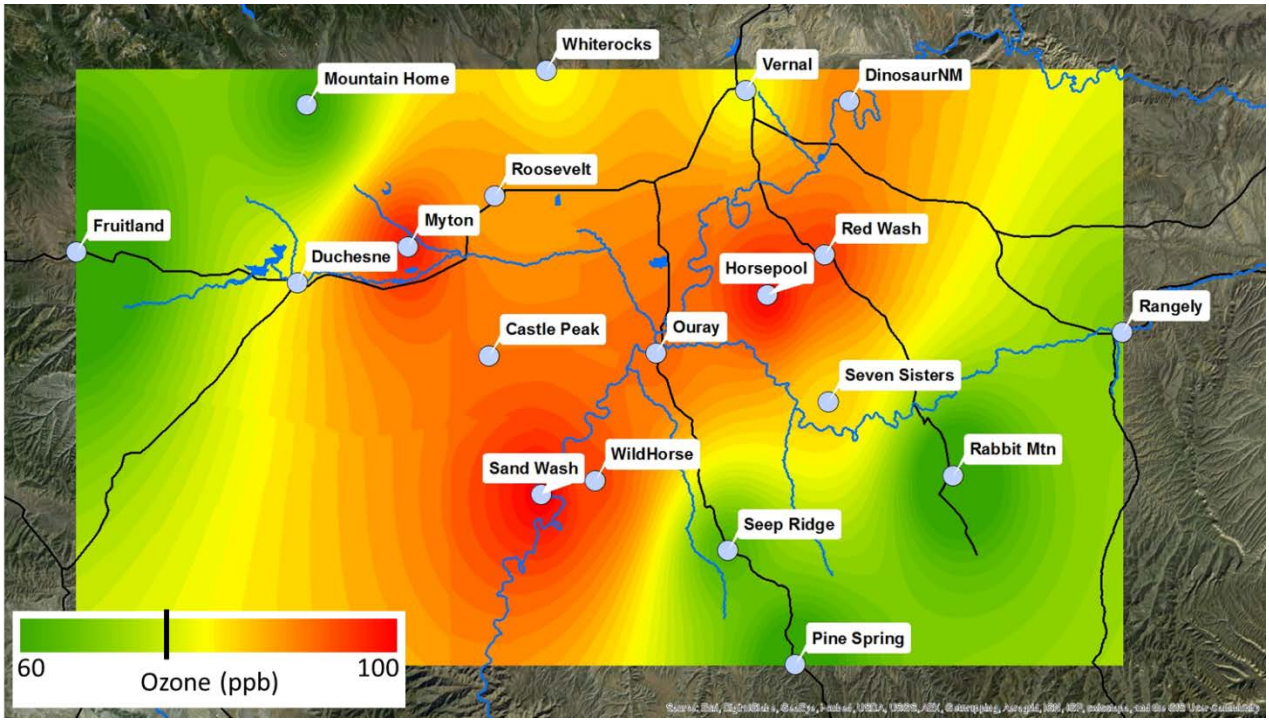

Figure 3-6. Daily maximum 8-hour average ozone concentrations for all sites in the Uintah Basin, 18 December 2013. The black line on the color scale indicates 75 ppb.

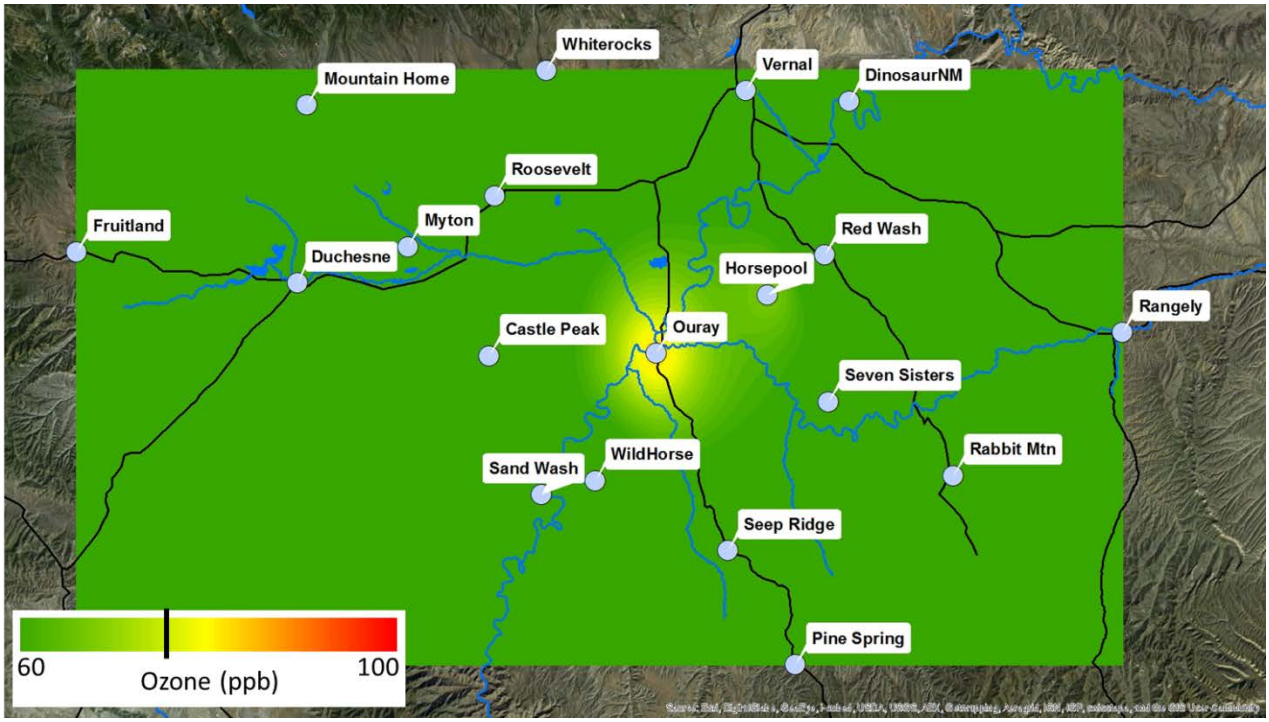

Figure 3-7 Daily maximum 8-hour average ozone concentrations for all sites in the Uintah Basin, 8 February 2014. The black line on the color scale indicates 75 ppb.

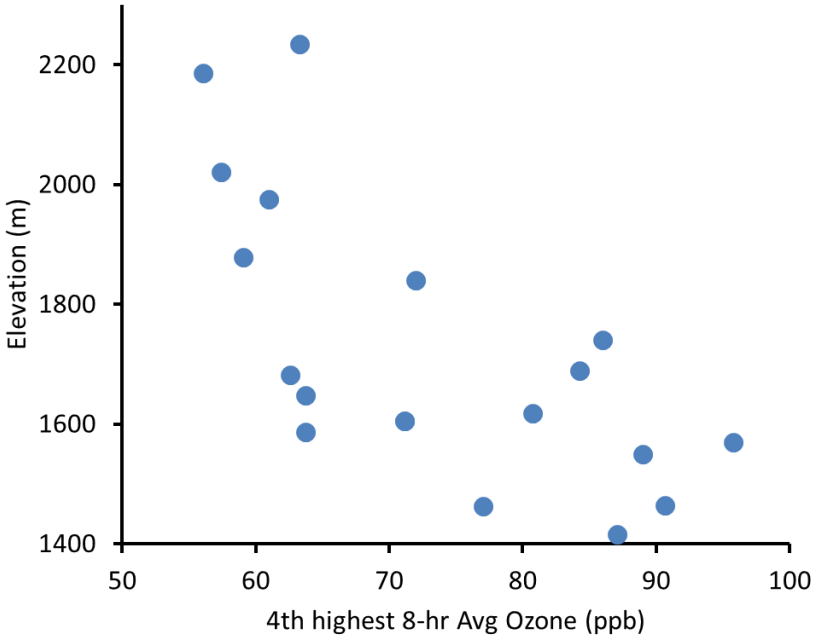

Figure 3-8. Fourth-highest daily maximum 8-hour average ozone versus site elevation for all sites in the Uintah Basin, winter 2013-14.

Figure 3-9 shows a time series of ozone concentrations at several sites in the Uintah Basin from July 2009 through 15 March, 2014. The Ouray and Red Wash air quality monitoring stations began operation in July 2009. During winter 2009-10, both sites experienced multiple exceedances of the level of the EPA ozone standard (75 ppb). Subsequently, monitors in Roosevelt, Vernal, and Rangely were added. As Figure 3-9 shows, exceedances of the ozone standard have been observed during four of the five winters in the Uintah Basin for which continuous ozone monitoring data is available.

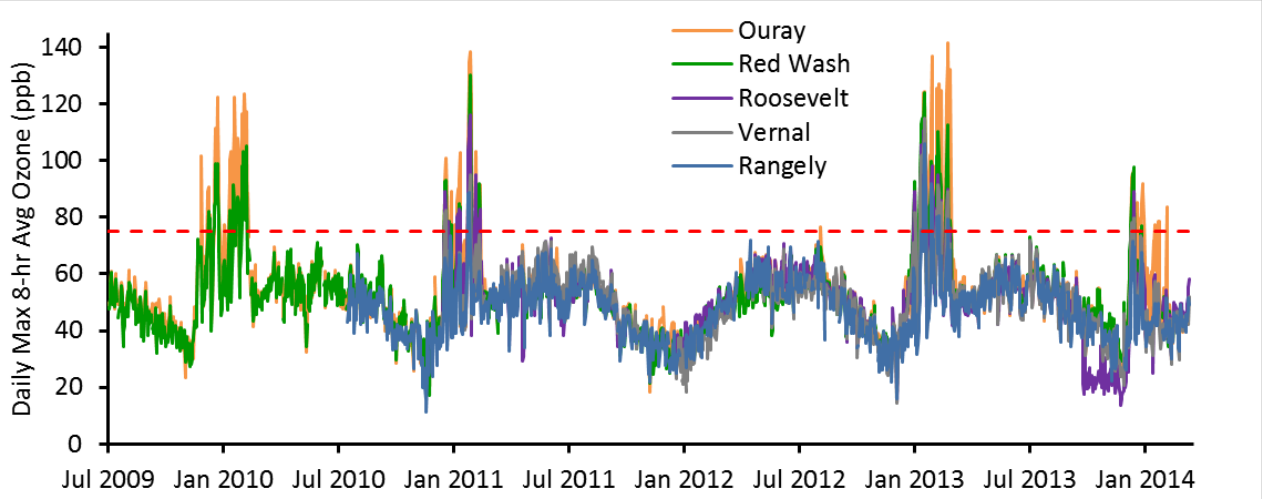

Figure 3-9. Time series of daily maximum 8-hour average ozone concentration at five sites in the Uintah Basin, July 2009-March 2014. The red dashed line shows 75 ppb, the EPA NAAQS for ozone.

Table 3-3 summarizes ozone statistics from the five sites shown in Figure 3-9 for each of the years that data are available. Data are organized by calendar year rather than by winter season since summertime exceedances have also occurred (albeit rarely) and since a nonattainment designation, if made by EPA, will be based on the average of the annual fourth highest daily maximum 8-hour average concentration averaged over three consecutive calendar years (i.e., the "ozone design value").

Table 3-3. Ozone summary statistics for five sites in the Uintah Basin over six calendar years. All values were calculated from daily maximum 8-hour average concentrations.

Year	Site	Mean	Median	Max	Min	4th High Daily Max	Exceedance Days
2009	Ouray	47.2	47.9	101.5	23.4	67.4	1
	Red Wash	44.8	43.7	72.3	27.3	67.6	0
	Vernal	--	--	--	--	--	--
	Roosevelt	--	--	--	--	--	--
	Rangely	--	--	--	--	--	--
2010	Ouray	56.7	54.5	123.6	20.3	117.3	40
	Red Wash	54.4	53.6	105.4	17.0	98.9	30
	Vernal	--	--	--	--	--	--
	Roosevelt	--	--	--	--	--	--
	Rangely	42.3	42.2	67.2	11.1	58.8	0
2011	Ouray	54.0	52.8	138.6	18.1	119.6	24
	Red Wash	51.6	51.8	130.2	21.3	98.3	21
	Vernal	55.5	55.6	95.1	33.1	84.9	7
	Roosevelt	56.2	54.7	116.3	29.3	103.6	19
	Rangely	48.6	50.0	88.6	21.9	73.4	3
2012	Ouray	49.3	50.5	76.5	18.8	67.6	1
	Red Wash	47.5	48.8	69.5	21.5	66.4	0
	Vernal	45.7	46.8	68.9	14.5	64.8	0
	Roosevelt	50.3	51.6	70.9	14.6	67.0	0
	Rangely	46.7	47.4	71.9	15.9	69.6	0
2013	Ouray	58.3	54.6	141.6	24.0	132.4	49
	Red Wash	57.8	54.8	124.0	29.0	114.0	44
	Vernal	53.2	52.9	114.9	20.5	102.1	25
	Roosevelt	50.5	51.8	110.8	13.6	104.0	31
	Rangely	50.8	50.7	106.1	22.3	91.0	11
2014 through Mar 31	Ouray	52.1	47.0	91.9	28.5	79.8	7
	Red Wash	43.4	43.6	52.6	30.5	50.5	0
	Vernal	42.3	42.6	57.5	28.0	54.3	0
	Roosevelt	45.3	45.0	63.8	25.0	58.3	0
	Rangely	42.4	42.3	51.8	30.0	49.7	0

3.3.2 Particulate Matter

As has been typical in previous years, $PM_{2.5}$ concentrations in Vernal tended to be higher than at other $PM_{2.5}$ measurement sites that operated during winter 2013-14 (Figure 3-10). Roosevelt $PM_{2.5}$ concentrations also tended to be higher than unpopulated areas with little urban source emissions. As noted above, however, the incomplete snow cover experienced during winter 2013-14 limited pollution-forming inversion conditions in the lowest parts of the Basin, especially after 1 January (see discussion above). As a result, more relatively high $PM_{2.5}$ days occurred in Ouray (though none exceeded the EPA standard) than were experienced at other sites. The 98th percentile of 24-h average $PM_{2.5}$ values (the EPA NAAQS metric for verifying annual compliance with the $PM_{2.5}$ standard), therefore, was slightly higher for Ouray than for Vernal and Roosevelt, even though Vernal experienced a higher maximum concentration for the winter. The map in Figure 3-11 shows higher 98th percentile $PM_{2.5}$ on the west side of the

Basin than the east, but this is likely due to poor spatial coverage of $PM_{2.5}$ measurements in the Basin. In reality, non-urban locations in the western Basin at higher elevation than Ouray likely experienced lower $PM_{2.5}$ than was observed in Ouray, Vernal, and Roosevelt.

Summertime 24-hour $PM_{2.5}$ concentrations exceeding the level of the NAAQS (35 µg/m^3) were observed in the Uintah Basin during summer 2012 (Figure 3-10). These and certain other summertime spikes in $PM_{2.5}$ concentrations have likely been due to wildfire smoke. A number of local and regional wildfires were active during summer 2012.

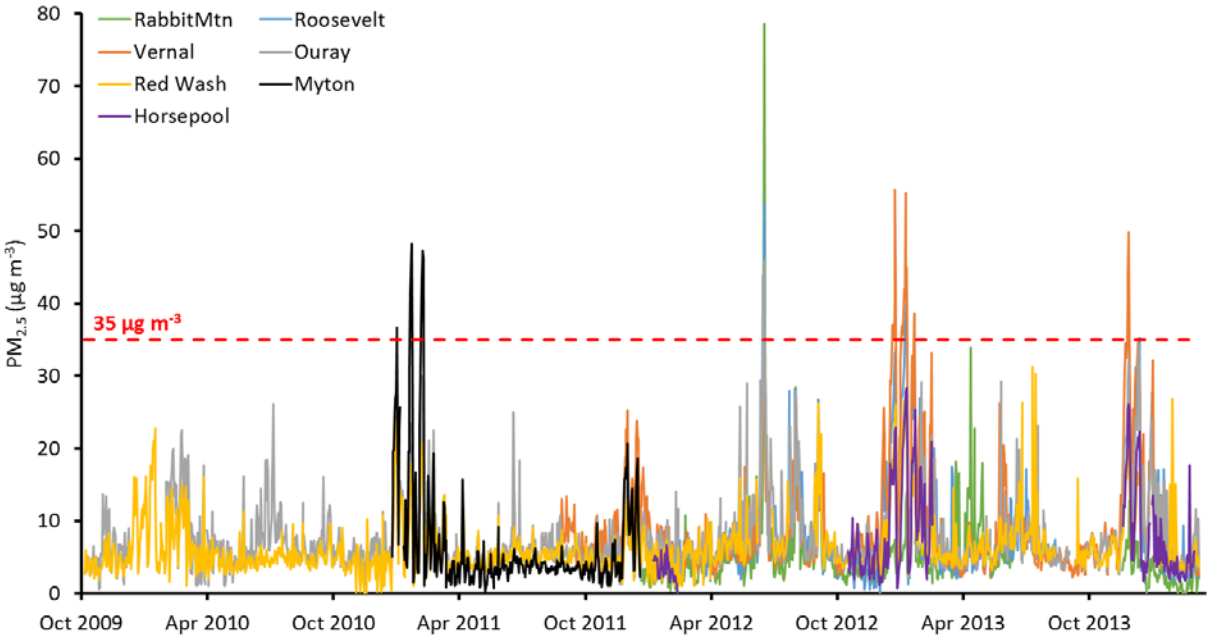

Figure 3-10. Time series of daily 24-hour average $PM_{2.5}$ concentrations at five sites in the Uintah Basin, October 2009-March 2014. The red dashed line shows 35 µg m^{-3}, the EPA standard for $PM_{2.5}$.

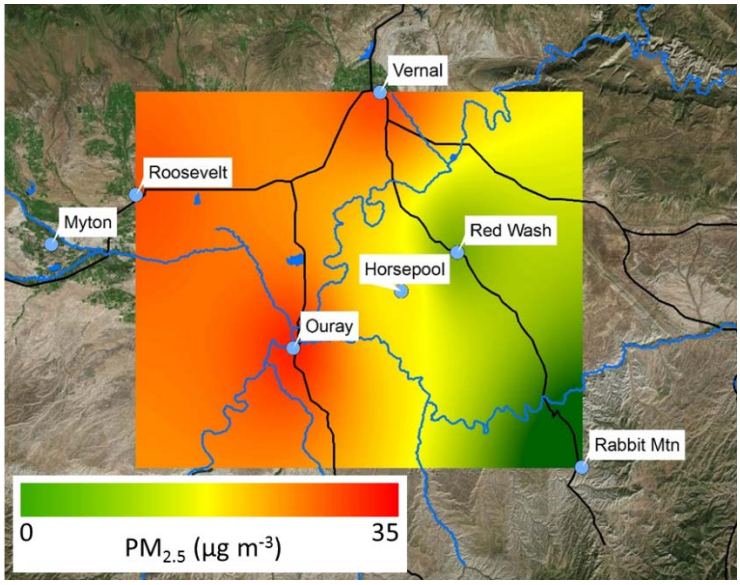

Figure 3-11. 98th percentile of 24-hour average $PM_{2.5}$ concentrations for all sites in the Uintah Basin, winter 2013-14.

$PM_{2.5}$ values in Vernal and Roosevelt have exceeded the level of the NAAQS during two of the three winters during which continuous measurements have been collected, and exceedances were also measured at Myton during winter 2010-11. However, no wintertime $PM_{2.5}$ exceedances have been observed distant from urban areas (Figure 3-10). While $PM_{2.5}$ increases at all sites during winter inversion episodes, and while those values can be near EPA standards, urban sources (which might include wood smoke, traffic-related emissions, or other sources) are apparently required to bring values in the Basin above EPA standards, at least at the present. Table 3-4 is a summary of $PM_{2.5}$ values at sites around the Uintah Basin from 2010 through March 2014.

Table 3-4. $PM_{2.5}$ summary statistics for the Uintah Basin over five calendar years. All values shown were calculated from daily 24-hour average concentrations.

Year	Site	Winter Mean	Winter Median	Winter Max	Winter Min	Annual # of Exceedance Days	Annual 98th Percentile Value
2010	Roosevelt	--	--	--	--	--	--
	Vernal	--	--	--	--	--	--
	Ouray	8.8	5.2	22.5	0.0	0	19.0
	Red Wash	7.2	5.8	22.7	0.0	0	16.0
	Myton	--	--	--	--	--	--
	Rabbit Mtn	--	--	--	--	--	--
	Horsepool	--	--	--	--	--	--
2011	Roosevelt	--	--	--	--	--	--
	Vernal	--	--	--	--	--	--
	Ouray	9.8	8.6	29.9	1.1	0	22.5
	Red Wash	7.8	6.5	23.6	1.0	0	17.7
	Myton	11.8	6.9	48.1	0.0	8	36.7
	Rabbit Mtn	--	--	--	--	--	--
	Horsepool	--	--	--	--	--	--
2012	Roosevelt	5.6	2.7	22.2	0.0	3	28.2
	Vernal	7.9	7.1	25.6	1.2	0	22.0
	Ouray	6.1	5.9	13.9	1.2	3	27.4
	Red Wash	4.8	4.4	10.6	0.0	0	15.9
	Myton	--	--	--	--	--	--
	Rabbit Mtn	2.7	2.5	10.7	0.0	4	20.2
	Horsepool	3.9	2.5	10.7	0.0	0	10.3
2013	Roosevelt	18.6	12.1	41.7	0.0	5	35.1
	Vernal	19.9	15.4	55.7	2.6	18	42.1
	Ouray	13.3	11.5	32.0	2.2	0	26.5
	Red Wash	10.8	8	26.6	3.0	0	25.9
	Myton	--	--	--	--	--	--
	Rabbit Mtn	4.9	3.7	13.9	0.0	0	18.0
	Horsepool	13.6	8.4	28.3	0.0	0	27.8
2014 through Mar 31	Roosevelt	8.1	4.1	35.3	0.0	1	29.8
	Vernal	9.5	6.6	32.1	2.2	0	30.3
	Ouray	9.2	6.8	34.3	2.3	0	31.5
	Red Wash	5.9	3.4	26.8	0.0	0	15.0
	Myton	--	--	--	--	--	--
	Rabbit Mtn	2.0	1.5	5.0	0.0	0	5.0
	Horsepool	5.5	4.0	22.3	0.0	0	21.5

3.3.3 Reactive Nitrogen

In *Final Report: 2013 Uinta Basin Winter Ozone Study* (Stoeckenius and McNally, 2014), we showed that NO_2 measurements at regulatory monitoring stations do not reflect true NO_2 values. NO_x measurements at these stations use molybdenum oxide catalysts to convert NO_2 to NO. Because the catalysts also convert other reactive nitrogen compounds (e.g., nitric acid, nitrous acid, peroxyacetyl nitrate, etc.) to NO, and because concentrations of these other compounds tend to be greater than concentrations of NO_2, NO_2 and NO_x values measured at regulatory monitoring stations are biased high. The ratio of NO_2 to other reactive nitrogen

compounds is likely to vary from site to site, so estimating true NO_2 concentrations (and true NO_x concentrations) from measured NO_2 values is problematic. NO values at regulatory monitors are not biased.

This section only discusses reactive nitrogen data collected by USU from Roosevelt and Horsepool. These sites have NO_x monitors that utilize photolytic NO_2 converters that do not suffer from the NO_y bias to which molybdenum oxide converters are subject. During winter 2013-14, as observed in previous years, NO_x was consistently higher at Roosevelt (11.5 [mean] ± 12.1 ppb [st. deviation]) than at Horsepool (5.1 ± 3.9 ppb), with more variability and a higher average for the season (Figure 3-12). The difference is likely due to urban NO_x sources that are more abundant in Roosevelt. Figure 3-13 shows that NO_y likewise was more abundant at Roosevelt (14.6 ±14.0) than at Horsepool (9.7 ± 8.4).

The difference between NO_y and NO_x, often termed NO_z, is a measure of the amount of non-NO_x reactive nitrogen in the atmosphere. NO_z is made up of nitric acid, nitrous acid, peroxyacetyl nitrate, and other byproducts and end products of the photochemistry that also produces ozone. NO_z concentrations at the two sites were similar (8.0 ± 6.7 at Roosevelt, 9.7 ± 8.4 at Horsepool), indicating similar levels of photochemical activity at the two sites (Figure 3-14).

NO_z concentrations dropped after the first of the year at both sites (Figure 3-14), coinciding with the end of significant ozone production. NO_x concentrations were not appreciably different between periods with ozone production and periods without (Figure 3-12), as has been observed in other years.

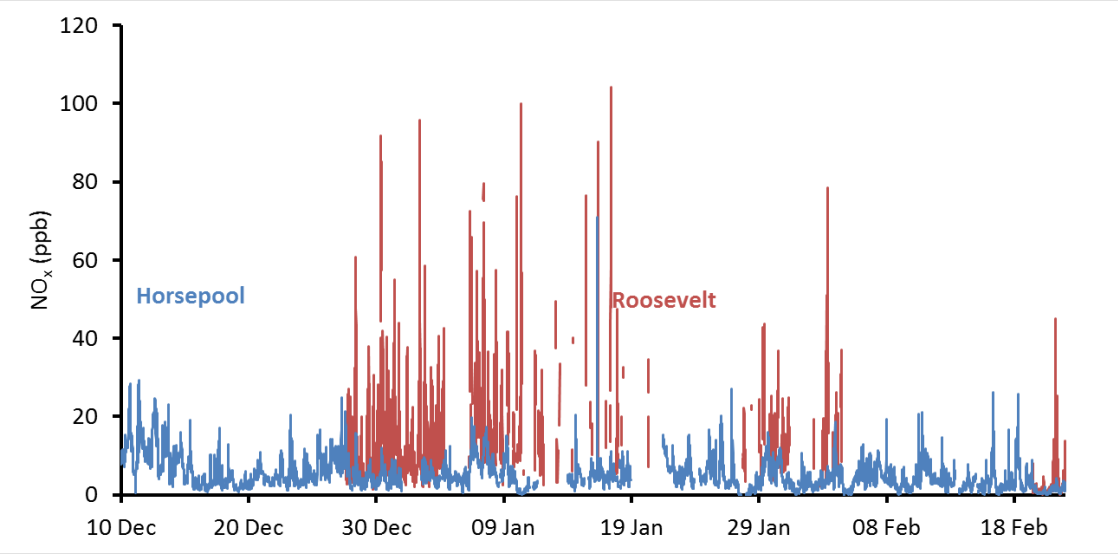

Figure 3-12. Time Series of NO_x at Horsepool and Roosevelt, winter 2013-14.

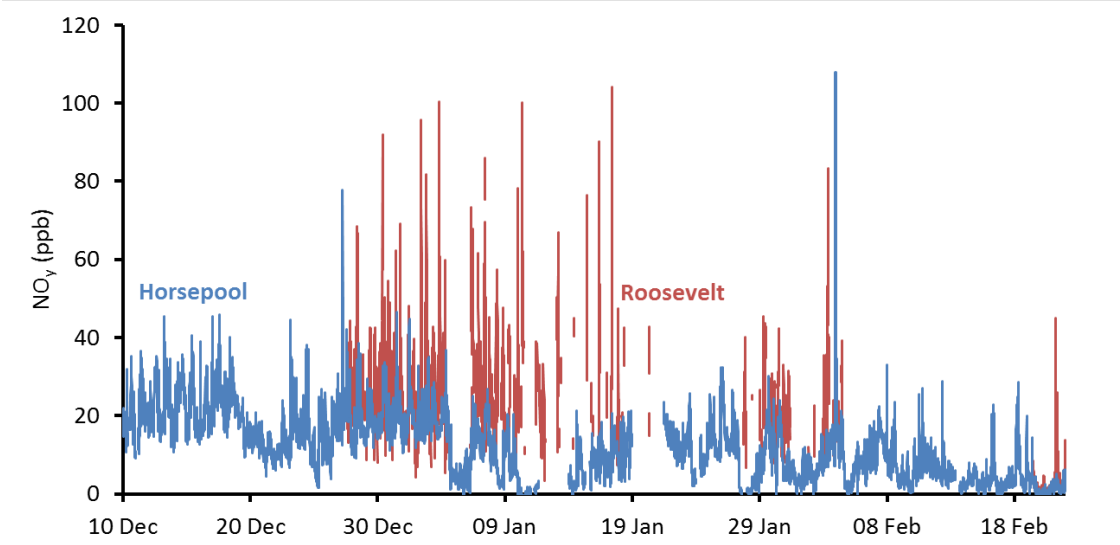

Figure 3-13. Time Series of NO_y at Horsepool and Roosevelt, winter 2013-14.

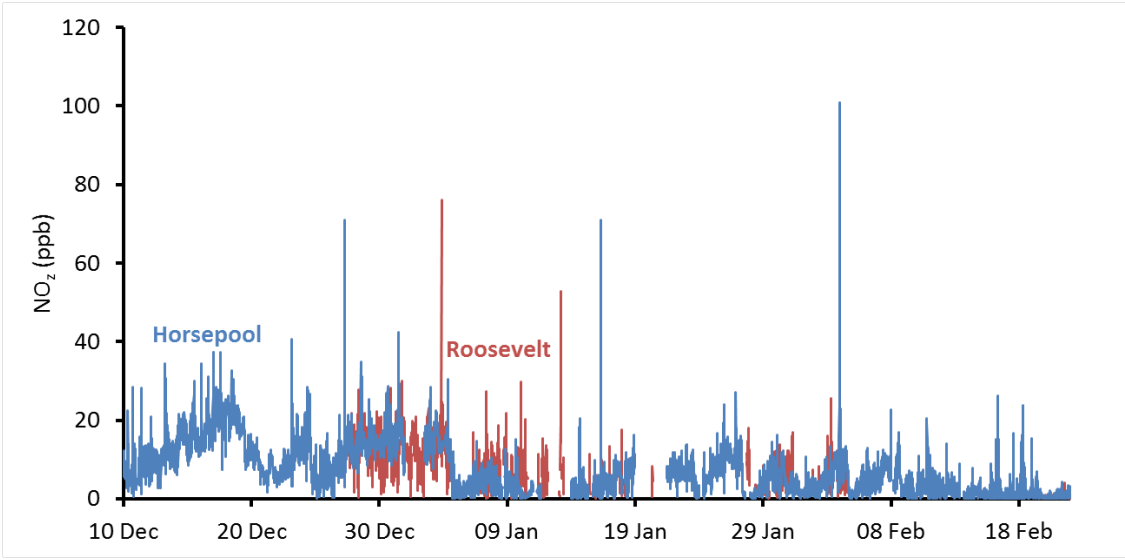

Figure 3-14. Time Series of NO_z at Horsepool and Roosevelt, winter 2013-14.

3.4 Acknowledgements

We are grateful to the Uintah Impact Mitigation Special Service District and the Utah Science, Technology, and Research Initiative for financial support of this work. We thank the Bureau of Land Management for providing equipment for remote ozone monitoring. We are also grateful to the Ute Indian Tribe for providing site access and to the Utah Department of Environmental Quality for providing space for our monitors at Roosevelt.

3.5 References

Lyman, S., and H. Shorthill (Eds.) (2013), *Final Report: 2012 Uintah Basin Winter Ozone and Air Quality Study*, *CRD13-320.32*, Office of Commercialization and Regional Development, Utah State University, Logan, Utah.

Martin, R.S., K. Moore, M. Mansfield, S. Hill, K. Harper, and H. Shorthill (2011), *Final Report: Uinta Basin Winter Ozone and Air Quality Study, EDL/11-039*, Energy Dynamics Laboratory, Utah State University Research Foundation, Logan, Utah.

Stoeckenius, T. and D. McNalley (Eds.) (2014), *Final Report: 2013 Uinta Basin Winter Ozone Study,* Environ International Corporation, Novato, California.

4.0 INTENSIVE CHEMICAL MEASUREMENTS AT HORSEPOOL

Authors
James M. Roberts, Patrick R. Veres, Bin Yuan, Carsten Warneke, Peter M. Edwards, Robert Wild, William Dube, Steven S. Brown, Martin Graus, Jessica Gilman, Brian Lerner, Joost A. de Gouw, Rui Li, Timothy Bates, Patricia Quinn, Abigail Koss, Shao-Meng Li, John Liggio, Hans Osthoff, Barry Lefer, James Flynn, Sergio Alvarez, Catalina Tsai, Jochen Stutz, David D. Parrish, Robert Zamora, Becky Alexander, and Maria Zatko

4.1 Introduction

The intensive measurements at the Horsepool sampling site during the Winter 2014 study were undertaken to provide additional information about radical sources, specifically nitrous acid (HONO). The site at which these measurements were conducted was the same as in the previous two years and is shown in Figure 2-1. The goals of the 2014 intensive study required a site configuration similar to that deployed during the 2012 intensive, as shown in Figure 4-1, with the exception that LIDAR measurements were deemed unnecessary hence were not deployed in 2014.

The picture in Figure 4-1 shows the location of the individual experiments at the site. The tower and instrument enclosures were very similar to those used during the 2012 intensive, and were geared towards intercomparisons of HONO measurements, exploration of vertical gradients, and assessment of potential inlet and interference effects. The other measurements were included with an emphasis on defining the chemistry that will be needed to interpret the HONO measurements and place them in context relative to both the photochemistry happening during the present season and the results of the previous two seasons. Table 4-1 lists the experiments deployed at Horsepool during the 2014 intensive.

Figure 4-1. The Horsepool measurement site as configured during the 2014 intensive study.

Table 4-1. Measurements deployed at the Horsepool site during the 2014 Intensive.

Measured Parameter	Method	Time Resolution	Detection Limit	Principal Investigator
NO, NO_2, NO_3, N_2O_5, NO_y, O_3	Cavity ring-down spectroscopy	1 sec	0.1 - 0.001 ppbv	Steve Brown/Rob Wild
NO, NO_2, NO_y fluxes	Photolytic, thermal conversion, chemiluminescence	1-10 sec	10 - 100 pptv	Jennifer Murphy
HONO, NO_2	Incoherent broadband absorption spectroscopy, ACES	1 min	0.2 ppbv	Steve Brown/Kyung-Eun Min
HONO	Long Path Absorption Photometer	3 min	10 pptv	Barry Lefer/James Flynn/Sergio Alvarez
Acyl Peroxynitrates, Nitryl Chloride ($ClNO_2$), HONO, HO_2NO_2	Iodide ion chemical ionization mass spectrometry (iCIMS)	1 - 5 sec	0.005 ppbv	Patrick Veres/Jim Roberts
CO_2 and Methane (CH_4)	Wavelength scanned cavity ring-down spectroscopy	1Hz every 5 sec	0.2 ppmv for CO_2, 2 ppbv for CH_4	Jim Roberts
O_3	UV Absorption	10 sec	1 ppbv	Jim Roberts
SO_2	UV fluorescence	1 min	0.1 ppbv	Jim Roberts
VOCs (see website for list)	In situ gas chromatography mass spectrometry	30 min	0.01 ppbv	Jessica Gilman/Brian Lerner/Joost de Gouw
Formaldehyde, Oxygenates, Aromatics, Acetonitrile	Proton-transfer reaction mass spectrometry / ToF	10 sec - 1 min	0.01 ppbv	Carsten Warneke/Joost de Gouw/Rui Li/Shao-Meng Li
HCHO	Liquid scrubber Hantzsch Reaction	1 min	100 pptv	Barry Lefer/James Flynn/Sergio Alvarez
O_3, NO_2, HONO, SO_2, HCHO, NO_3	Long Path - Differential Optical Absorption Spectroscopy (LP-DOAS)	5 min	1ppb, 80ppt, 20ppt, 250ppt, 200ppt, 2ppt	Jochen Stutz/Catalina Tsai
Acids: HNO_3, HCl, HONO, HNCO, carboxylic acids, substituted phenols	Negative ion proton transfer mass spectrometry / ToF	1 - 10 sec	0.01 ppbv	Bin Yuan/John Liggio
Size-Resolved Aerosol Surface Area	SMPS, APS	15 min		
Aerosol Chemical Composition	Particle into Liquid Sampler (PiLS)	10 min		Tim Bates/Trish Quinn
Snow Composition:Anions/Cations	Ion chromatography	N/A		Trish Quinn/Tim Bates
Aerosol and Snow Nitrate Isotopes	Isotope Mass Spectrometry	N/A		Becky Alexander
Photolysis Rates	Spectral radiometry	1 min		Hans Osthoff
Photolysis Rates	Broadband radiometry upwards/downwards	1 min		Bob Zamora
Meteorological Data	Weather station	1 min		Allen White
Boundary Layer Height, Vertical	SODAR, Sonic anemometers	1 min		Allen White

This section will summarize the major findings from the 2014 Horsepool intensive site with emphasis on the outstanding questions, i.e. sources of radicals. The fundamental differences between the three intensive years can be summarized by the data in Figure 4-2 which shows the timelines of ozone measurements. The three years had the two extremes, low ozone during

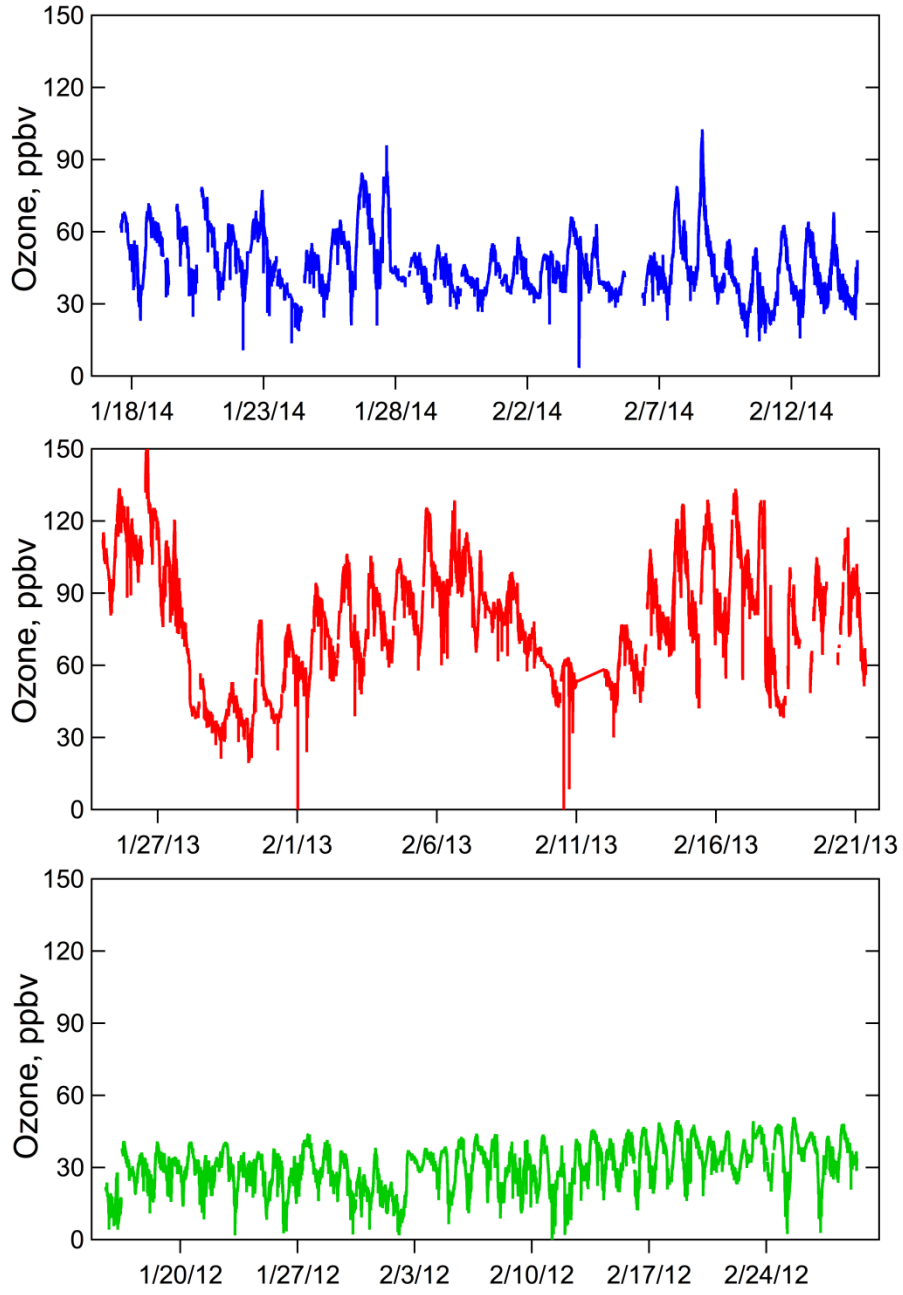

Figure 4-2. Ozone summary for all three years. The top trace (blue) shows the 2014 data, the middle trace (red) shows the 2013 data, and the bottom trace (green) shows the 2012 data.

the 2012 study when there was bare ground and no stable cold pool, high ozone in 2013 when there was snow cover and persistent cold pool events lasting more than a week, and 2014 when there was some snow cover, but cold pool events that only lasted a few days. The details of the 2014 measurements will be discussed below. The data on which these analyses are based can be found on the website: http://www.esrl.noaa.gov/csd/groups/csd7/measurements/2014ubwos/.

4.2 Volatile Organic Compounds (VOCs)

VOC composition of primary hydrocarbons measured at the Horsepool site in the Uintah Basin was the same for all three years (see Figure 4-3). The mean mixing ratios of the hydrocarbons varied by a factor of approximately 4 (see Figure 4-4). For example, the observed mean propane (the third most abundant hydrocarbon in raw natural gas) was 31 ppbv, 134 ppbv, and 67 ppbv for 2012, 2013, and 2014, respectively. By comparison, mean propane observed at a wintertime site within the Denver-Julesburg Basin in northeastern Colorado in 2011 was 27 ppbv [Gilman et al. 2013] and the range of mean propane values for 28 U.S. cities is 0.29-6.05 ppbv [Baker et al. 2008].

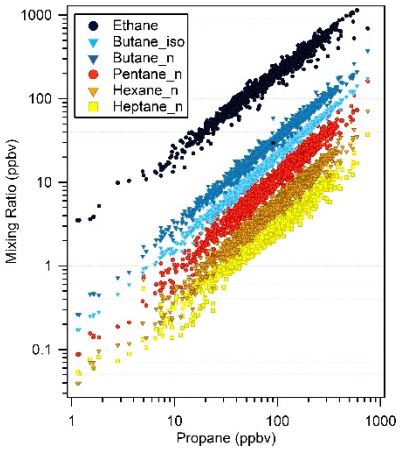

Figure 4-3. Correlations of C_2-C_6 alkanes to propane in 2014. The very tight correlations of all light alkanes to propane ($r>0.95$, $r^2>0.90$) suggest that these species are associated with the same emission source. The enhancement ratios (linear slope of correlation plot) of alkanes to propane are most similar to the composition of raw natural gas. The observed enhancement ratios of the alkanes were similar for all 3 winters indicating that leakage or raw natural gas into the atmosphere is the dominate emission source of hydrocarbons in the Uintah Basin.

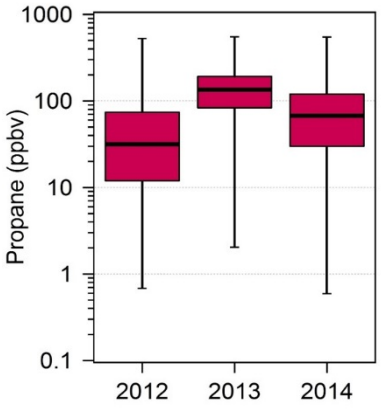

Figure 4-4. Distribution of observed propane values for 2012-14 at the Horsepool Site. The box represents the 75th (top) and 25th (bottom) percentiles. The median (50th percentile) is shown by the thick line within the box, and the whiskers are the maximum and minimum observed values. The mean propane increased by a factor of 4 in 2013 and a factor of 2 in 2014 compared to 2012 (baseline) values. Temporal correlations indicate that meteorology had the largest effect on the observed mixing ratios. Cold pool stagnation events in 2013 resulted in the highest overall observed VOC mixing ratios [see Stoeckenius and McNally, 2014, Chapter 5].

Primary emissions of methanol, particularly from near-by sources were observed in all years as indicated by short-term spikes in ambient concentrations [see Stoeckenius and McNally, 2014, Chapter 5]. Additionally, methanol has weak correlations with other secondary organics such as acetaldehyde indicating that methanol is mostly from primary sources. The mean observed mixing ratios varied by a factor of 4 (see Figure 4-5). Methanol is used in large quantities throughout the Uintah Basin as an anti-freezing agent. Observed mixing ratios are higher than expected for wintertime continental air (~ 5 ppbv) but are of the same order of magnitude measured at summertime sites heavily influenced by natural biogenic emissions as well as sites heavily influenced by industrial operations (Gilman et al., 2008).

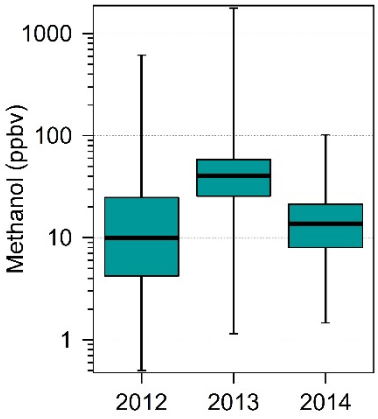

Figure 4-5. Distribution of observed methanol values for 2012-2014. The mean methanol increased by a factor of 4 in 2013 and a factor of 2 in 2014 compared to 2012 (baseline) values.

The composition of oxygenated VOCs and C_2-C_4 alkyl nitrates formed in the atmosphere from the photochemical oxidation of primary hydrocarbons was also similar for all 3 years. The mean mixing ratios of oxygenated VOCs varied by a factor of approximately 10 (see Figure 4-6). The most abundant alkyl nitrate measured by the GC-MS in 2012 and 2014 was iso-propyl nitrate and the mean increased by a factor of 4 from 2012 (no snow) to 2014 (partial snow conditions), which is twice as large as the observed increase in primary hydrocarbons . Alkyl nitrates were not measured in 2013. The composition is largely determined by the mixture of primary hydrocarbons and the abundance is dictated by meteorology which drives the photochemical production of ozone, oxygenated VOCs, and alkyl nitrates. The fact that the oxygenated VOCs and alkyl nitrates increased by twice as much as the primary hydrocarbons indicates that photochemical formation of these species does not have a direct, linear relationship with the concentration of the VOC precursors (i.e., decreasing hydrocarbons by X amount will not necessarily decrease secondary products by the same amount).

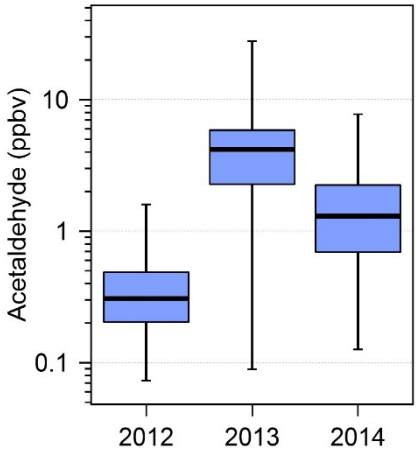

Figure 4-6. Distribution of observed acetaldehyde values for 2012-2014. The mean acetaldehyde increased by a factor of 11 in 2013 and a factor of 3.6 in 2014 compared to 2013 (baseline) values.

The photochemical formation of oxygenated VOCs occurred at similar rates in 2013 and 2014 even though the observed ambient mixing ratios were lower in 2014 (see Figure 4-7). This suggests that the chemistry was similar between the last 2 years of the experiment.

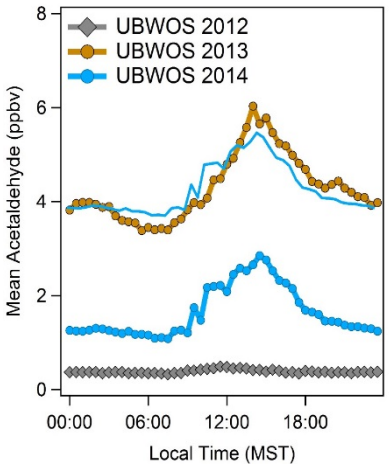

Figure 4-7. Diurnal profiles of mean acetaldehyde for 2012-2014. The lighter blue trace is the 2014 diurnal profile offset so that the value at midnight is equal to 2013 values. The 2013 and 2014 diurnal profiles are very similar suggesting that the photochemical formation of this species as essentially equivalent for both years.

The composition of the OH reactivity was remarkably similar for 3 years of this study (see Figure 4-8). OH reactivity is a product of reactivity of a species with the hydroxyl radical (k_{OH}) and its ambient concentration. It is a simple metric used to identify key reactive species that may participate in the photochemical formation of ozone. The magnitude of the OH reactivity of the measured VOCs varied by a factor of 3 (see Figure 4-9). Very tight correlations between the VOC OH reactivity and propane for all 3 years is used as direct evidence that (i) the overall composition of VOCs was similar for all 3 years in spite of differences in abundance and varying degrees of photochemistry, and (ii) the primary emissions of hydrocarbons and the secondary products formed from their oxidation is related to a single dominant source of VOCs within the Uintah Basin.

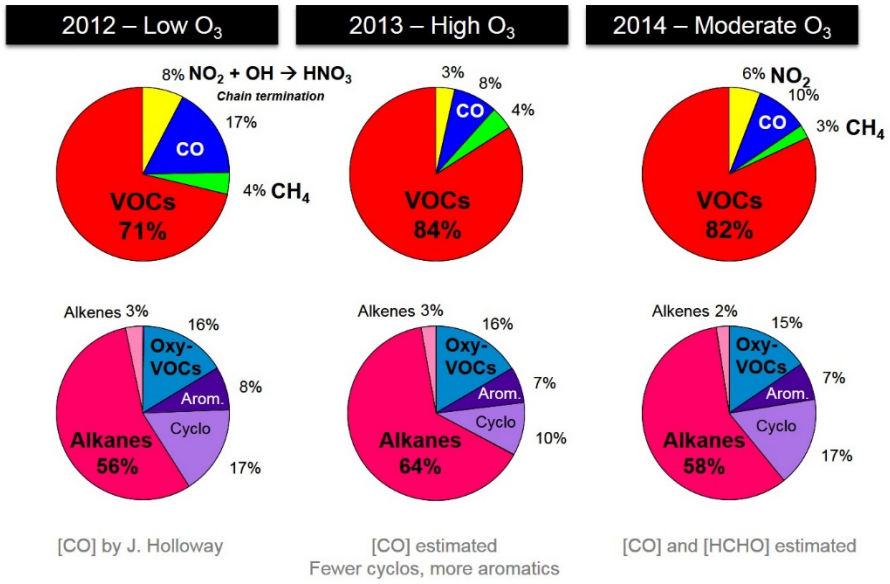

Figure 4-8. Composition of the OH reactivity. All species are included in the top row (VOCs are red, CH_4 is green, CO is blue, and NO_2 is yellow). VOCs are the dominate contribution to the OH reactivity. Reaction of OH + NO_2 is a net sink of OH radicals and quenches the recycling of OH radicals. The bottom row is the OH reactivity of all measured VOC species separated by compound class. Alkanes, which are fairly unreactive species, are the dominant contributors to OH reactivity due to their large abundances. Cycloalkanes, oxygenated VOCs, and aromatics are also important contributors to the OH reactivity. The overall abundance of alkenes was very low so that these species, which are highly reactive, were only a minor contributor to the OH reactivity.

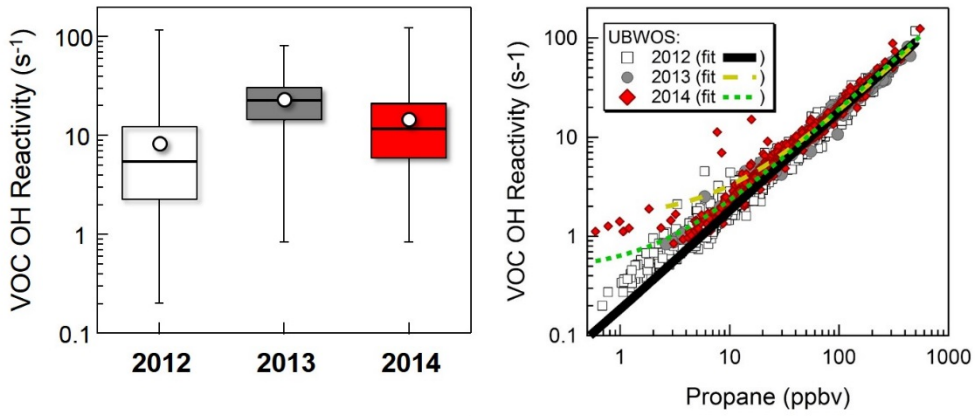

Year	Median (s^{-1})	Mean (s^{-1})	Max (s^{-1})
2012	5.4	8	117
2013	22.6	23	81
2014	11.7	15	124

Year	y-int	slope	r^2
2012	*0.004*	0.181	**0.97**
2013	1.5	0.172	**0.99**
2014	0.45	0.188	**0.99**

Figure 4-9. LEFT: Distribution of observed OH reactivity of all measured VOCs for 2012-2014. The mean VOC-OH reactivity increased by a factor of 2.9 in 2013 and a factor of 1.9 in 2014 relative to 2012 (baseline) values. RIGHT: Correlation plot of the VOC-OH reactivity to propane mixing ratios for 2012-2014. The similar slopes and the very tight correlations (r_2>0.97) show that the overall composition of VOCs was similar for all 3 years and that the VOC-OH reactivity is highly dependent of a single, dominant source of VOCs in the Uintah Basin.

4.2.1 Formaldehyde

Formaldehyde measurements during the 2014 intensive are entirely consistent with the results from UBWOS 2013 when differences in meteorology between the two years are taken into account. This is readily apparent in Figures 4-10(a-d), which show the timelines of CH_2O and O_3 measurements for each year, and close-ups of O_3 build-up events. The CH_2O and O_3 levels and diurnal behavior look similar for the 2013 event and the first 3.5 days of the 2014 build-up before the clean-out. The CH_2O is from a combination of primary and (30%) and secondary (75%) sources and background (5%) [see Stoeckenius and McNally, 2014, Chapter 5]. The secondary formaldehyde is accompanied by a large number of other carbonyl compounds, some of which are measured, most of which were not, that produce radicals when photolyzed. These carbonyl compounds are the major radical sources driving O_3 events.

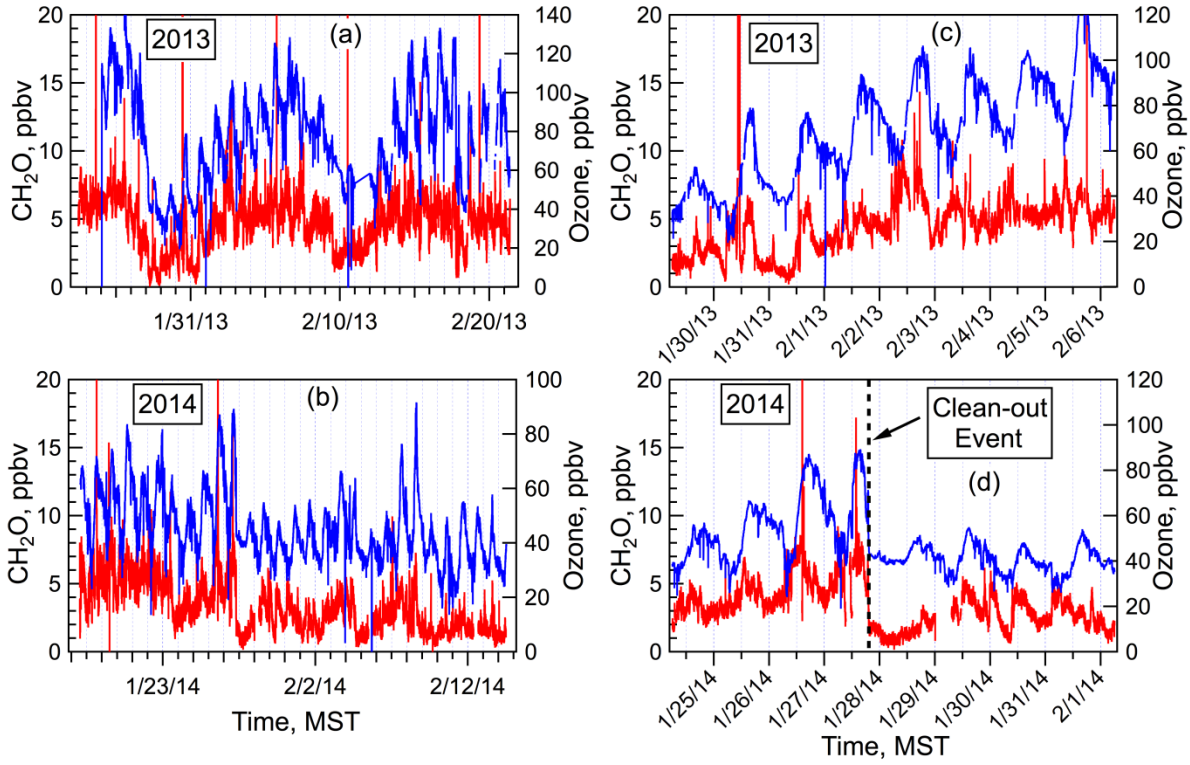

Figure 4-10. Timelines of all the formaldehyde and ozone measured during UBWOS 2013 (a) and UBWOS 2014 (b), and details of the main build-up period observed in 2013 (c) and the partial build-up period in 2014 (d) that was cut short by a shift in meteorology. The blue lines are the measured ozone and the red liens the measured formaldehyde. Short term spikes in formaldehye concentrations from local sources can be seen on both years.

4.3 Oxides of Nitrogen

The oxides of nitrogen (NOx = NO + NO_2) are the main catalysts for ozone formation, and together with their atmospheric chemical products form a family of compounds known as odd-nitrogen (NOy). The detailed chemistry of NOy has many features that can be used to interpret how the photochemistry proceeds in an air basin. The relative levels of NOx present provide the basis for assessing the efficiency of radical chemistry. NOx product species, chiefly HNO_3, PANs and alkyl nitrates, build up due to the same photochemistry that produces ozone, hence we expect broad correlations of these products (collectively termed NOz = NOy- NOx) with O_3.

The average NOx levels vs. time of day observed during the 2014 study are shown in Figure 4-11 along with those observed in 2012 and 2013. The NOx levels observed in all three studies are remarkably similar, with the daytime 2014 data being slightly higher than the other two years. As a result, the potential for photochemical ozone formation was similar for all three years, from the point of view of NOx chemistry. The mid-day average NOx levels of 5-7 ppbv are close to the optimum levels for ozone production under the conditions found in the Uintah basin in

the wintertime. This optimum can be thought of as the trade-off between NOx high enough to carry the radical chain that produces O_3 but not so high that the reaction of OH with NO_2 is a significant radical sink. These aspects of the UBWOS 2012 and UBWOS 2013 measurements are discussed by Edwards et al., [2013; 2014].

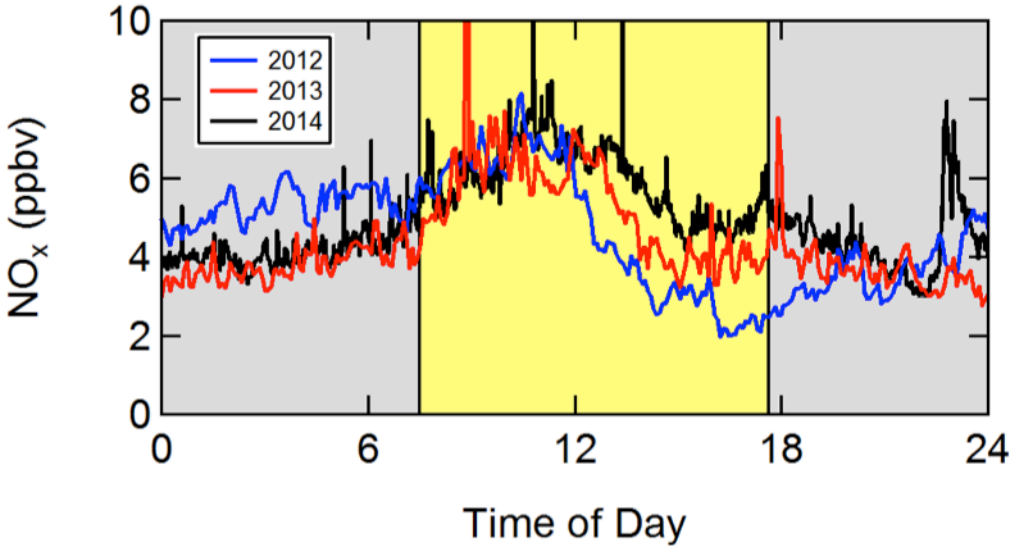

Figure 4-11. Average NOx levels measured at the Horsepool site versus time of day for the three intensive years.

The main differences among the 3 intensive years are the levels of NOy that built up in the basin as a result of NOx chemistry. The observed NOy concentrations fall in the same order as the amounts of O_3 formed during those years, with 2013 being the highest, 2014 the next highest and 2012 the lowest (Figure 4-12). The diurnal profiles of NOy are different among the years, with 2014 and especially 2013 showing distinct mid-day maxima. These differences are best visualized by examining the quantity NOz, defined as NOy-NOx, which is simply the sum of all the NOx product species. NOz, shown versus time of day in Figure 4-13, was lowest in 2012 and had almost no variation with time of day, was highest in 2013 and had a mid-afternoon maximum, corresponding to photochemical conversion of NOx to products, and was of intermediate magnitude in 2014, but still had a mid-afternoon maximum.

The compositions of NOz during the three years are summarized as pie charts in Figure 4-14 for both day and night periods. The size of the pie wedges indicate the percentage of NOz corresponding to each compound. Nitric acid is the most abundant NOz species during the day, with PAN and “Other” being the next most abundant. At this site, “Other” encompasses organic

nitrates, peroxynitric acid ($HOONO_2$) and some fraction or particle nitrate.[6] Nitrous acid (HONO) was not a major contributor to NOz, even in the daytime 2013 measurements which we now believe had significant interferences (see section below on HONO).

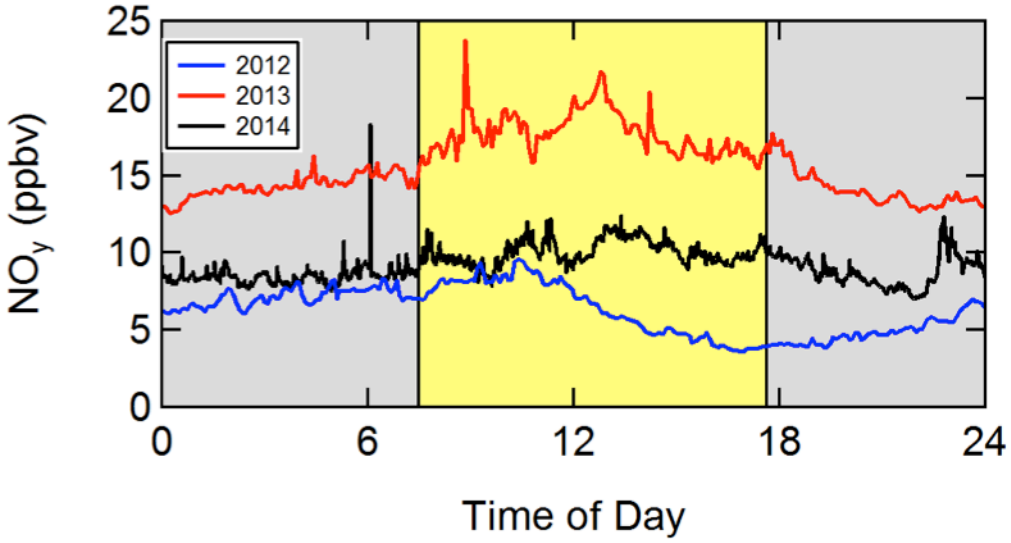

Figure 4-12. The average levels of NOy versus time of day measured at the Horsepool site during the three intensive years.

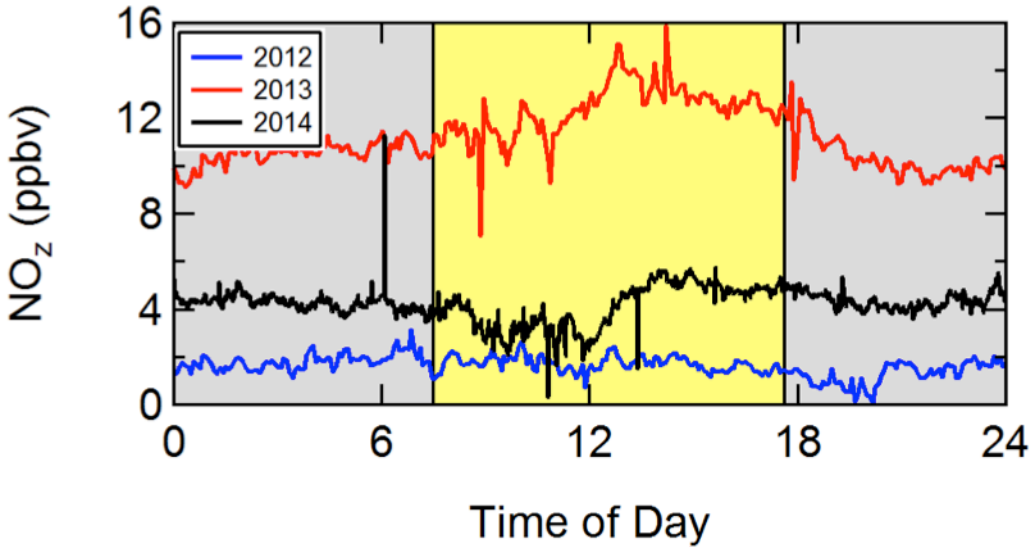

Figure 4-13. The average levels of NOz versus time of day measured at the Horsepool site

[6] It is generally recognized that open tube NOy convertors of the type used in this study convert volatile particle nitrate (mostly $NH4NO_3$), but not refractory nitrate (e.g. $NaNO_3$). The relative sizes of these particle nitrate pools differ from site to site, but are often roughly equal.

during the three intensive years.

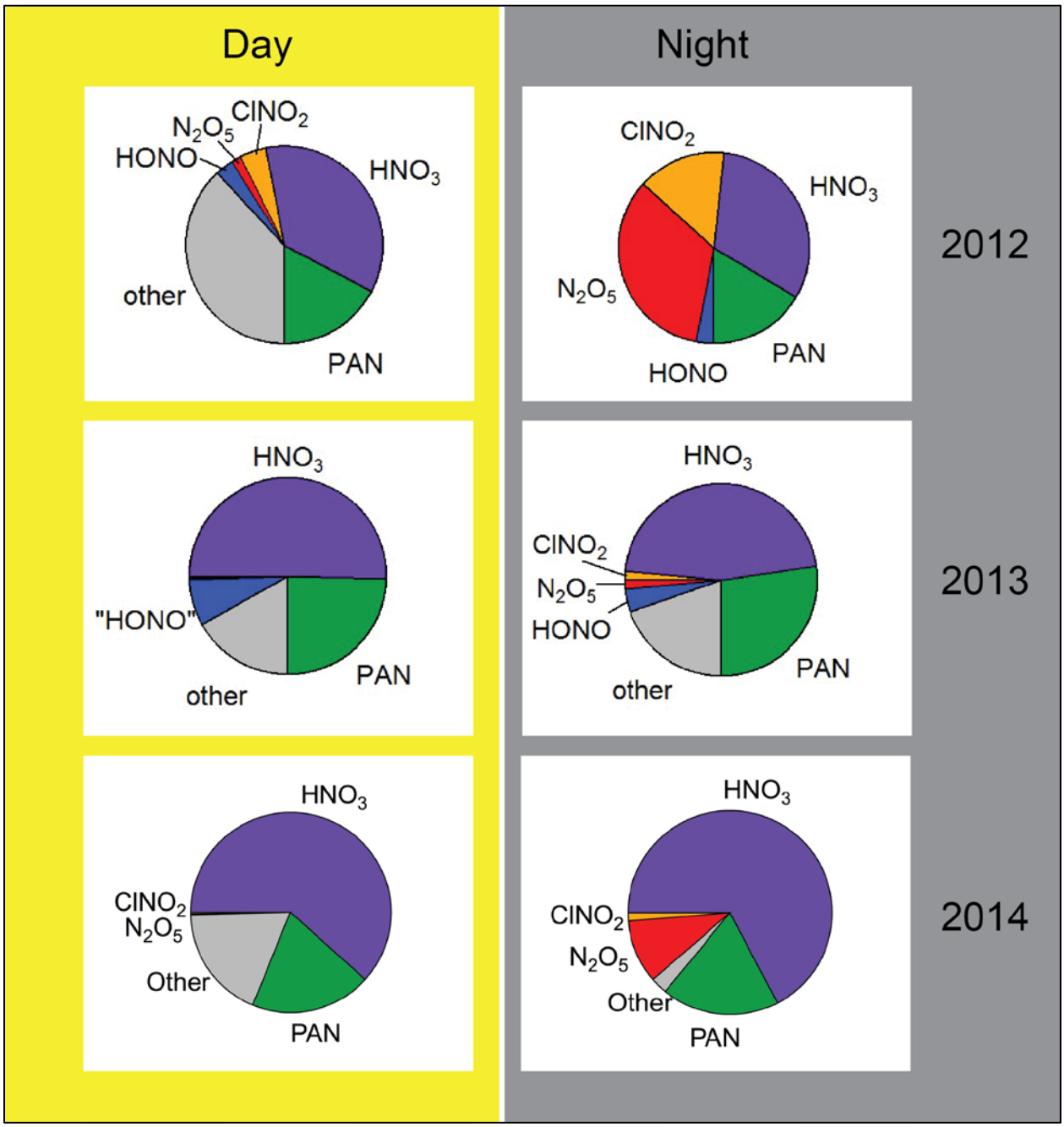

Figure 4-14. Proportions of the individual compounds that made up NOz for each year classified by day or night. The daytime 2013 HONO measurement was left in, as reported, but is now believed to have significant interferences.

4.3.1 NO_3 and N_2O_5

Nighttime chemistry of NO_2 and O_3 will produce N_2O_5, first through reaction of O_3 and NO_2 to produce NO_3 and then reaction of NO_3 with NO_2. N_2O_5 can heterogeneously react to form HNO_3, a major sink of reactive nitrogen. The amount of N_2O_5 that reacts heterogeneously at night influences the total amount of photochemically active NO_x available during the day, since it reverts back to NO_x in sunlight.

Using the NO_2 and O_3 measurements and a known reaction rate constant, we can calculate $P(NO_3)$ the production rate of NO_3. Assuming that sinks of N_2O_5 are large compared to those of NO_3, a steady-state approximation allows us to calculate the lifetime of N_2O_5 (τ_{N2O5}) by dividing measured N_2O_5 concentrations by the NO_3 production rate:

$$\tau_{N2O5} = [N_2O_5]/P(NO_3)$$

This lifetime can be interpreted as a measure of N_2O_5 reactivity, and is plotted as solid lines in Figure 4-15, which shows lifetimes approximately 3.5 times longer in 2012 than 2013. Since this calculation is based on a steady-state assumption, the times of day where this may hold are midnight to 7 in the morning.

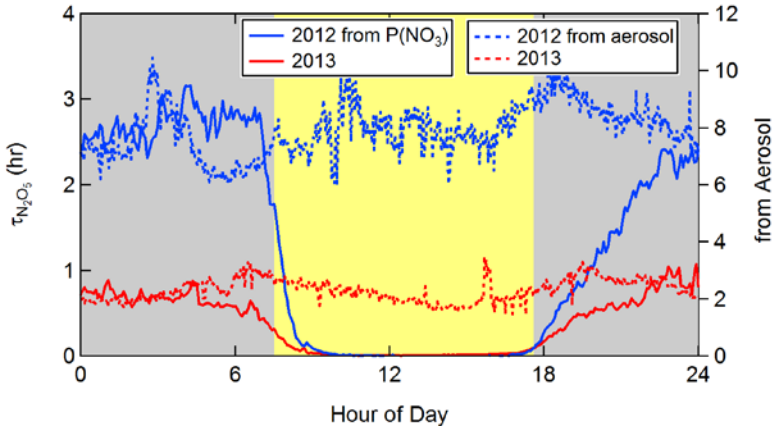

Figure 4-15. Lifetimes of N_2O_5 implied by the steady state analysis and $P(NO_3)$ (solid lines) and estimated for loss to aerosol (dashed line).

The heterogeneous reaction of N_2O_5 can occur on aerosol or ground surfaces. Using aerosol measurements from the NOAA Pacific Marine Laboratory PMEL, adjusted for hygroscopic growth, we can calculate the expected N_2O_5 lifetime due to aerosol uptake,

$$\tau_{N2O5} = 4/(\gamma c S_A)$$

where γ is the uptake coefficient (set to 0.02 for a hydrated particle, [Chang et al., 2011]), c is the mean molecular speed, and S_A the aerosol surface area density. The resulting calculated

lifetimes, shown as dotted lines in Figure 4-15, are consistent with the lifetime calculation based on $P(NO_3)$ during the midnight – 07:00 steady state period.

Some of the difference in N_2O_5 lifetime between the 2012 and 2013 winter studies seen in Figure 4-15 may be explained by different inlet heights. Figure 4-16 shows inlet positions for N_2O_5 sampling for the three different winter campaigns. The blue dot marks the inlet height in 2012, the red dot marks the height in 2013 and the two black dots mark the sampling heights used in 2014.

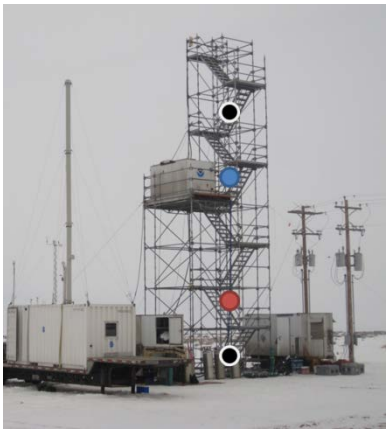

Figure 4-16. Tower used for sampling during the UBWOS 2014 intensive study at the Horsepool site. The indicated sampling levels were 1m, 3m, 7m and 14m agl.

Significant N_2O_5 uptake to the ground would result in a vertical gradient of N_2O_5 lifetime. To check this possibility, we placed two inlets (marked with black dots) on the tower and alternated between the two. Repeating the above N_2O_5 lifetime analysis based on $P(NO_3)$ for these two heights results in the solid and dotted black lines shown in Figure 4-17.

The difference of approximately a factor 2 between the two inlet heights used in 2014 shows that there is some vertical gradient of N_2O_5 lifetime, most likely due to uptake on the snow surface. However, this gradient is not nearly large enough to account for the difference N_2O_5 lifetimes between 2012 and 2013. This finding is consistent with the conclusion that uptake to aerosol is the major factor in determining the lifetimes of N_2O_5, explaining much of the difference in the nighttime chemistry of reactive nitrogen in 2012 and 2013.

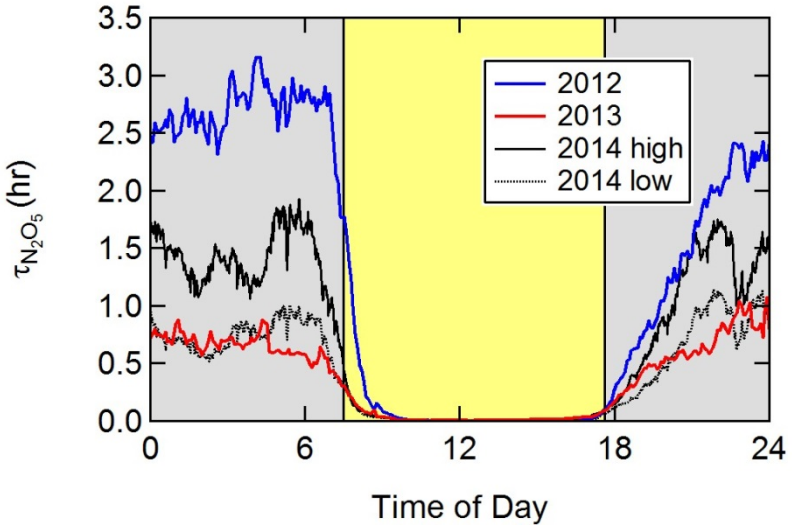

Figure 4-17. The lifetimes of N_2O_5 implied by the formation rates and ambient concentrations for the three UBWOS intensive years and two inlet heights in 2014.

4.3.2 Acylperoxy nitrates (PANs) and Nitryl Chloride ($ClNO_2$)

PANs and $ClNO_2$ were measured with the I^- CIMS instrument in a manner similar to that used during the 2012 and 2013 studies. The chief differences in the 2014 procedures were that an automatic routine was devised to switch from a hot (150°C) to room temperature inlet, and a dual inlet system was devised to automatically switch between two inlets used for both the I^- CIMS instrument and other instruments measuring HONO (see below). The multi-instrument inlets were configured either in the top (14 m agl) and bottom (1 m agl) position in order to observe gradients, or with one short and one long inlet at height of the instrument enclosure to check for inlet interferences. The hot and cold inlet configuration allows for routine assessment of potential interferences in the PAN measurement due to peroxyacetic acid. The results of the PAN and $ClNO_2$ measurements are summarized in this section.

The major PAN-type species in the Uintah basin is acetyl peroxynitrate ($CH_3C(O)OONO_2$ = PAN), which is produced from almost every VOC having 2-carbons or more, especially alkanes. The levels of PAN observed in 2014 were intermediate to the high levels observed in 2013 and the low levels in 2012, as shown in Figure 4-18 along with representative examples from 3 different urban areas. The distribution of PAN in 2014 was most like that observed in the summer of 2010 in Pasadena, CA.,

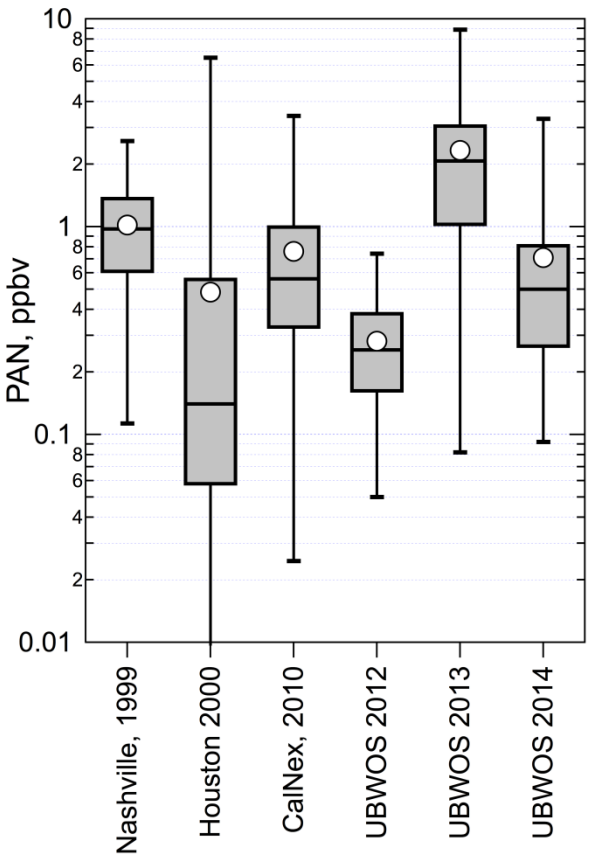

Figure 4-18. Distributions of PAN levels measured during the three UBWOS campaigns and during three summer campaigns in urban areas.

One important feature of PAN chemistry is that it is formed from the same NOx-VOC chemistry that makes O_3, therefore a correlation of PAN with O_3 is expected during active photochemistry. The correlation of O_3 and PAN measured during UBWOS 2014 is shown in Figure 4-19 along with correlations from the 2012 and 2013 Horsepool intensives, and TexAQS 2000 campaign in Houston, TX. The differences in these O_3 PAN correlations between the TexAQS 2000 and the UBWOS data sets reflect the faster PAN loss rates operative in the summertime in Houston. In addition to such correlations, the role of PAN as a key intermediate provides a diagnostic in the comparison of models and measurements. While models can often predict O_3 close to measured levels, it is not clear that the model is getting that answer for the right reason. PAN provides a good diagnostic because it reflects both the VOC and NOx photochemistry happening in a given airshed, hence provides a critical test of model mechanisms. Such a comparison was successfully done for the UBWOS 2013 study [Edwards et al., 2014], providing support for the conclusion that box modeling with the Master Chemical Mechanism (MCM) done for that year is reasonably accurate.

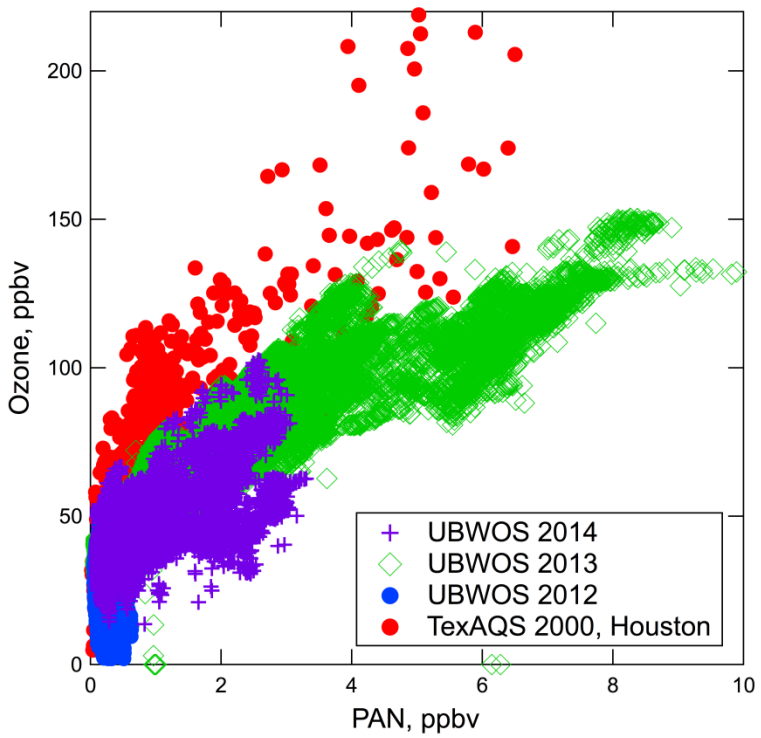

Figure 4-19. The correlations of O_3 and PAN for the three UBWOS Intensives at Horsepool, along with that from the TexAQS 2000 Summertime study in Houston TX.

The PAN CIMS was configured with a variety of inlets over the course of the intensive study. Early in the experiment the instrument had two inlets of identical length and material (PFA thermostated at 30°C), one placed at 18.3 m above the ground and the other placed at 1m above the snow field immediately to the south of the tower as shown in Figure 4-20. The CIMS sampled alternately from one inlet or the other, switching every half hour. The PAN data for this early period of gradient measurements is shown in Figure 4-21 and in general shows small differences in PAN with height, with the top inlet measuring slightly higher than the lower, with the exception of the mornings of 23 and 27 January during which PAN measured through the upper inlet measurement was substantially lower than through the bottom inlet (the reasons for these anomalous gradients are as yet unknown).

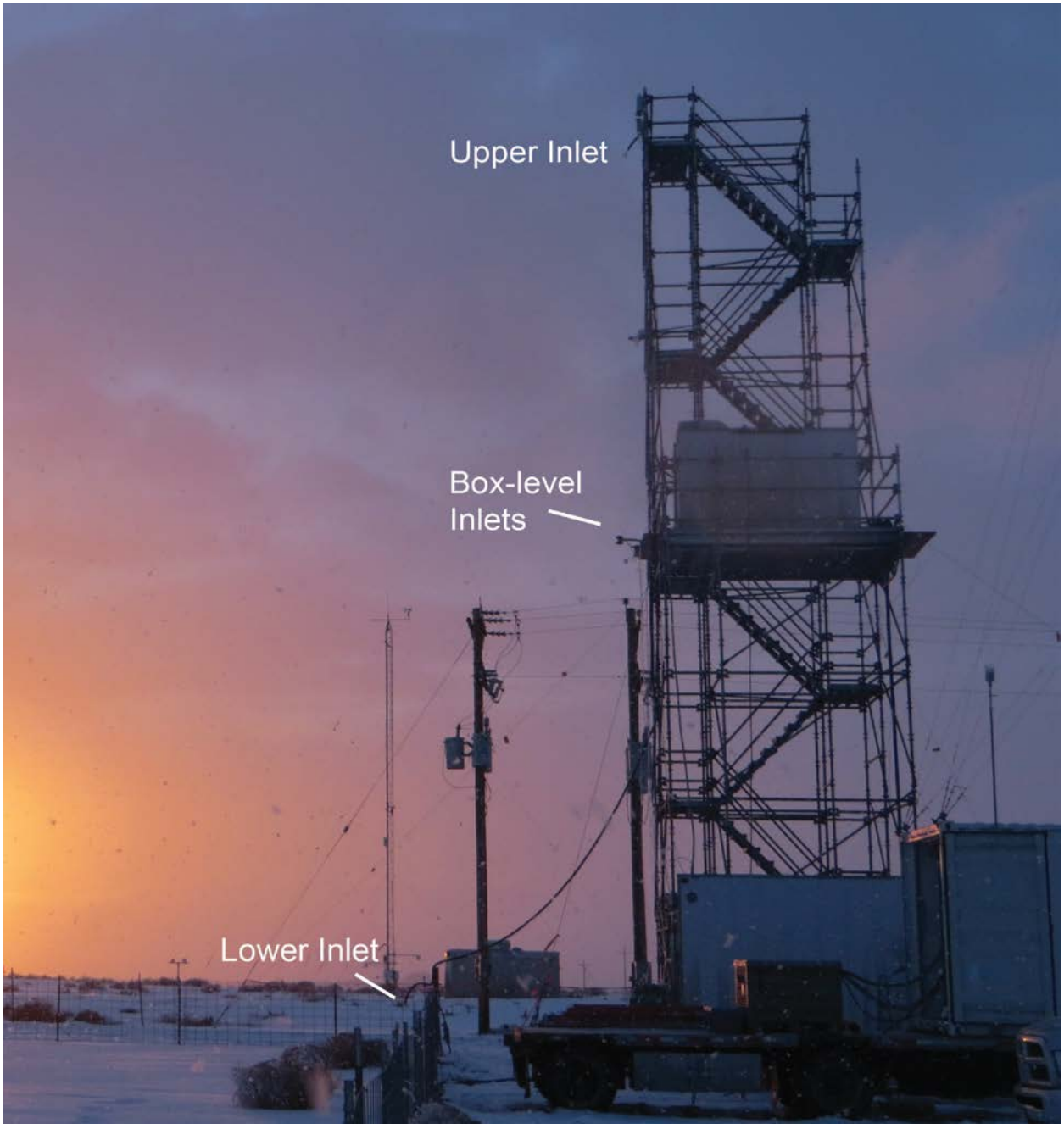

Figure 4-20. A photograph of the sampling tower showing the location of the inlet used for the CIMS and HONO experiments during UBWOS 2014.

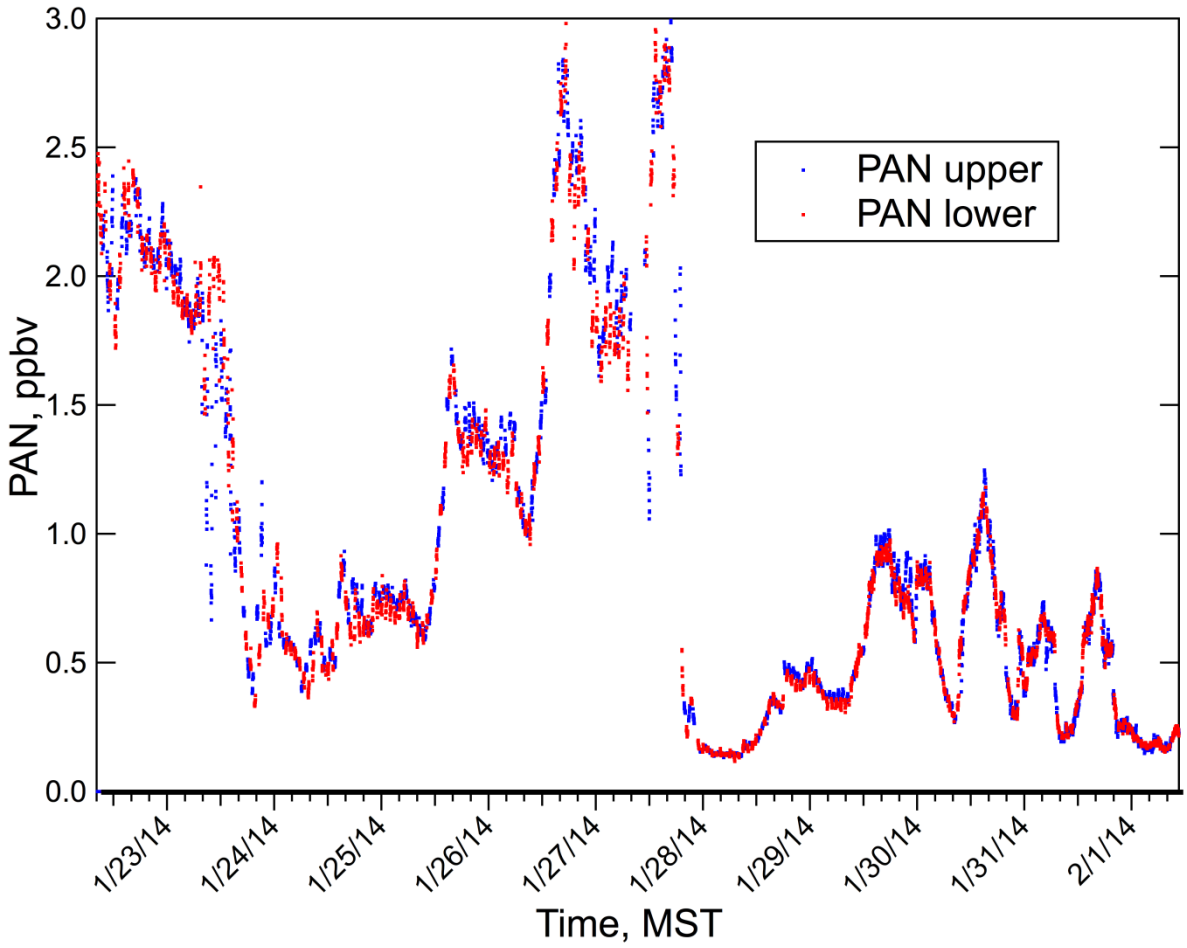

Figure 4-21. Timeline of PAN measurements during the time when the PAN CIMS was switching between the top inlet at 18.3 m and the bottom inlet at 1m.

Nitryl chloride ($ClNO_2$) was measured with the same instrument as PANs, so is discussed in this section. The important features of $ClNO_2$ chemistry are that it is only formed at night, through the reactions of N_2O_5 with chloride on surfaces, and is rapidly photolyzed to form chlorine atoms and NO_2, providing a radical that can initiate photochemistry. The $ClNO_2$ levels measured in 2014 are compared to values from the previous 2 years and several other urban areas in Figure 4-22. The 2014 levels were lower than during the other 2 UBWOS measurement periods, for reasons that may have to do with a combination of lower particle chloride concentrations as compared to 2012 and lower aerosol surface area loadings as compared to 2013. The higher Pasadena data reflect the presence of sea salt derived soluble chloride in that air basin [Mielke et al., 2013], and conversely, the lower Weld County data reflect lower soluble chloride in that air basin [Riedel et al., 2013].

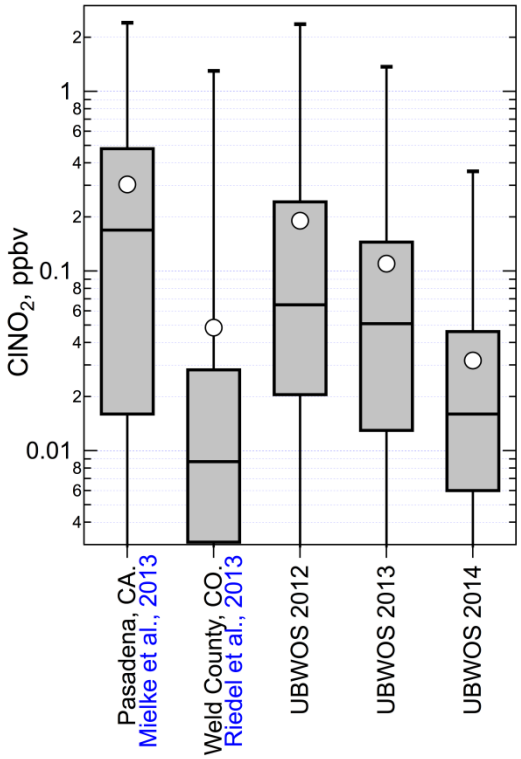

Figure 4-22. The distribution of $ClNO_2$ measured during the 3 UBWOS intensive studies at the Horsepool site compared to two data sets from Pasadena, CA., in summer 2010 and Weld County, CO., in winter 2011.

Possible snow surface reactions are an interesting aspect of $ClNO_2$ chemistry. Snow in this environment is highly perturbed by deposition of pollutants, particularly nitrogen oxides but also sulfate and chloride. The 2014 intensive had several time periods when there were inlets at different heights for extended lengths of time (days) when instruments sampled alternately from each inlet. One such period of $ClNO_2$ measurements in shown in Figure 4-23 when strong gradients were observed on some nights implying formation of $ClNO_2$ on snow surfaces. The snow measurements of chloride showed concentrations of at most 20 μM, however it should be noted that this was the average amount in the first 3 cm of the snow. Previous work on the efficiency of N_2O_5 conversion to $ClNO_2$, versus hydrolysis, shows quite low efficiencies at such low [Cl^-] [Roberts et al., 2009]. At temperatures found during UBWOS 2014, a quasi-liquid layer is present on the snow surface which might have sufficient Cl to permit the reaction of N_2O_5 to form $ClNO_2$. This is a likely scenario if the major sources of chloride to the snow or ground involve deposition of gases and particles.

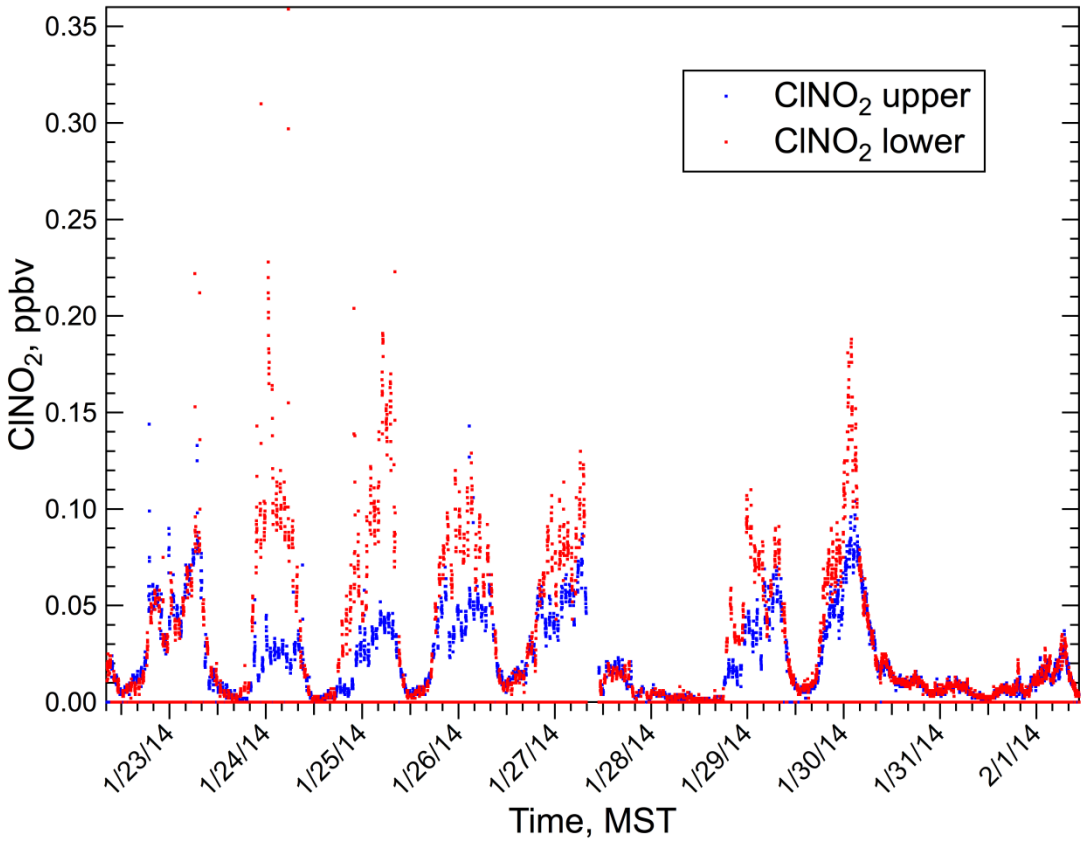

Figure 4-23. Timeline showing $ClNO_2$ levels measured through the top and bottom inlets.

4.4 Acetate Ion CIMS

During UBWOS 2014, a time-of-flight chemical ionization mass spectrometer (ToF-CIMS) using acetate as reagent ion was deployed at the Horsepool site to measure organic and inorganic acids. The instrument (ToF-CIMS) used in 2014 was selected over the quadruple CIMS used in 2012 and 2013, since the time-of-flight MS detector has a mass resolution up to 4000, compared with the unity mass resolution of a quadruple detector. The high mass resolution of ToF-CIMS is able to separate the signals of isobaric masses. For example, the signals of propionic acid ($C_3H_5O_2^-$) and glyoxylic acid ($C_2HO_3^-$) in acetate CIMS both have nominal mass of 73, but the signals of the two compounds are separated in the ToF mass spectra (Figure 4-24). Differencing the signals of methyl acrylic acid ($C_4H_5O_2^-$) from the fluorine impurity (CF_3O^-) is also demonstrated in Figure 4-24. The powerful ToF-CIMS can measure much more species in the atmosphere.

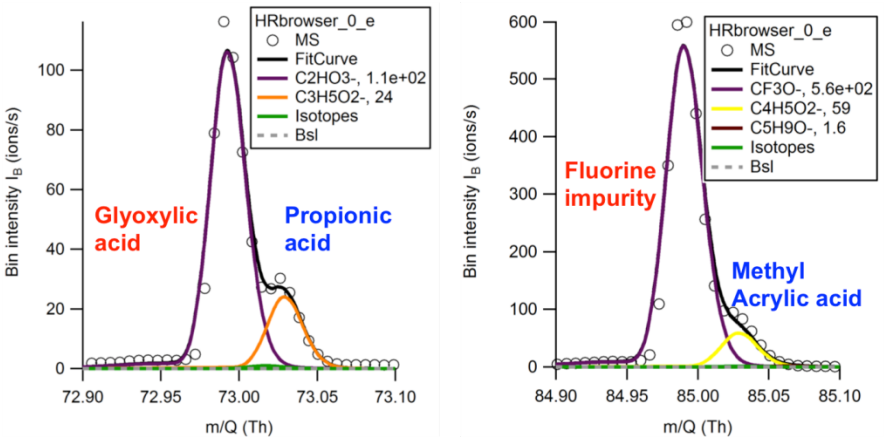

Figure 4-24. An example of high resolution fitting to ToF-CIMS mass spectra: m/Q 73 (left) and m/Q 85 (right).

One species that is measured in the three UBWOS campaigns is formic acid. Formic acid is mainly from secondary formation of hydrocarbon oxidation. This is consistent with daytime concentration maxima in the three different campaigns. The concentrations of formic acid were highest in 2013, followed by 2014 and then 2012 (Figure 4-25). It indicates that the photochemistry in 2014 is in somewhere between the conditions of 2012 and 2013. This observation is in agreement with ozone measurements. As discussed by several papers from UBWOS studies, the 2012 study was performed in the period without snow cover and no ozone enhancement was observed. In 2013, several ozone episodes were encountered.

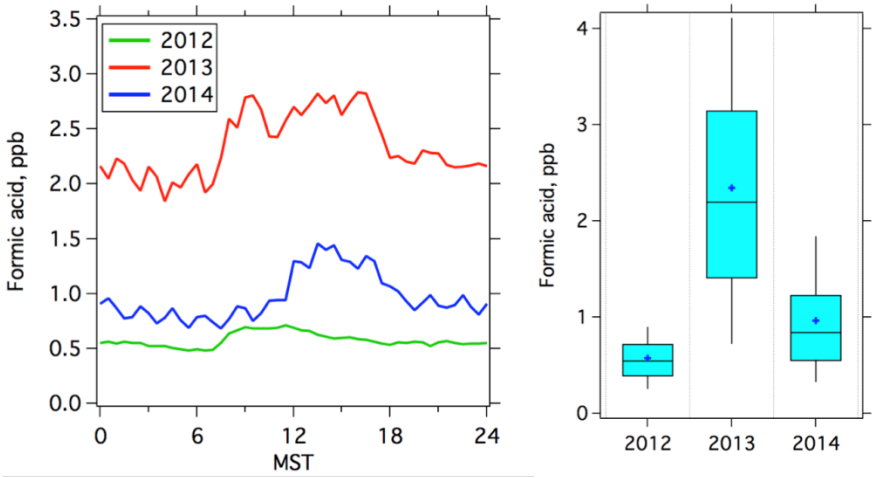

Figure 4-25. Comparison of formic acid concentrations in 2012-2014 at Horsepool site during UBWOS campaigns: (left) diurnal variations; (right) box-whisker plot. The blue markers are arithmetic mean of the concentrations.

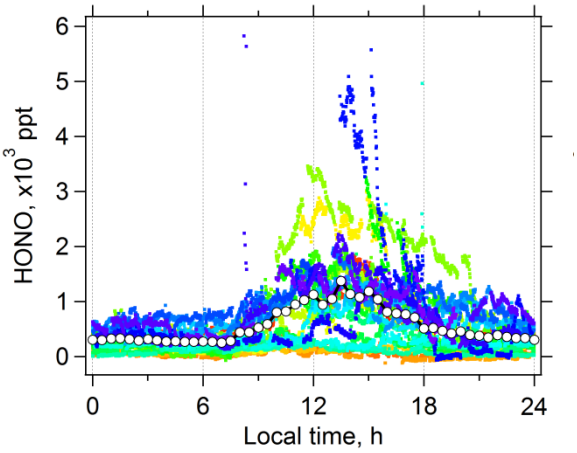

Figure 4-26. Diurnal variations of m/z 46 (NO_2^-) signals in acetate CIMS during UBWOS 2013. The open circles show the average over the whole campaign.

The other important species measured by acetate CIMS is HONO. HONO signal is recorded at m/z 46 (NO_2^-) in acetate CIMS. Very high levels of NO_2^- were measured during UBWOS 2013 with a maximum during the daytime (Figure 4-26). The noontime average of NO_2^- signals was equivalent to over 1 ppb of HONO and NO_2^- was as high as 5 ppb on several occasions during UBWOS 2013. These high levels of HONO were found to be inconsistent with ozone photochemistry in the atmosphere (Stoeckenius and McNalley, 2014). Laboratory experiments after the 2013 study showed that peroxynitric acid (HO_2NO_2) can also contribute to the signals of m/z 46 in acetate CIMS (Figure 4-27). Box model simulations show that peroxynitric acid can reach up to 0.5 ppb during the ozone accumulation periods (P. Edwards, personal communication, 2014). Typical polar/snow/ice measurements of HO_2NO_2 acquired in Antarctica ranged up to only 50 pptv [Slusher et al., 2002]. The NO_2^- signals in acetate CIMS measured in UBWOS 2014 are shown in Figure 4-28. The signals were generally lower than 1 ppb throughout the 2014 campaign. The average signal of NO_2^- in 2014 is also much lower than those measured in 2013. The lower NO_2^- signals in 2014 may be a result of several aspects: (1) the photochemistry in 2014 was not as strong as 2013 and peroxynitric acid produced from the reaction of NO_2 with HO_2 radicals was lower; (2) The setup of the acetate CIMS used in 2013 and 2014 has several differences, including acetic anhydride amount introduced into the radioactive ion source and flow tube pressures. These differences may affect calibration factors for both HONO and peroxynitric acid; (3) HONO may also be formed from peroxynitric acid in the inlet and the inlet configurations (e.g. resident time, temperature of the inlet) may be a large influencing factor for this processes.

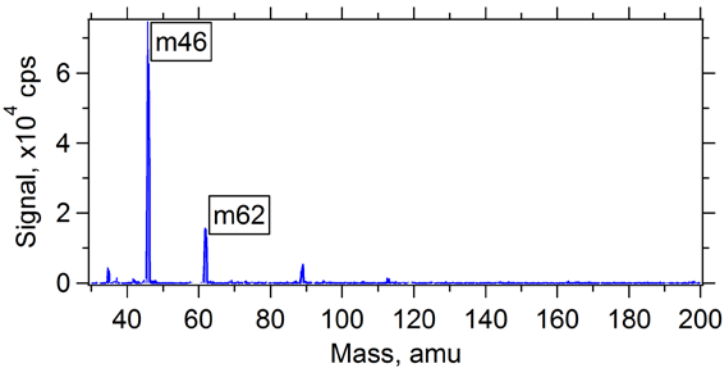

Figure 4-27. Mass spectrum of HO_2NO_2 in the acetate CIMS. There is trace amount of nitric acid (HNO_3) in the solution that may contribute to m/z 62 (NO_3^-) in the mass spectrum.

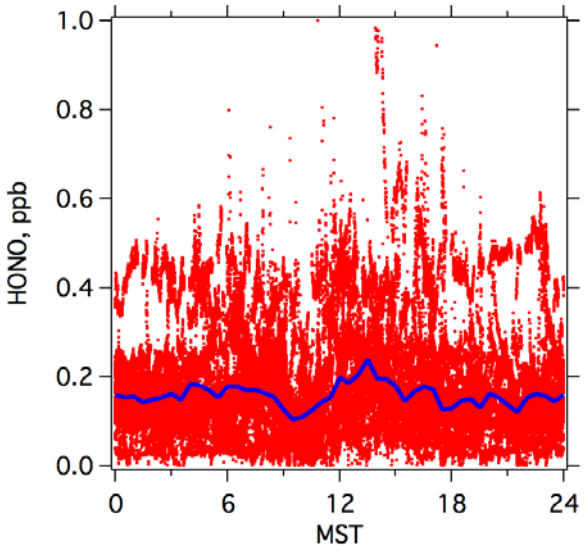

Figure 4-28. Diurnal variation of m/z 46 (NO_2^-) signals in acetate CIMS during UBWOS 2014. Blue trace is the average in the whole campaign.

4.4.1 Nitrous Acid (HONO) Summary

The principal unsolved questions around winter ozone left over from UBWOS 2013 revolved around the validity of the high daytime HONO measurements observed during that year, and the possibility of reactions on the snow source that only impact the lowest layer of the very stable PBL. The levels of HONO measured during UBWOS 2013 averaged slightly more than 1 ppbv and had an early afternoon maximum. These levels of HONO translated to unreasonably large radical sources leading to a profound over-prediction of O_3 by the MCM box model if assumed to be distributed throughout the whole box [Edwards et al., 2013]. The 2013 HONO measurements were made at two heights during part of the 2013 intensive, and there was evidence of a daytime snow source of HONO, partly resolving the conflict between the high

source and O_3 production since such a snow source would result in a rapid decrease in HONO with height, thus limiting the radical source.

The UBWOS 2014 intensive measurements at Horsepool included deployment of four *in situ* instruments and one open-path optical method for HONO (Table 4-2). In addition a number of inlet tests were performed, including varying the length of inlets and sampling points. Where possible, two in situ measurements were placed on the same inlet, however this was not possible for the Acetate-ToF due to pressure feedback issues, and in the case of the LOPAP, which uses a scrubbing coil at the inlet. Comparisons of these methods were done by placing all the inlets at the same location (the point marked "Box Level Inlets" in Figure 4-20, which is at 9.1m agl). Configuration of the DOAS instrument and light path were essentially the same as those deployed during UBWOS 2012, with similar retroreflector heights of 28m, 45m, and 68m agl relative to Horsepool base elevation, while the average heights of the light paths above the ground were somewhat lower than 2012 due to the slope of the terrain.

The iCIMS measurement of HO_2NO_2 was a key addition to the portfolio in UBWOS 2014 and enabled some important diagnostic analyses on the possible interference of HO_2NO_2 in the HONO instruments as described in Veres et al., 2015 and described here. The instrument configuration, shown in Figure 4-29 was different from previous years in that automated valves were included to permit the inlet dissociation zone to be by-passed, and sampling to be switched between two inlets. Peroxynitric acid was observed at two different ions depending on inlet mode, either $I{\bullet}HO_2NO_2^-$ (m/z = 206) when the air was passed through the room temperature inlet, or $I{\bullet}HO_2^-$ (m/z = 160) when the air passed through the dissociator at 130°C. The HO_2NO_2 signals due to each ion were calibrated in the laboratory after the project, and timelines for measurements in both modes are shown to be in quite reasonable agreement (Figure 4-30), with exception of higher signal for the $I{\bullet}HO_2^-$ ion during the very cleanest periods, likely due to ambient HO_2 radicals, which will also be detected at that ion.

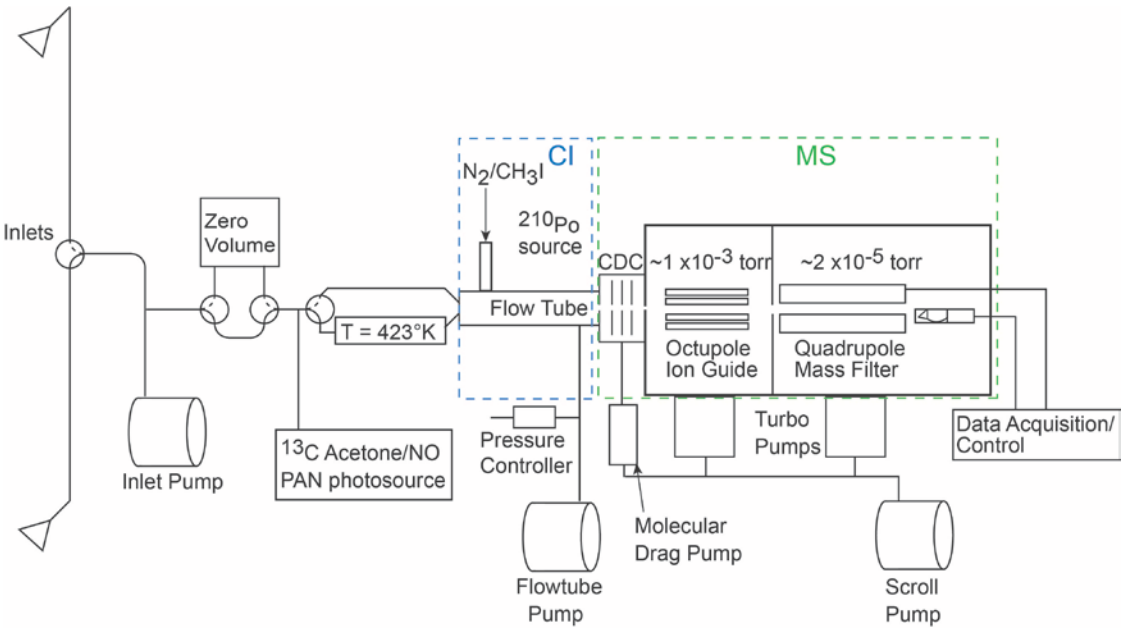

Figure 4-29. Schematic diagram of the iCIMS used to measure nitrogen species during UBWOS 2014.

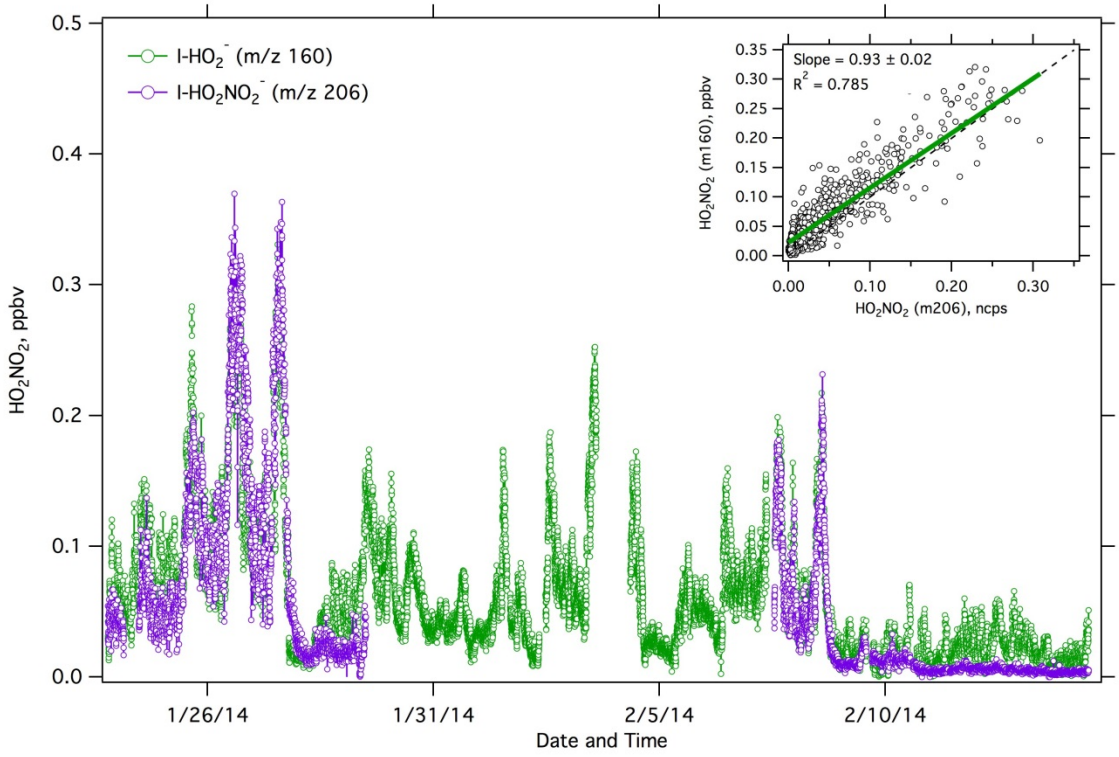

Figure 4-30. Timelines of the two different measurements of HO_2NO_2 made by the iCIMS during UBWOS 2014.

A summary of HONO measurements is shown in Figure 4-31 showing all measurements for all three UBWOS campaigns, and two additional data sets for comparison. Several features are clear: while the UBWOS measurements were only slightly higher than those observed in Pasadena, the UBWOS 2013 data showed an early afternoon maximum which would correspond to a very large OH radical source. In contrast, the highest HONO in Pasadena was observed at night. The long-path DOAS HONO was the lowest of the UBWOS 2014 datasets, and the other datasets had medians that were 2-3 times higher, and their highest observations were considerably higher than the DOAS. Some reasons for the higher numbers include the fact that the DOAS data are spatially and temporally averaged, and some of the high values may be due to interferences in the *in situ* measurements.

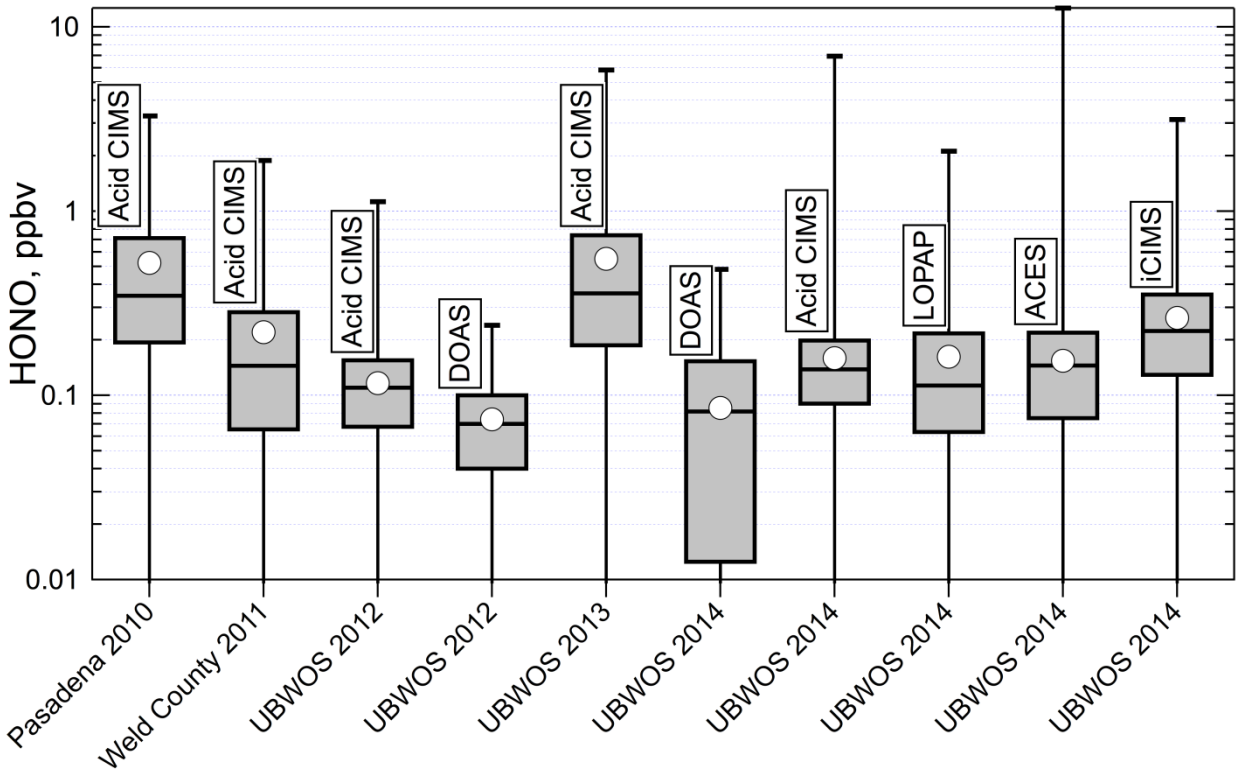

Figure 4-31. Summary of HONO measurements from the three UBWOS campaigns and two previous campaigns that used the Acid CIMS instrument. Symbols used in each box and whisker are the same as previous such plots.

The timeline of HONO measurements shown in Figure 4-32 corresponded to a period of approximately 5 days during which all the in situ instruments were measuring and had at least one inlet at box-level. This subset of the data will be referred to as the "common period", and will be used to examine instrument performance. The timeline (Figure 4-32a) shows considerable variability among the results, with the DOAS generally lower than the *in situ* methods. Comparison of results by correlation with either LOPAP (Figure 4-32b) or DOAS (Figure 4-32c) confirm this. Other intercomparison studies of HONO measurement techniques

have been conducted, mostly under summertime urban conditions, however there is evidence of intereferences in *in situ* measurements such as mist chamber and LOPAP techniques in cold polar environments, including one study that reports a 15% interference in a LOPAP instrument from HO_2NO_2 [Legrand, 2014].

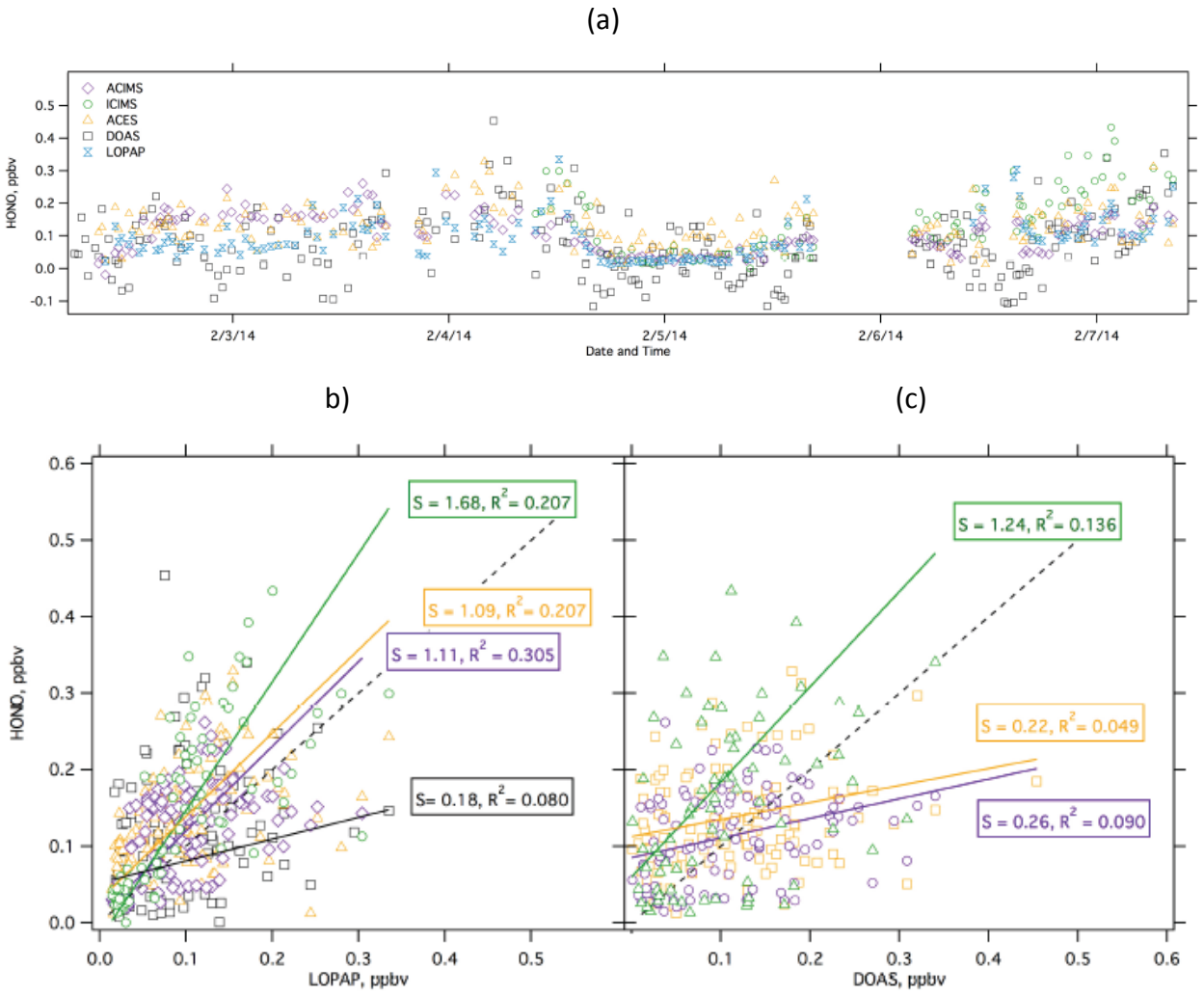

Figure 4-32. Comparison of the four *in situ* and DOAS HONO measurements. Panel (a) shows the timeline of the "common period" (see text), and panels (b) & (c) show the correlations of HONO measurements with either the LOPAP (panel b) or DOAS (panel c). The legend in panel (b) is the same as in panel (a), and the symbol colors in in panel (c) are the same as in the legend in panel (a).

The comparison of HO_2NO_2 and HONO signals detected by the iCIMS when the instrument alternated between a 30°C 20m long inlet, and an ambient temperature inlet of 3m length provided a key tests of inlet interferences due to HO_2NO_2. The results of a two day period with the iCIMS in this configuration are shown in Figures 4-33(a&b). These figures show daytime signals for HO_2NO_2 measured through the short inlet that are present in the HONO signal

measured through the warm long inlet. Our tentative conclusion from this is that inlet effects can result in HO_2NO_2 being detected as HONO, hence interfering with that measurement. The precise mechanism for this effect is not entirely clear since the gas phase decomposition of HO_2NO_2 proceeds via the radical channel;

$$HO_2NO_2 + M \Rightarrow HO_2 + NO_2$$

This mechanism is also thought to dominate in acidic aqueous solution [Goldstein et al., 2005]. The neutral pH mechanism of solution-phase decomposition proceeds through formation of O_2 and nitrite about 50% of the time [Goldstein et al., 1998];

$$HO_2NO_2 + surface_{(aq)} \Rightarrow H^+ + NO_4^-$$

$$NO_4^- \Rightarrow NO_2^- + O_2$$

$$NO_2^- + H^+ \Rightarrow HONO$$

The surface of the inlets was made out of PFA Teflon, and based on temperature and absolute humidity, would not have had liquid water on it. However, the tests imply that there is a surface reaction that forms nitrite, and hence nitrous acid, similar to the laboratory observations of Zhu, et al., [1993] on glass surfaces. The diurnal profiles of these HO_2NO_2 and HONO signals is consistent with this view, as concentrations HO_2NO_2 peak in the daylight due to its photochemical source and are much lower at night. The conclusion from this test is that all the measurements that employed a long inlet were most likely compromised by this effect, and have an apparent daytime signal of HONO that is actually due to HO_2NO_2.

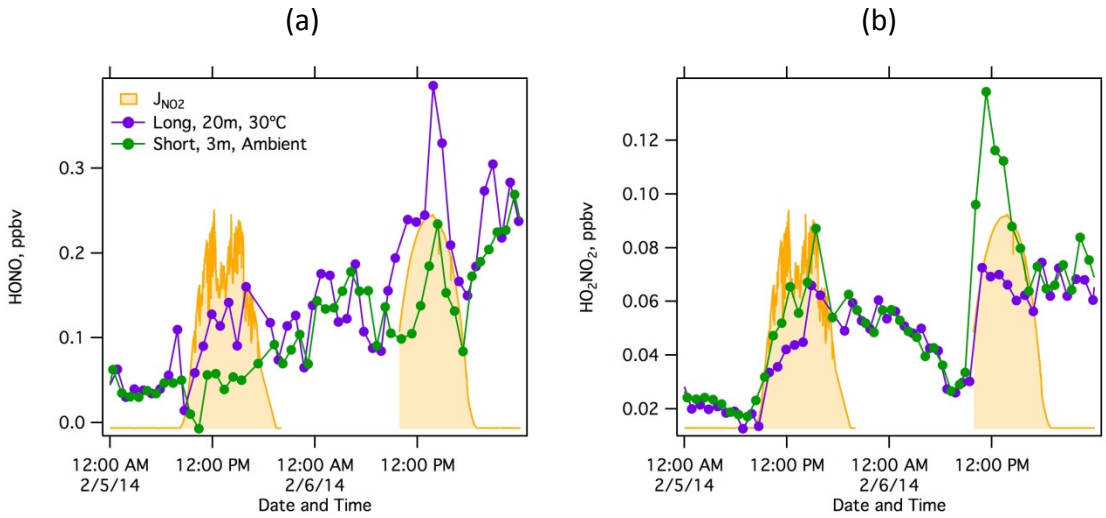

Figure 4-33. The timelines of the short and long inlet tests performed with the iCIMS. Panel (a) shows the HONO, and panel (b) shows the HO_2NO_2 detected.

The possibility of chemical interferences in the techniques that used solution-phase or gas-phase ion chemistries also needs to be considered. Such an interference would be due to the

particular chemistry involved in the HONO detection scheme. Definitive conclusions about interferences will require thorough laboratory investigations. However there are some conclusions that can be drawn based on current evidence in the literature and our preliminary work. The Acid CIMS results from UBWOS 2013 imply a significant interference at NO_2^- due to HO_2NO_2, that may be a fundamental aspect of the ion chemistry. The thermodynamics that govern the acetate ion NI-PT-CIMS usually involve a simple proton transfer, the probability of which is governed by gas-phase acidities, and any reaction for which the ΔG is negative will undergo the following proton abstraction reaction;

$$CH_3C(O)O^- + HA \Rightarrow CH_3C(O)OH + A^-$$

In practice, acetate ions are often clustered with H_2O or acetic acid, changing the thermodynamics slightly, but often making the reaction rate faster. Unfortunately, the gas phase acidity of HO_2NO_2 has not been measured, but its aqueous-phase acidity constant, pKa is about 6.8, implying that the gas phase acidity would not be favorable, based on our experience that gas phase acidity roughly correlates with pKa. The complicating factor for HO_2NO_2, and its conjugate anion, $O_2NO_2^-$ are that the HO_2-NO_2, and O_2-NO_2- bonds are quite weak, presenting the possibility of the reaction;

$$CH_3C(O)O^- + HO_2NO_2 \Rightarrow CH_3C(O)OH + O_2 + NO_2^-$$

which would constitute a direct interference in the Acid CIMS measurement. A good correlation of the Acid CIMS signal due to HO_2NO_2 would be evidence of such in interference. Figure 4-34 shows a good correlation between HONO measured by the Acid CIMS in the daytime, and the HO_2NO_2 measured by the iCIMS, yielding strong evidence for this chemical interference. Another piece of evidence for this interference is that the average apparent Acid CIMS HONO signal observed in 2013 was consistent with the HO_2NO_2 predicted by the MCM model [Edwards et al., 2014]. Further laboratory tests will be needed to confirm this interference.

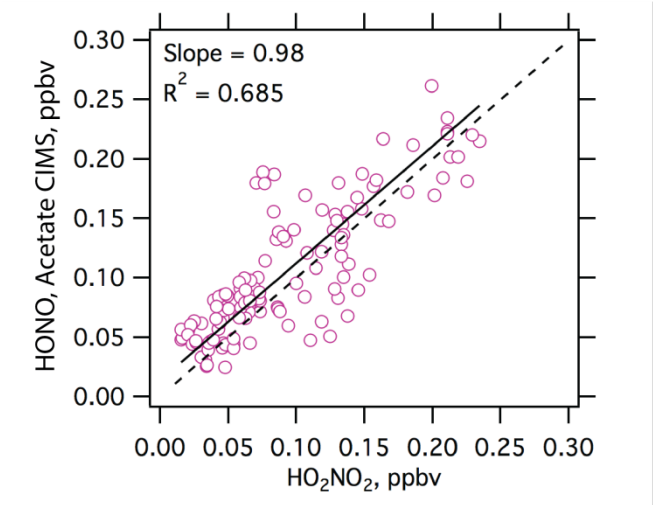

Figure 4-34. The correlation of HONO measured during the daytime by the acetate ion CIMS and the HO_2NO_2 measured by the iCIMS during UBWOS 2014.

The other instrument for which a chemical interference is known or suspected is the LOPAP method. A 15% interference has been estimated for the response of the LOPAP to PNA in laboratory studies [Legrande et al., 2014]. The average diurnal profiles of LOPAP HONO and iCIMS PNA are shown in Figure 4-35 and show very similar temporal profiles. This is circumstantial evidence for some interference in the LOPAP method although it would need to be larger than the 15% reported above. The LOPAP instrument used in UBWOS 2014 is the same instrument deployed in the Wyoming Upper Green River Basin ozone study described by Rappengluck et al,. [2014]. While not definitive, the UBWOS results imply that the high daytime HONO observed in Wyoming might have some contribution from PNA.

A summary of the performance and current assessments of the inlet and chemical interferences are given in Table 4-2. While these methods may function well in some environments, e.g. summertime urban areas, in the UBWOS environment, unusually high PNA compromises all but the DOAS measurement. Accordingly, we will use only the DOAS measurements in further assessments of HONO in the daytime and potential ground or snow sources.

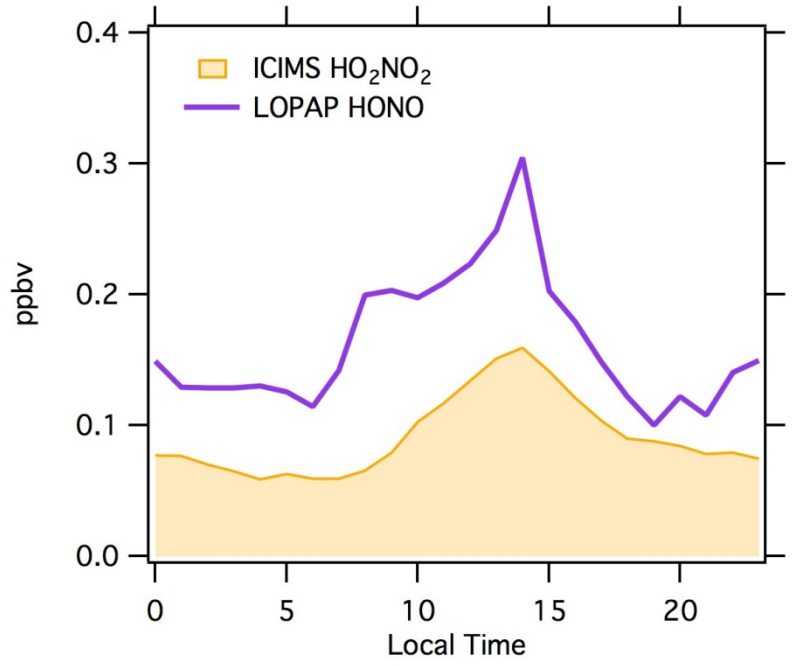

Figure 4-35. Average diurnal profiles of HONO observed by the LOPAP, and PNA observed by the iCIMS during UBWOS 2014.

Table 4-2. Summary of the HONO measurements during UBWOS 2014.

Instrument Name	Principle of Operation	Detection Limit	Time Constant	Inlet Interference[a]	Chemical Interference[a]
Acid CIMS	Acetate ion NI-PT-CIMS	10 pptv	10 sec	+	+
LOPAP	Chemical Derivatization UV-Absorption	10 pptv	3 min	?	+
iCIMS	Iodide ion CIMS			+	-
ACES	Broad-band Cavity Enhanced Spectroscopy	0.2 ppbv	1 min	+	-
DOAS	Long-path UV Absorption Spectroscopy	30 pptv	20 min	-	-

[(a)] A '+' indicates an observable effect, '-' indicates no observable effect; potential LOPAP inlet interferences could not be assessed independently.

The DOAS results are summarized in Figure 4-36 which shows the diurnal profile of both UBWOS 2014 and UBWOS 2012 data. The profiles for all three light path heights show similar values and temporal changes with the exception of afternoon values during 2014, which showed distinctly higher values, and a gradient, with higher values at the surface. This surface source is consistent with some process or processes that release HONO at the snow surface. The height profile implied by this source is broadly consistent with the gradient analysis described in the UBWOS 2013 Final Report. The conclusions from the UBWOS 2013 analysis therefore also pertain to UBWOS 2014, this apparent HONO source is only a minor contributor to the photochemical radical budget of the polluted boundary layer in the Uintah Basin.

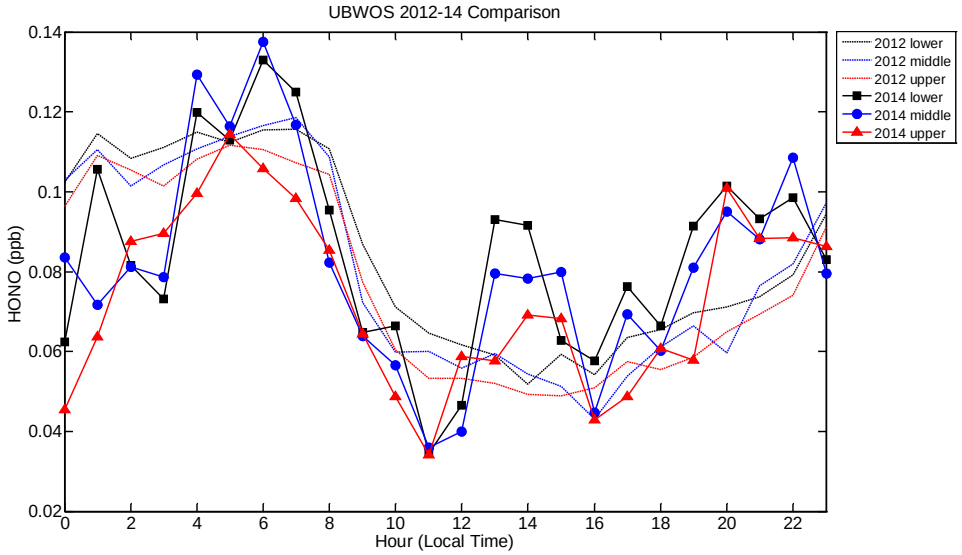

Figure 4-36. Comparison of the diurnal profiles of HONO measured by DOAS in 2012 (dashed lines), and 2014 (solid lines), for all three light paths.

4.4.2 Snow Chemistry

During the UBWOS 2014 Horsepool intensive period, the concentrations of sulfate, nitrate, and calcium in the surface snow increased with time [Figure 4-37] until a snow fall event on January 30, 2014 that blanketed the surface layer. Nitrate concentrations were more than an order of magnitude higher than sulfate concentrations. Sulfate and nitrate concentrations in 2014 were similar to those measured in 2013. Calcium concentrations, however, were much higher in 2014 because of the exposed soil that was blown onto the surface snow. Particulate and dissolved organic carbon and black carbon concentrations were all higher prior to the snow-fall event [Figure 4-38]. The high concentrations of soil in the surface snow were responsible for most of the measured aerosol light absorption.

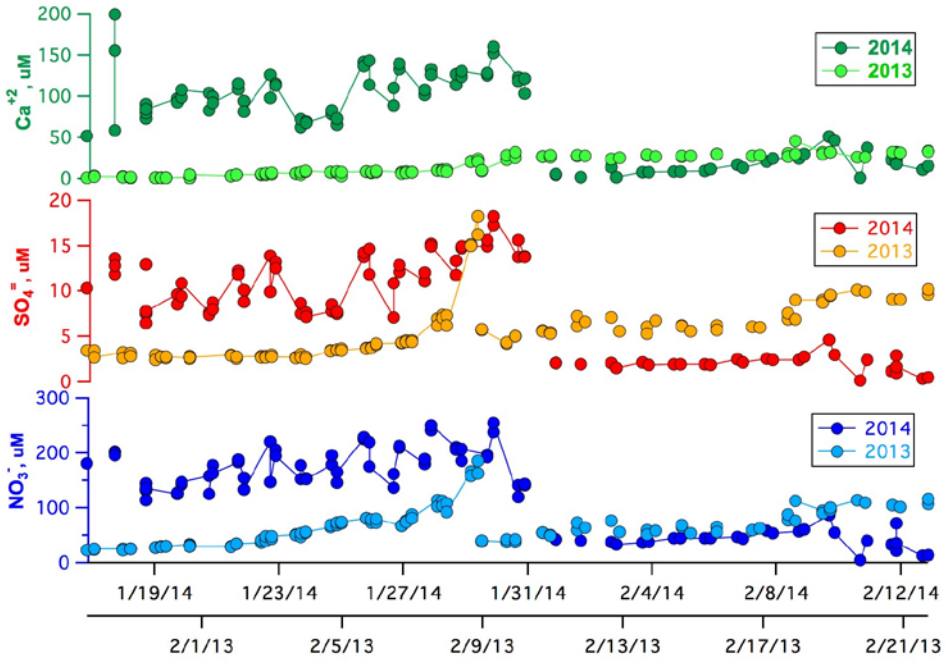

Figure 4-37. The concentrations of sulfate, nitrate, and calcium in the surface snow during UBWOS 2014.

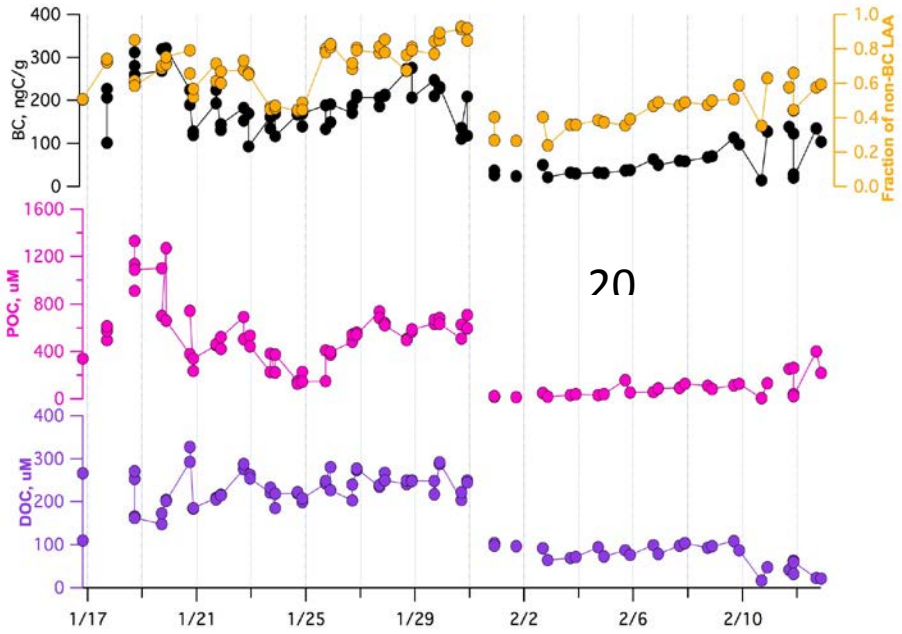

Figure 4-38. Particulate and dissolved organic carbon and black carbon concentrations measured in the surface snow during UBWOS 2014.

The observations of the nitrogen isotopic composition of nitrate ($d^{15}N(NO_3^-)$) in snow and atmospheric aerosol during UBWOS 2014 showed that active snow photochemistry was only apparent on days with fresh snowfall. There was no fresh snowfall for over a month before the campaign start date, which allowed for continuous deposition of dust onto the snow surface. Dust hampers snow photochemistry primarily because dust absorbs ultraviolet radiation. Figure 4-39 shows data from three (out of twelve) snowpits sampled on January 22, January 31, and February 4, 2014. Figure 4-39b from January 22 shows the existence of a surface dusty layer with high concentrations of light absorbing impurities. The aerosol $\delta^{15}N(NO_3^-)$ value shown in Figure 4-39a is similar to $\delta^{15}N$ values of anthropogenic NO_x sources, suggesting minimal influence of snow-sourced NO_x on atmospheric nitrate abundance. Similarly, the snowpit profile of $\delta^{15}N(NO_3^-)$ from January 22 is not suggestive of active snow photochemistry. Figures 4-39a and 4-39b are representative of all snowpits dug before fresh snowfall occurred midway through the campaign. Three inches of snow fell between January 30th and January 31st and the dusty layer was buried beneath the fresh snow (Figure 4-39d). Figure 4-39c shows that snow $\delta^{15}N(NO_3^-)$ values are lowest at the surface and increase with depth until the top of the dusty layer, a profile indicative of active snow photochemistry within this fresh layer of snow. The aerosol $\delta^{15}N(NO_3^-)$ values are lower on January 31st compared to the other days of the campaign, further suggesting that active photochemistry is releasing reactive nitrogen to the overlying atmosphere immediately after fresh snowfall. The next snowpit from February 4 (Figures 4-39e and f) was dug five days after the fresh snow event. By this time, a new dusty layer had formed on the surface of the snow (Figure 4-39f). The air and snow $\delta^{15}N(NO_3^-)$ values suggest that the degree of photochemical activity in snow had decreased (Figure 4-39e)

compared to January 31. Future work will include the use of a snow chemistry model constrained by these observations to quantify the flux of reactive nitrogen from the snow during the 2014 campaign.

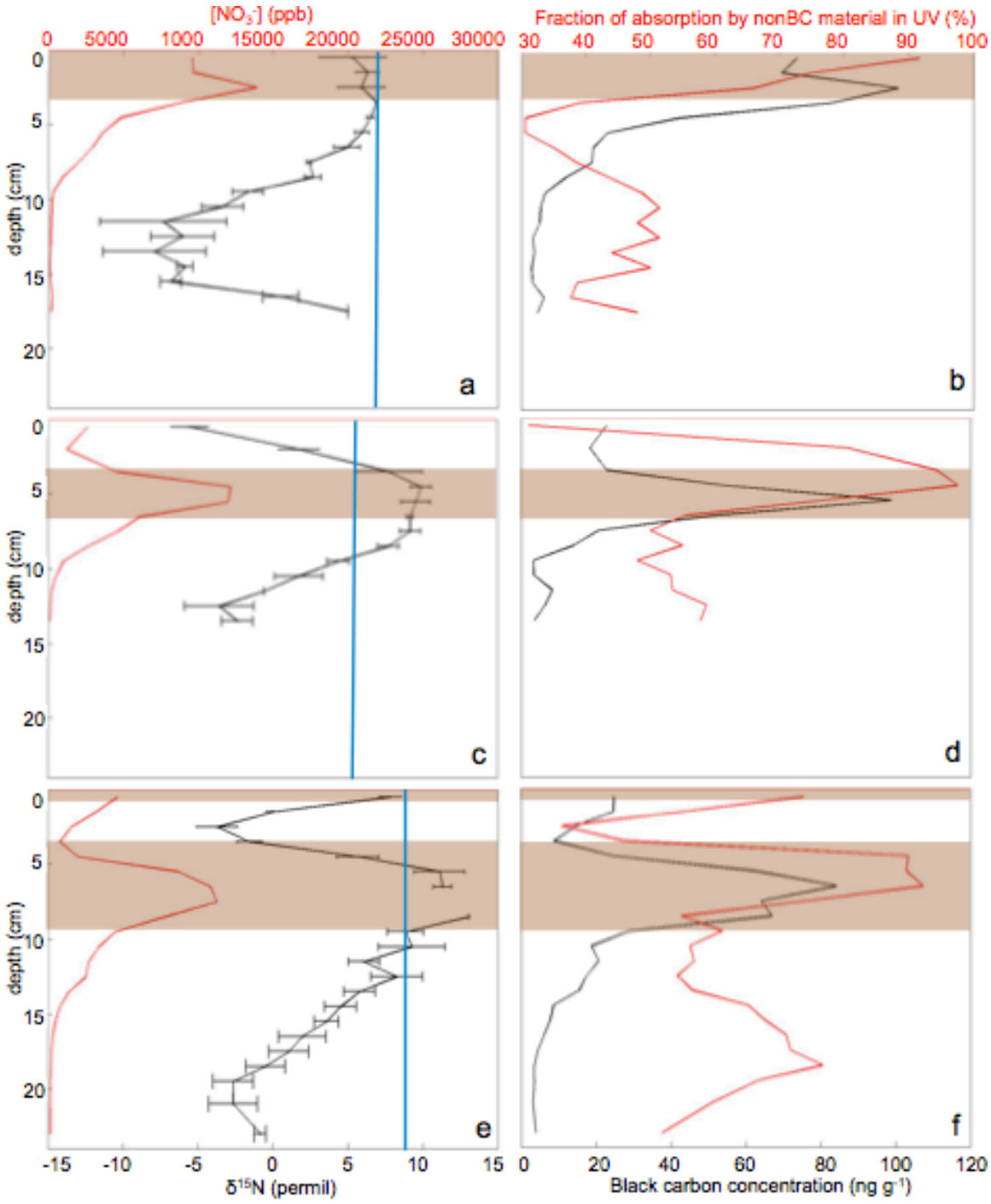

Figure 4-39. Chemistry (left column) and optical data (right column) measured in snow and air on January 22nd (a, b), January 31st (c, d), and February 4th (e,f). The brown shading shows the location of the dusty layer in each snowpit. Panels a, c, e: Snow nitrate concentrations (ppb, red), $\delta^{15}N(NO_3^-)$ in snow (‰, black) and air (blue). Panels b, d, f: Snow black carbon concentrations (ng g^{-1}, black) and fraction of ultraviolet absorption by non-black carbon material in snow (%, red).

4.4.3 Particulate Matter

The average diameter of the submicrometer atmospheric aerosol in 2014 was between that measured in 2012 and 2013 [Figure 4-40]. As a result, the average $PM_{2.5}$ ambient relative humidity (RH) surface area was also between that calculated for 2012 and 2013. The average surface area was 60, 270, and 160 um^2 cm^{-3} in 2012, 2013 and 2014, respectively. In 2014 there were periods when the aerosol concentrations became very low and new particle nucleation was observed (Figure 4-41, January 29). During the stagnation periods, the aerosol number size grew during the afternoon but decreased again during the night most likely from dilution with air from above the inversion. Campaign averaged nitrate and ammonium data from the aerosol mass spectrometer showed a minimum in concentrations at 0600-0700 and an increase in concentrations until 2000-2100 [Figure 4-42]. Ammonium and nitrate were highly correlated in a ratio (0.32) roughly consistent with NH_4NO_3, which is 0.290. No diurnal cycle was evident in the sulfate or particulate organic matter concentrations, implying deposition at night did not have a large impact on ambient levels of these particles..

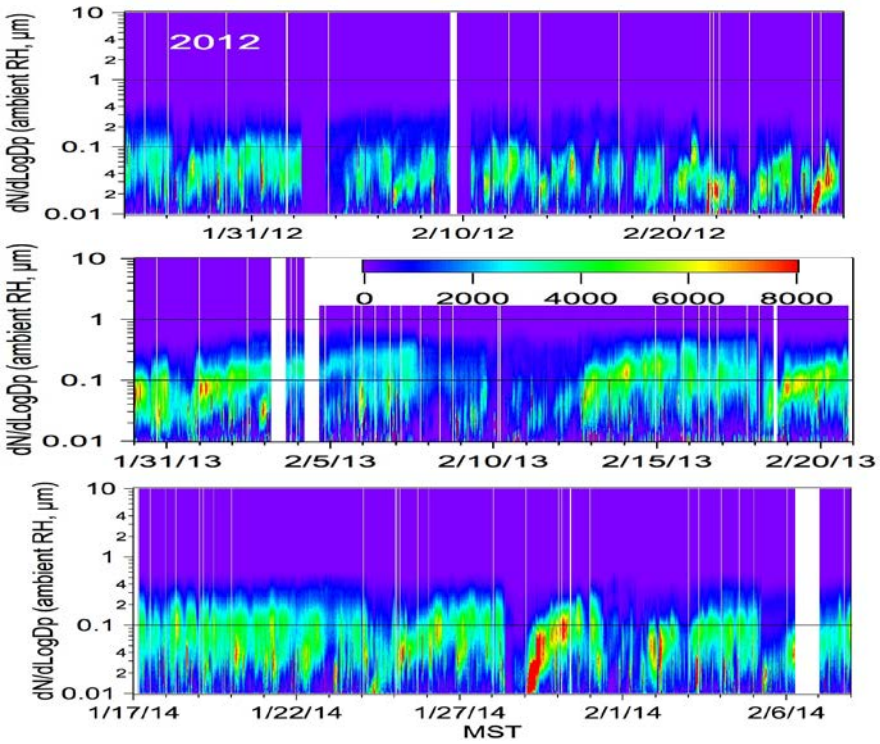

Figure 4-40. Distributions of aerosol diameter for the 2012, 2013, and 2014 UBWOS intensives.

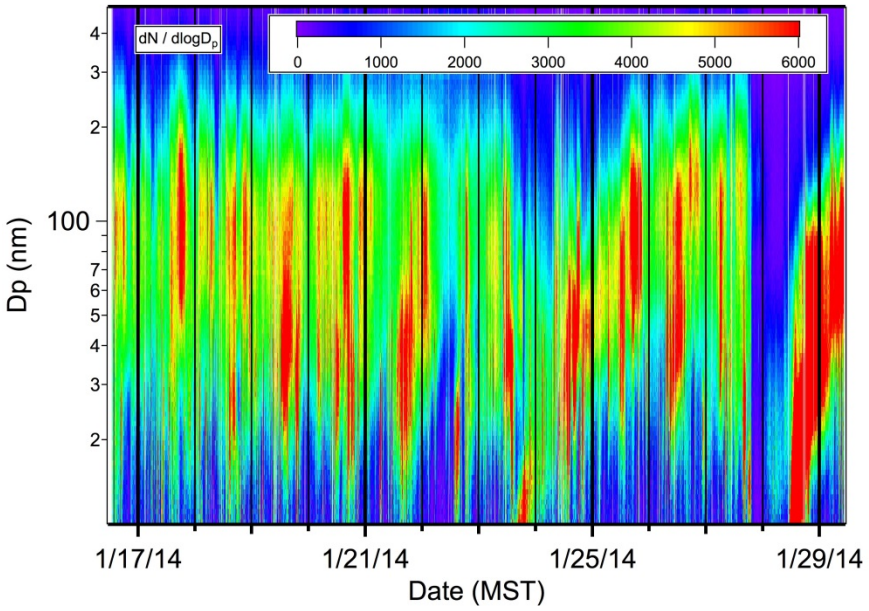

Figure 4-41. Size spectra of atmospheric particles during the early part of the UBOS 2014 Horsepool intensive.

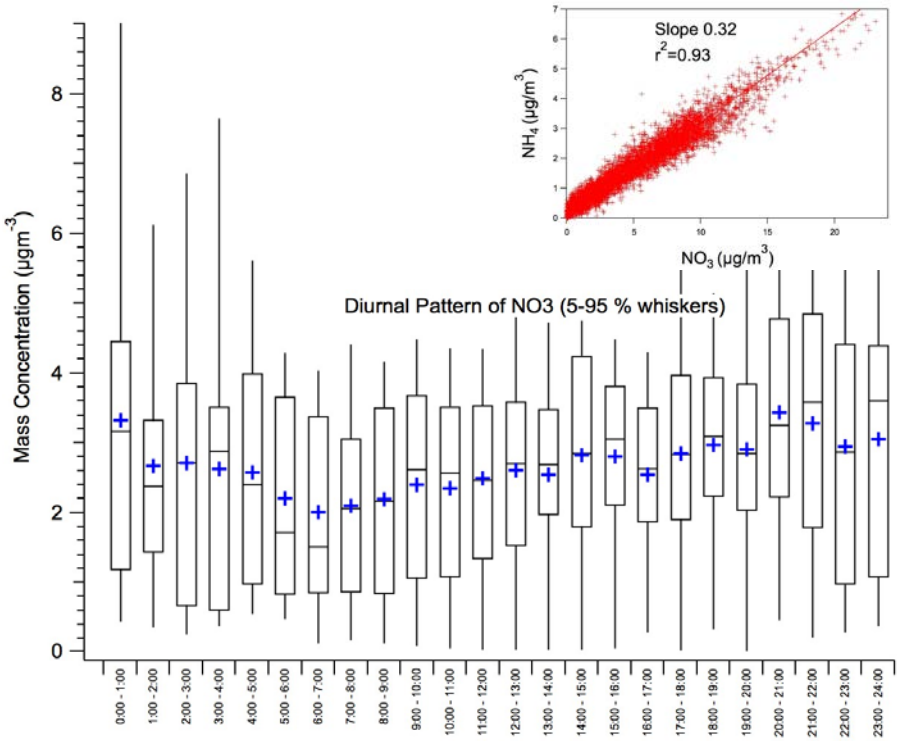

Figure 4-42. Aerosol mass concentration as a function of time of day during the UBWOS 2014 Horsepool intensive study.

Non-soil $PM_{2.5}$ mass concentrations in 2014 occasionally reached levels measured in 2013 although on average were greater than in 2012 and less than in 2014 [Figure 4-43]. Total $PM_{2.5}$ was highest during 2014 with the addition of the soil particles. Soil concentrations were generally highest during the day presumably a result of the increased vehicle traffic re-suspending soil from snow-free roads.

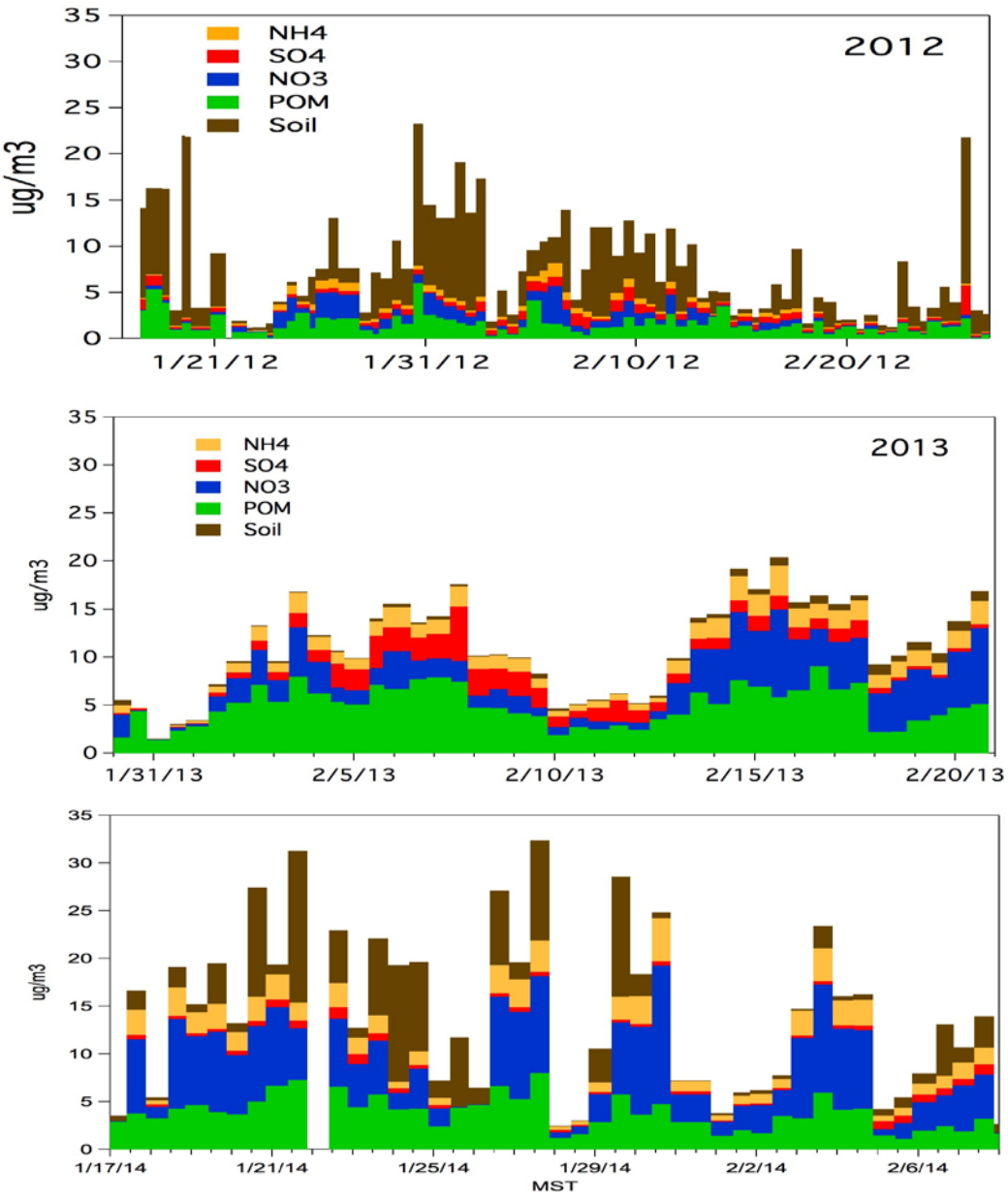

Figure 4-43. Contributions to aerosol mass during the 2012, 2013, and 2104 UBOS intensive studies at Horsepool.

4.5 Conclusions

The Uintah Basin did not experience prolonged intense O_3 events during the 2014 campaign, rather there were several instances when stagnant cold pools started to form and O_3 started to build-up as was observed in 2013, only to have the cold pool break-up. While the cold pool events did not last as long, the chemistry observed during them mimicked the first few days of typical ozone events seen in the 2013 data. Results from the UBWOS 2014 Horsepool intensive study settle the major outstanding questions that remain from the previous two campaigns. The *in situ* measurements of HONO were all found to be compromised to some extent by a combination of inlet effects due to HO_2NO_2 decomposition, and chemical interferences. The long path DOAS measurement, which does not suffer from these effects, showed HONO to be essentially the same as during the 2012 intensive, with the addition of a surface source of HONO during the afternoon. The timing and gradient of the daytime HONO implies a snow chemistry source that could be due to prompt HO_2NO_2 decomposition, or due to build-up and storage of NO_2^- overnight on the snow surface, with volatilization driven by acid deposition. This surface HONO does not represent a significant radical source to the entire boundary layer. As in the 2013 intensive, formaldehyde and associated carbonyls are the major radical sources driving O_3 production. The VOC-NOx chemistry that takes place during O_3 episodes tends to amplify the OVOC and alkylnitrate products. These findings amplify the need to understand the location, nature, and magnitude of the VOC sources in the Uintah Basin.

4.6 References

Baker, A.K. et al., (2008), Measurements of nonmethane hydrocarbons in 28 United States cities, *Atmos. Environ.*, 42, 170-182, doi.org/10.1016/j.atmoenv.2007.09.007.

Chang, W. L., P. V. Bhave, S. S. Brown, N. Riemer, J. Stutz, and D. Dabdub (2011), Heterogeneous atmospheric chemistry, ambient measurements, and model calculations of N_2O_5: A review, *Aer. Sci. Technol.*, *45*, 655-685, doi:10.1080/02786826.2010.551672.

Edwards, P.M. et al., (2013), Ozone photochemistry in an oil and natural gas extraction region during winter: Simulation of a snow-free season in the Uintah Basin, Utah. *Atmos. Chem. Phys.*, 13, 8955-8971.

Edwards, P.M. et al., (2014), High winter ozone pollution from carbonyl photolysis in an oil and gas basin, *Nature,* accepted.

Gilman, J.B. et al., (2008), Measurements of volatile organic compounds during the 2006 TexAQS/GoMACCS campaign: Industrial influences, regional characteristics, and diurnal dependencies of the OH reactivity, *J. Geophys. Res.*, 114, doi: 10.1029/2008JD011525.

Gilman, J.B., B.M. Lerner, W.C. Kuster, J.A. deGouw, (2013), Source signature of volatile organic compounds from oil and natural gas operations in Northeastern Colorado, *Environ. Sci Technol.*, 47, 1297-1305.

Goldstein, S., G. Czapski, J. Lind, G. Merenyi, (1998) Mechanism of Decomposition of Peroxynitric Ion (O_2NOO^-): Evidence for the Formation of $O_2\bullet^-$ and $\bullet NO_2$ Radicals, *Inorg. Chem.*, 37, 3943-3947.

Goldstein, S., J. Lind, G. Merenyi, (2005) Chemistry of peroxynitrates as compared to peroxynitrates, *Chem. Rev.,* 105, 2457-2470, doi:10.1021/cr0307087.

Legrand, M. et al., (2014), Large mixing ratios of atmospheric nitrous acid (HONO) at Concordia (East Antarctic Plateau) in summer: a strong source from surface snow?, *Atmos. Chem. Phys.*, 14, 9968-9976, doi: 10.5194/acp-14-9963-2014.

Mielke, L. H., et al. (2013), Heterogeneous formation of nitryl chloride and its role as a nocturnal NOx reservoir species during CalNex-LA 2010, *J. Geophys. Res.*, *118*, doi:10.1029/2013JD019655.

Riedel, T. P., et al. (2013), Chlorine activation within urban or power plant plumes: Vertically resolved $ClNO_2$ and Cl_2 measurements from a tall tower in a polluted continental setting, *J. Geophys. Res.*, *118*, doi:10.1002/jgrd.50637.

Roberts et al., (2009) Laboratory Studies of Products of N_2O_5 Uptake on Cl^- Containing Substrates, *Geophys. Res. Lett.*, 36, L20808, doi:10.1029/2009GL040448.

Slusher, D. L., et al. (2002), Measurements of pernitric acid at the South Pole during ISCAT 2000, *Geophys. Res. Lett.*, *29*, doi:10.1029/2002GL015703.

Stoeckenius, T. and D. McNally, 2014. 2013 Uinta Basin Winter Ozone Study. Till Stoeckenius and Dennis McNally, eds., ENVIRON International Corp., Novato, CA, March. Available at http://www.deq.utah.gov/locations/U/uintahbasin/ozone/strategies/studies/UBOS-2013.htm.

Veres, Patrick R., James M. Roberts, Robert Wild, Peter M. Edwards, Steve S. Brown, Timothy S. Bates, Patricia K. Quinn, James E. Johnson, Robert J. Zamora, and Joost de Gouw, Peroxynitric acid (HO_2NO_2) measurements during the UBWOS 2013 and 2014 studies using iodide ion chemical ionization mass spectrometry, Atmos. Chem. Phys., submitted, 2015.

Zhu, T., G. Yarwood, J. Chen, and H. Niki. (1993), Evidence for the heterogeneous formation of nitrous acid from peroxynitric acid in environmental chambers, *Environmental Science & Technology,* 27, No. 5: 982-983.

5.0 EMISSION INVENTORY DEVELOPMENT ACTIVITIES

Authors
Patrick Barickman, Utah Division of Air Quality
Stuart McKeen, National Oceanic and Atmospheric Administration
Ravan Ahmadov, National Oceanic and Atmospheric Administration
Seth Lyman, Bingham Entrepreneurship & Energy Research Center, Utah State University, Vernal, Utah

5.1 Introduction

With the exception of the NOAA "Top Down" inventory described in section 5.2, the oil and gas emission inventories used for photochemical modeling in the Uinta Basin have been based on the WRAP Phase III inventory work updated in 2009 by the Western Regional Air Partnership (WRAP).[i] Efforts have been underway during 2014 to create a new inventory for the Basin that is no longer tied to the Phase III inventory and work plans are in place to continue this effort during 2015. This chapter outlines the state of the inventory along with several projects now underway among research groups and regulatory agencies who share responsibilities in the Basin.

The Bureau of Land Management, through the Air Resource Management Strategy (ARMS) study, updated the Phase III inventory to a 2010 base year and used this inventory to perform full-year episode modeling in support of NEPA analysis.[ii] The Bingham Research Center at USU in Vernal has now taken over the analysis and refinement of the ARMS study and is currently working on updating the emissions inventory for this model. The WRAP has completed full-year modeling of 2008 base year ozone modeling as the first step of a multi-year modeling project to provide regional modeling resources to states in the Western US.[iii] In addition, EPA, ORD (Office of Research and Development) have been working on full-year ozone modeling covering the entire US using the National Emissions Inventory database (NEI).

The Utah Division of Air Quality (UDAQ) provided a significant update to the WRAP Phase III inventory for its submission to the EPA's 2011 NEI.[iv] This inventory has been used by the photochemical modeling group at UDAQ for winter ozone simulations during a January, 2013 episode allowing observations taken during the 2013 UBOS field campaign to be used in model performance evaluation. A top-down inventory, described in section 5.2, has been used by photochemical modelers at NOAA in Boulder, Colorado.

5.2 The NOAA Top-Down Oil and Gas Inventory

Details of a top-down based oil/gas sector emissions inventory, and its application within a regional 3-D photochemical study of the Uinta Basin, are provided in *Ahmadov et al.* [2014][v]. The inventory is based on the 55,000 kg/hr methane flux estimate from the Basin determined during a single aircraft flight during the 2012 UBOS study [*Karion et al*., 2013][vi]. Surface measurements of methane, VOC and NOy at the Horsepool site collected during the 2012 and

2013 UBOS studies are then used to derive emission ratios relative to methane, allowing estimates of total basin-wide emissions for NOy and several dozen speciated VOC when scaled to the *Karion et al*. [2013] estimate. When these emissions are applied within the WRF/Chem regional model, the high O_3 events observed during 2013 are well reproduced, and model biases of O_3 precursors are acceptably small. This is in stark contrast to poor model performance with simulations using U.S. EPA NEI-2011 (version 1) oil/gas sector emissions, or no emission from the oil/gas sector. The *Ahmadov et al.* [2014] study provides further analyses of O_3 sensitivity to NOy and VOC emission perturbations, the relative importance of alkane versus aromatic VOC emissions, and the relative importance of oil/gas sector versus other anthropogenic sources in the Basin using the top-down inventory as a reference. Basin-wide total emissions from this inventory are based solely on UBOS observations, but there are inherent assumptions used to derive the methane flux estimate, emission ratios, and other inventory pieces required to build the final gridded emissions product used in the 3-D simulations. The relationship between these assumptions and uncertainties within the top-down based oil/gas sector emissions are discussed in more detail in section 5.2.1. Reducing uncertainties in the top-down approach benefits its usefulness as an evaluation tool for the bottom-up based oil/gas sector emissions used within other UBOS related model platforms and programs.

The main impetus for deriving a top-down emissions inventory is the high correlations between primary nonoxygenated VOC and CH_4 exhibited in the measurements collected at Horsepool during the 2012 and 2013 field campaigns. Pearson r^2 correlation coefficients from linear regressions of nearly all these VOC range from 0.85 to 0.98, suggesting a common source to these VOC and CH_4. Examples of VOC-CH_4 correlation and regression fits are shown for toluene (r^2=0.90) in Figure 5-1a, and NOy-CH_4 (r^2=0.65) in Figure 5-1b. Though the patterns in the NOy-CH_4 scatter plot suggest multiple source signatures, there is an obvious correlation, accounting for 65% of the variance between the two species. Any reliable emission/model application for the UB is forced to either simulate or incorporate the specie-specie ratios that are clearly and consistently present in the observations. Though absent any information on specific sources, the top-down inventory implicitly incorporates the observationally based species-specie ratio information when applied within a gridded model framework. The observed total flux of CH_4 from the UB is an additional constraint that models need to either accurately simulate or incorporate, which again is an implicit component of the top-down inventory.

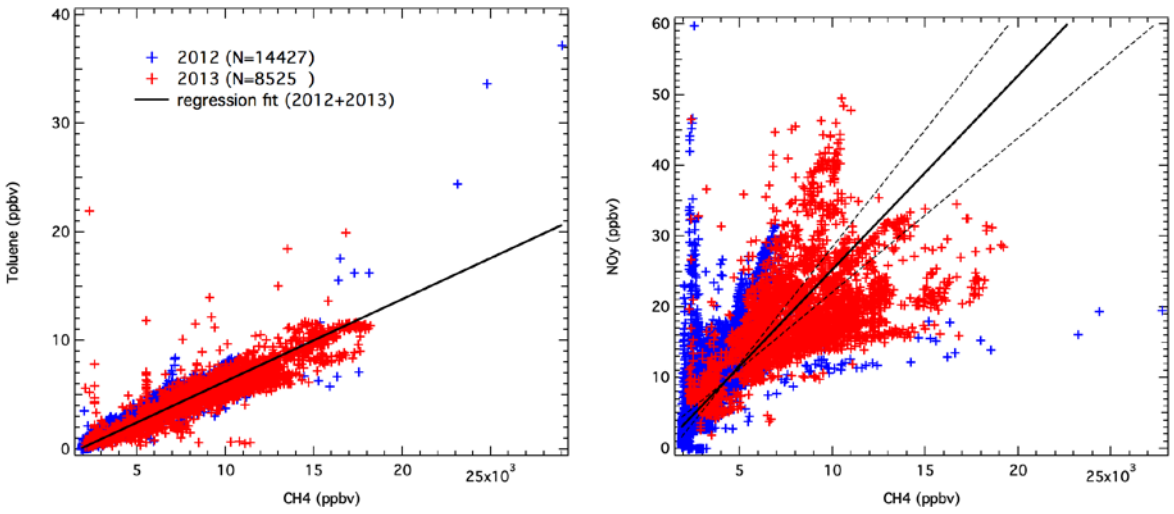

Figure 5-1a,b. Scatter plots and regression slopes derived from observations collected between 10am to 4pm (MST) at Horsepool during the winters of 2012 and 2013. Dotted lines in the NOy-CH_4 scatter plot are regression slopes derived from NOy versus CH_4 (lower), and CH_4 versus NOy (upper). Solid lines are regression slope averages adopted in the top-down inventory.

Quantifying the accuracy of the top-down inventory is difficult if not impossible with existing data. In terms of the VOC-CH_4 ratios used, *Helmig et al*. [2014][vii] applied the same top-down approach to place the UB oil/gas sector VOC emissions within a broader, more global perspective. Using VOC and CH_4 measurements from an entirely different set of instruments, and the CH_4 flux of *Karion et al.* [2013], they report the UB C2 – C7 VOC mass emission rate to be 194 ± 56 x 10^6 kg yr^{-1}. They report VOC-CH_4 ratios for 7 of the most significant VOC, and these ratios are all within 15% of the NOAA determinations used by *Ahmadov et al*. [2014], independently confirming these ratios used in the top-down inventory.

A recent submission by Koss et al. [2015][viii] provides an independent check on the Karion et al., methane estimate and by extension, the VOC inventory. The analysis relies on ambient VOC data from both the 2012 and 2013 UBWOS intensive studies at the Horsepool site, as well as measurements of PBL depth, and an estimate of the geographic size of the Basin. Ratios of aromatic HC were used to quantify the second-order reaction with OH radical and to ratio-out the effects of first order loss processes, which in the case of these compounds consist primarily mixing out of the basin. A volume emission rate for benzene (4.1±0.4 x 10^5 molecules $cm^{-3}s^{-1}$), was estimated using a mass balance approach with loss due to OH radical estimated from changes in VOC ratios. The volume of the cold pool air mass trapped within the basin was then calculated and used to obtain a mass emission rate of benzene, and by virtue of the benzene-methane correlations, the mass emission rate of methane, which turned out to fall in the range 14-39 x 10^3 kg hr^{-1} corresponding to the range of observed polluted layer altitudes in 2013 (1600m – 1700m asl). However, since the Karion et al., measurements were made in 2012 in the absence of cold pool conditions, Koss et al., increased this estimate according to the faction of wells located outside the 2013 cold pool (40 – 50%) that would likely have contributed to the

Karion et al. observations. The resulting methane emission range of 27-57 x10^3 kg methane hr^{-1} overlaps with the estimate of Karion et al., of 55±15 x10^3 kg methane hr^{-1}. While there is certainly room for improvement in methane emissions estimates, these results indicate that there does not appear to be a large difference in emissions between the two years. It is of interest to note that the Koss et al., estimate is based on a numerical integration of measurements taken over a seven day period at the beginning of February, 2013 and can therefore be thought of as representing a weekly average in contrast to the single day measurement of Karion et al., [2013].

The usefulness of the UBOS speciated VOC measurements and top-down approach to explain the observed levels of NOy, VOC and other O_3 precursors for the UB has been demonstrated in two model applications. *Edwards et al*. [2014][ix] applied a similar set of VOC ratios, derived from the same NOAA Horsepool data, within a box-model application for the Feb 1 – Feb 6, 2013 UBOS O_3 stagnation event. Using a simple representation for dilution, and a comprehensive photochemical treatment, they report excellent comparisons with O_3, PAN, PPN, CH_3CHO, MEK and acetone using the Horsepool dataset, illustrating that expected secondary oxidation products are consistent with the VOC and NOy mix used to force the model. *Ahmadov et al*. [2014] demonstrate the relative performance of the top-down inventory through comparisons of WRF/Chem model results with simulations using the most recent bottom-up inventory (NI-2011, version 1). The bias statistics in that study show significantly better agreement for NOy, NOx species, PAN, primary VOC and oxygenated-VOC using the top-down inventory for both 2012 and 2013. The correlation statistics are also significantly improved for 2013 using the top-down inventory.

Several simplifying assumptions related to NOy and individual VOC were made in the top-down inventory of *Ahmadov et al.* [2014] that deserve further investigation. Some of them are listed below along with recommendations for testing or reducing the impact of the assumptions in future top-down inventory improvements.

5.2.1 Uncertainties in Basin-wide CH_4 emissions:

The Basin-wide oil/gas sector emissions within the NOAA top-down inventory depend primarily on the boundary layer measurements of methane flux from the Feb. 3, 2012 NOAA instrumented flight with a stated uncertainty of 30% (*Karion et al*. [2013]). But due to wind direction and flight limitations, this flux estimate is limited to roughly the eastern two-thirds of the UB, and is thus a lower limit to Basin-wide methane emissions. A sufficient sampling of flux determinations under meteorological conditions conducive to light aircraft measurements would reduce this fundamental uncertainty and provide a reference point for future trend information and analysis. Though methane fluxes alone are fundamentally important, fluxes of NOy, VOC, CH_2O, and other hydroxy-radical sources would provide additional valuable information in terms of constraints to UB model applications, and source-apportionment determinations determined from Lagrangian or Bayesian based data-inversion techniques.

5.2.2 Uncertainty in emission ratios

Emission ratios within the top-down inventory are assumed to be equivalent to measured concentration ratios. This assumption is only valid if NOy and individual VOC are not rapidly removed by photochemical or heterogeneous processes, which would have the effect of underestimation within the top-down inventory for those species undergoing significant removal. For NOy, the rate of HNO_3 and organic nitrate deposition to snow surfaces, or their possible sources from heterogeneous chemistry at the snow-air interface, are not know within the UB, and could potentially be necessary when deriving emission ratios from NOy measurements made near the surface.

As explained in *Ahmadov et al.* [2014], the ratio determinations in the top-down inventory were determined from a simplest-approach, first-order perspective, without going into sampling or windowing strategies that could further impact emission ratio determinations. For example, the linear regressions assume all measurements are perfect. More accurate regression slopes and associated uncertainties could be derived using 2-sided statistical methods that include information on measurement precision and accuracy. Regressions are limited to data collected in the 10:00 am to 4:00 pm time window, which is justified on the basis of higher spatial representativeness during hours when the planetary boundary layer is active. Though data from both 2012 and 2013 are used in the regression analysis, emission ratios are inherently similar to ratios derived using 2013 data only, due to the substantially higher levels of NOy and VOC in 2013 compared to 2012 (observed median values a factor of 5 to 7 higher). An inventory based only on ratios from 2012 data would have somewhat different methane ratios for NOy and some VOC compared to the top-down inventory adopted in *Ahmadov et al.* [2014]. The higher weighting of 2013 data in the regressions is justified by the argument that specie-specie correlations are more locally influenced and representative of the Basin during 2013, and more regionally influenced from larger scale meteorological forcing in 2012. Such questions related to appropriate data windows, and the effects of meteorological forcing on slope determinations from specie-specie correlations can best be addressed with further analysis of VOC and NOy measurements made at different locations.

5.2.3 Uncertainty in spatial and temporal allocation of emissions

Spatially, oil/gas emissions in the top-down inventory are simply allocated according to well numbers in a given model grid cell, using well location information from the Department of Oil, Gas and Mining, Utah Department of Natural Resources[x], valid as of May of 2012. No distinction is made for well type or activity in the apportionment. An additional premise is that ratios of individual species relative to methane derived from the Horsepool observations are representative of all oil/gas emissions throughout the Basin. Thus, oil/gas sector emissions for NOy and each VOC species have the same spatial pattern as the top-down oil/gas sector emissions shown for CH_4 in Figure 5-2.

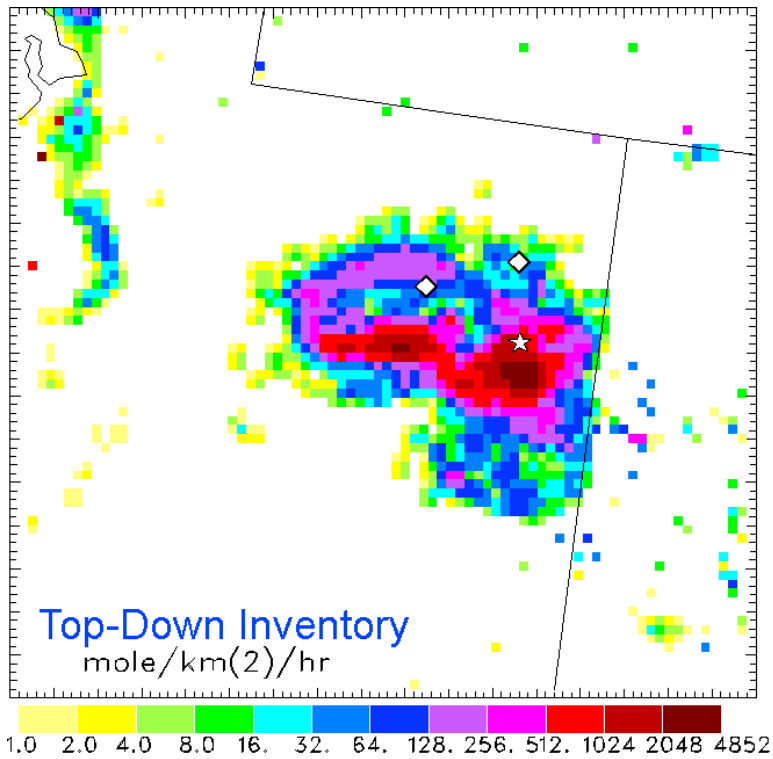

Figure 5-2. Spatial distribution of CH_4 emissions used in the top-down inventory. Diamonds are Roosevelt (to the west) and Vernal (to the east), the star is the location of the Horsepool site.

Comparative analysis of NOy and VOC measurements at other locations made during UBOS may be useful in assessing the applicability of these assumptions. However, the real need is the accurate location and relative magnitude of the specific oil/gas sector emissions responsible for the Basin-wide emission totals. Mobile van-based surveys [e.g. *Warneke et al*., 2014][xi] provide emission information for specific extraction operations and locations, while aircraft measurements from 2013 show basin-wide regional differences in NOx emissions [*Oltmans et al.*, 2014][xii]. An obvious improvement to the top-down inventory would be to incorporate such spatial information within the formalism.

Temporally, oil/gas emissions in the top-down inventory are simply held constant, regardless of time of day, day of year, and are assumed the same for both 2012 and 2013 winters. Further information on the relative importance of process-specific sources is needed to better estimate the impact on time of day temporal apportionment. For example, the top-down inventory cannot incorporate diurnal or daily variations in vehicular traffic in the temporal apportionment of NOy emissions since information on the relative importance of vehicle traffic compared to other NOy sources in the Basin is lacking. Moreover, while some VOC and NOy emission sources in the UB may originate from "continuous" operations, any atmospheric sample collected at Horsepool is an integrated quantity over thousands of discrete releases occurring upwind. The fraction of these sources that can be considered sporadic, process or event specific, or accidental could have implications for diurnal or daily temporal emission patterns needed in

model applications. Information on yearly or seasonal trends in drilling, well capping, well depletion, and transmission are potentially important for constraining temporal allocations on those time scales. Indirectly, the WRF/Chem simulations show a stronger negative bias in primary species for the 2013 simulations compared to 2012, suggesting an increase in oil/gas sector activity responsible for the VOC and NOy observed at Horsepool. But meteorological biases within the model related to snow cover and its impact on planetary boundary layer depth between the two years cannot be excluded as a factor contributing to these bias differences.

5.3 Bingham Research Center Studies

5.3.1 Non-combustion measurements

Investigations of inversion episodes in the Uintah Basin have shown that formaldehyde and other carbonyls are key precursors to wintertime ozone formation. Three principal categories of carbonyl sources exist in the Basin: combustion-related primary emissions, non-combustion primary emissions, and secondary atmospheric formations (from photochemical reactions involving organic compounds). Combustion-related emissions of formaldehyde are relatively well characterized, and EPA emission factors for formaldehyde are available for some oil- and gas-related combustion processes, though emission factors for other carbonyls are less readily available. Photochemical production of carbonyls from organic compounds is represented in the chemical mechanisms utilized by regional-scale air quality models (e.g., CAMx and CMAQ), and while these mechanisms are imperfect, a basic computational framework for estimating atmospheric production of carbonyls exists.

On the other hand, non-combustion primary emissions of carbonyls from oil and gas processes are completely uncharacterized. To our knowledge, no measurements of non-combustion carbonyl emissions from oil and gas sources have ever been collected in the Uintah Basin or elsewhere. Analyses of ambient air in the Basin have indicated that non-combustion emissions of carbonyls from oil- and gas-related sources may be an important component of total emissions. These analyses also suggest that formaldehyde emissions from non-combustion sources in oil- and gas-producing areas are connected with methanol emissions in some cases. Methanol is used as a deicer and solvent in oil and gas operations, and it is likely that some methanol degrades to formaldehyde during use, although it is not clear where in the production process the degradation occurs.

Measurements of carbonyl concentrations in methanol and produced water were collected in the Uintah Basin during winter 2013-14. These measurements show that used and aged methanol and produced water have higher formaldehyde concentrations than new methanol (Figures 5-3 and 5-4). A number of other carbonyls were also observed in methanol (Figure 5-5), but they were not consistently correlated with formaldehyde (Table 5-1). Formaldehyde may be formed from methanol degradation, but the mechanism by which these other carbonyls are produced is unclear. Aldehydes, routinely used as a component of hydraulic fracturing

fluid,[7] may be a source of carbonyls to produced water or oil and gas production streams. Carbonyls could also be produced in high-temperature and/or high-pressure oil and gas processes (e.g., well-site separation, glycol dehydration, or gas purification).

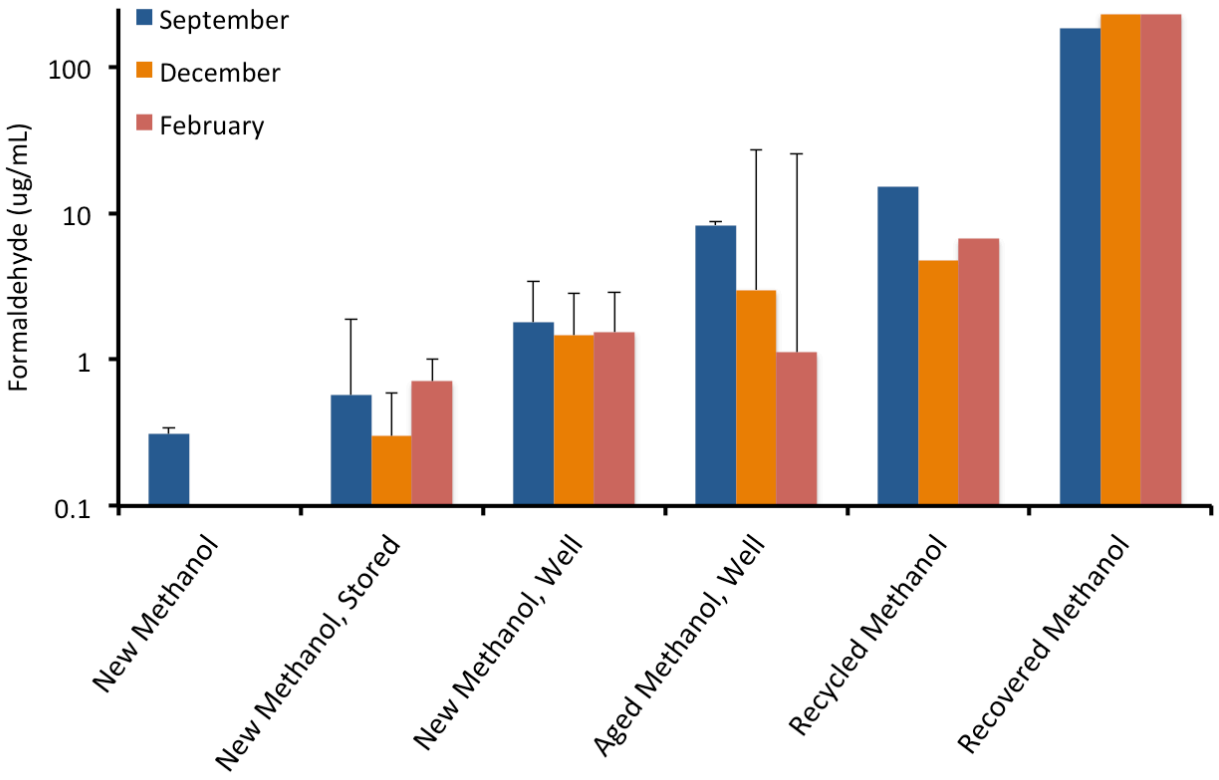

Figure 5-3. Concentrations of formaldehyde in methanol at various stages of storage and use at Uintah Basin oil and gas facilities, winter 2013-14. "New Methanol" had not undergone any post-shipping storage or use. "New Methanol, Stored" was unused and stored in large, centralized tanks. "New Methanol, Well" was stored in wellsite tanks. "Aged Methanol, Well" had been in wellsite storage tanks since winter 2012-13. "Recycled Methanol" had been recovered after use, purified via distillation, and transferred to a wellsite storage tank. "Recovered Methanol" had been recovered after use but not yet purified. The top of each bar is the mean concentration. Whiskers represent 95% confidence intervals.

[7] See table of "chemical used most often" at http://fracfocus.org/chemical-use.

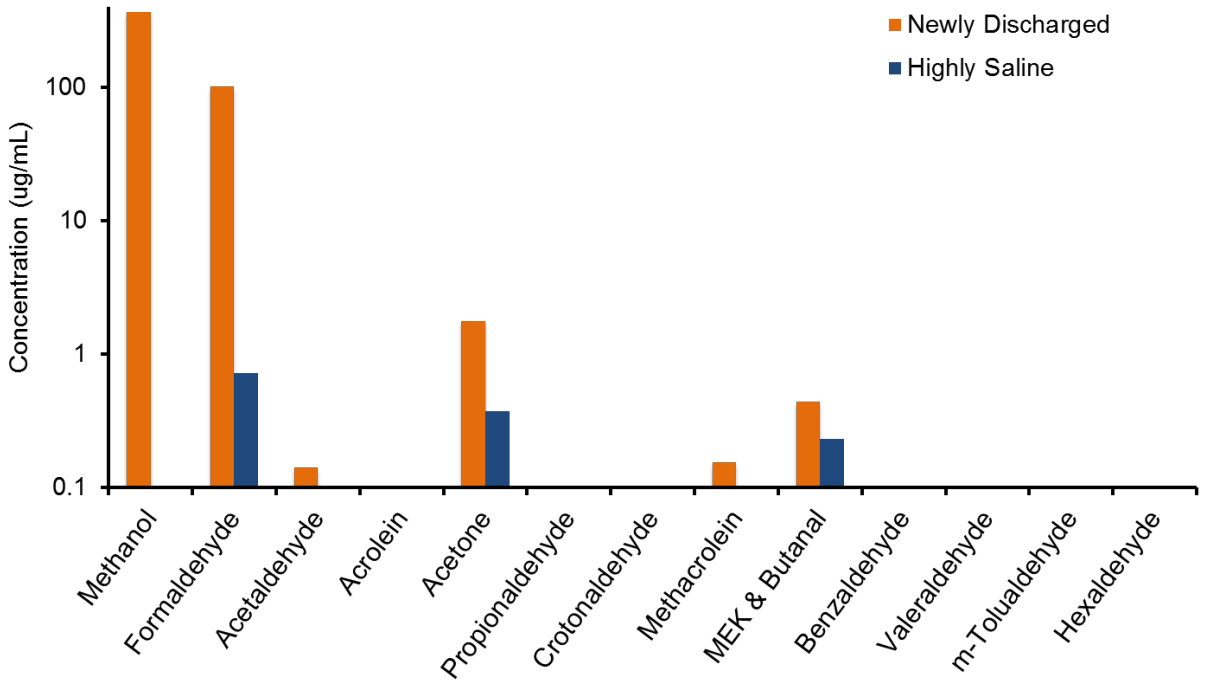

Figure 5-4. Concentrations of methanol and carbonyls in produced water from storage ponds in the Uintah Basin, winter 2013-14. "Newly Discharged" was water recently offloaded from trucks. "Highly Saline" was water that had undergone extensive evaporation in storage ponds.

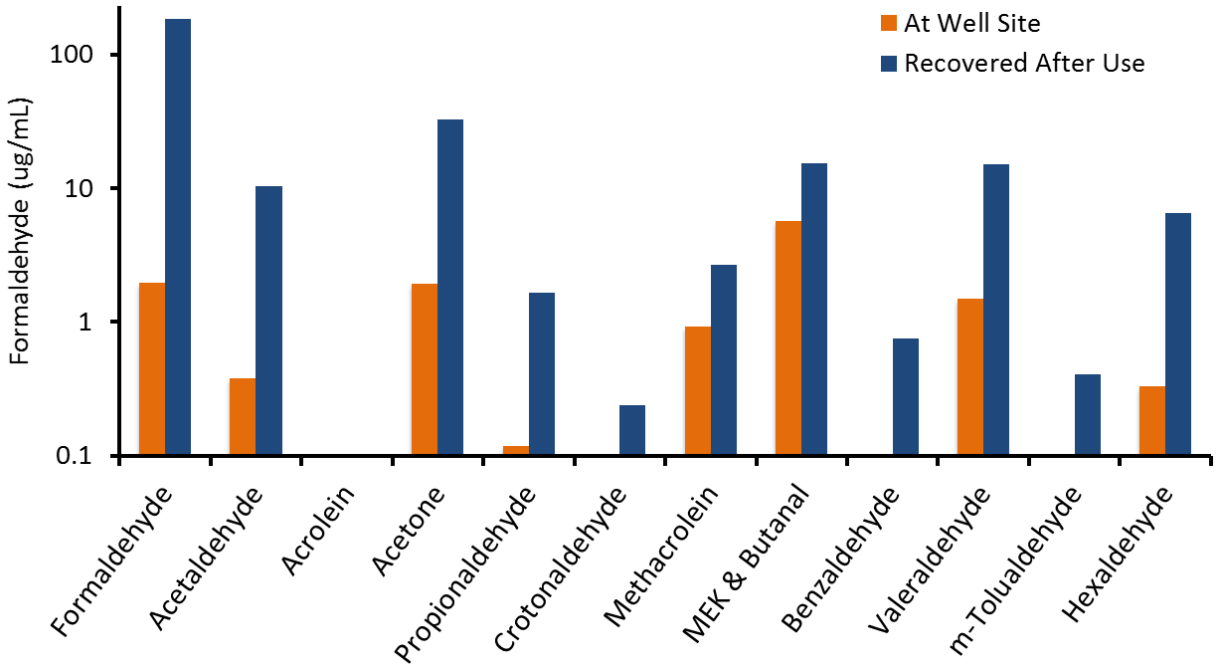

Figure 5-5. Concentrations of formaldehyde and other carbonyls in methanol samples from storage tanks at well sites (same as "New Methanol at Well," Figure 5-3) and recovered after injection into gas lines (same as "Recovered Methanol," Figure 5-3).

Table 5-1. Correlation of individual carbonyls in methanol with formaldehyde.

Carbonyl	Correlation Coefficient (r) with Formaldehyde
Formaldehyde	1.00
Acetaldehyde	0.45
Acrolein	0.00
Acetone	0.49
Propionaldehyde	0.53
Crotonaldehyde	0.08
Methacrolein	0.31
MEK & Butanal	0.43
Benzaldehyde	0.87
Valeraldehyde	0.59
m-Tolualdehyde	0.24
Hexaldehyde	0.77

Utah State University, with research funding from UDAQ, has undertaken a 12-month study to develop an emissions inventory for formaldehyde and other carbonyls in the Uintah Basin. Emissions measurements at likely non-combustion sources will help determine the role formaldehyde plays in wintertime ozone production. It is uncertain which oil and gas equipment or processes are important non-combustion sources of carbonyls to the atmosphere, but candidates include:

- Three-phase separators
- Glycol dehydrators
- Well site storage tanks (crude oil, condensate, and produced water)
- Produced water impoundments
- Deicing processes (due to possible degradation of methanol to formaldehyde)
- Hydraulic fracturing operations, especially flowback
- Distillation and heating processes

Emissions from distillation and heating processes will not be measured for this project because these sources are often embedded within larger oil and gas facilities (e.g., compressor stations, gas plants), and isolating these emissions from other sources would be impossible without direct facility access.

Carbonyls will be collected with DNPH sorbent cartridges. Air is pulled through the cartridges during sampling to collect carbonyls, and in the laboratory, carbonyls are extracted from the cartridges with acetonitrile and analyzed by high performance liquid chromatography.

Individual pieces of equipment at well sites will be measured via bag sampling. In this method, a bag encloses the component to be tested (e.g., leaky fitting, separator pressure relief valve, solar-powered methanol pump), and measurements of carbonyl concentrations inside and outside of the bag are taken. The difference between inside and outside concentrations is multiplied by the flow rate through the bag to determine the component's emission rate.

We will also measure emissions from potential sources via plume characterization/inverse modeling. In this method, carbonyls from upwind and downwind of an emission source and meteorology (wind speed and direction, temperature, humidity, pressure, and solar radiation) are measured. After collection, the meteorological data and the site's physical characteristics are used to build a plume dispersion computer model of emissions from the potential source. Finally, the measured concentrations of carbonyls are used to adjust the dispersion model's emission rate until the modeled emission plume best matches the measured air concentrations. This method works best with constant, steady wind speed and direction; it does not work well during inversion events. Sample collection, therefore, will necessarily occur at the beginning and end of the winter season.

We will use peer-reviewed literature, reports, and the measurement campaign to estimate the carbonyl emissions of various oil and gas sources. We will compare this information to the representation of carbonyl emissions of oil and gas sources in currently available speciation profiles for the SMOKE emissions model, elucidating potential speciation profile modifications that could be recommended to improve model performance. Since the potential modifications will be preliminary, a second phase of the project will be required for model sensitivity testing and refinement to determine how changes to carbonyl emissions influence photochemical model accuracy.

5.3.2 Hydrocarbons from soils near well pads

A number of recent studies provide evidence that actual emission rates of methane and other hydrocarbons may be higher than current inventories report (Tollefson, 2013[xiii]; Petron et al., 2012[xiv]). Some potentially significant sources of greenhouse gases and ozone-forming hydrocarbons have been excluded from inventories because little or nothing is known about how much these sources emit (Beusse et al., 2013; Bar-Ilan et al., 2009). These uncharacterized sources could account for much of the apparent discrepancy between inventoried and actual emissions.

One such uncharacterized source is near-well soil emissions. Problems with well casings or cementing processes may lead to underground emissions of gas or oil from the wellbore, and leaks in subsurface piping at well sites are also possible. Soil gas measurements such as those conducted by the United States Geological Survey (USGS) in Utah (Stolp et al., 2006[xv]) can provide evidence that leaks exist, but they cannot quantify the emission rate of leaked gas from the soil to the atmosphere.

With funding from the Utah Bureau of Land Management (BLM) and the Department of Energy (DOE), and in cooperation with BLM and USGS, USU's Bingham Research Center is measuring emissions of methane and nonmethane hydrocarbons from soils near a number of wells in Moab, Clay Basin, and Uintah Basin, Utah. Measurements are being collected using a modified version of the EPA emission isolation dynamic flux chamber (Eklund, 1992[xvi]) that is currently widely used for air toxics emissions (Figure 5-6).

Figure 5-6. USU flux chamber samples soil emissions at a well site in Utah.

The dynamic flux chamber measures soil emissions as the difference in concentrations inside and outside the chamber. This differential concentration is multiplied by the flow rate and divided by the surface area covered by the chamber to calculate the emission (or deposition) flux. The chamber system connects to a laser-based methane analyzer (LGR Ultraportable Greenhouse Gas Analyzer) and inertized stainless steel evacuated air sampling canisters. The LGR analyzer delivers measurements in real time, while canisters are filled and subsequently analyzed for C2-C12 hydrocarbon concentrations at the Bingham Research Center laboratory.

Measurements so far have shown that soil gas concentrations of methane are correlated with methane emission rates from soils (Figure 5-7), and emissions of nonmethane hydrocarbons are also correlated with soil gas concentrations. Emissions of methane and nonmethane hydrocarbons can be high at some wells, but the emission rate tends to decrease rapidly with increasing distance from well heads (Figure 5-8), and the contribution of methane and nonmethane hydrocarbon emissions from soils at well pads to total emissions from all oil- and gas-related sources is at this time expected to be low.

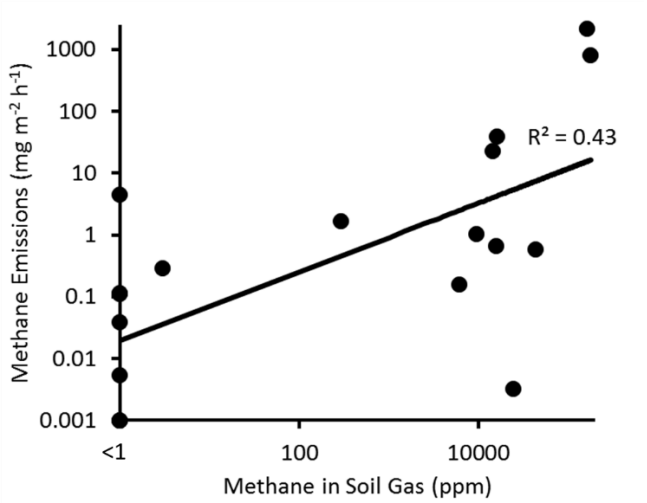

Figure 5-7. Methane in soil gas vs. methane emission rate from soil on well pads in Utah.

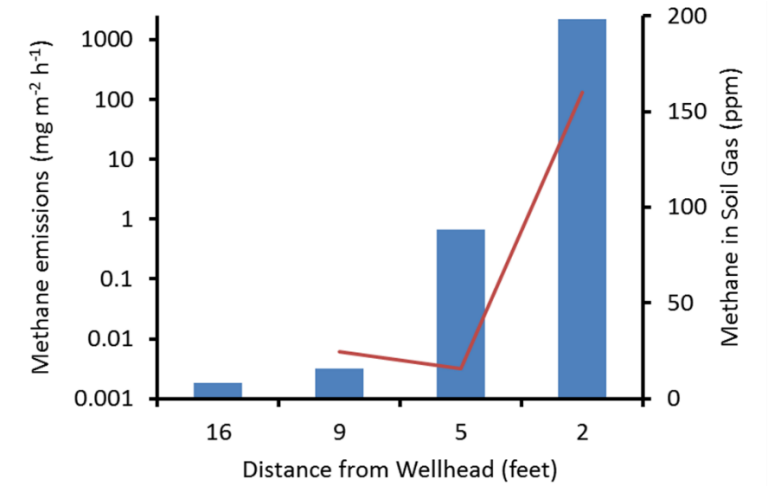

Figure 5-8. Methane emission rate and soil gas concentration in relation to distance from the wellhead at a gas well in Utah. The blue bars represent emission rate, and the red line represents soil gas methane.

5.3.3 Emission characterization for produced water ponds and land farms

Emissions of methane and nonmethane hydrocarbons from produced water in storage tanks and from evaporation ponds or other surface impoundments are excluded from most current oil and gas emissions inventories (Beusse et al., 2013[xvii]; Bar-Ilan et al., 2009[xviii]). While very few measurements of emissions from produced water surface impoundments have been made, no publicly-available measurements of emissions from produced water storage tanks have been made, and no publicly-available measurements of emissions from land farms have been made. Emissions from produced water surface impoundments in the Uintah Basin were measured by

USU's Bingham Research Center during winter 2012-13. Results of this study were detailed by Lyman et al (2013)[xix].

In June 2014, the Bingham Research Center received funding to perform additional measurements of hydrocarbon emissions from produced water and land farms in the Uintah Basin. This study will allow for characterization of emissions from produced water surface impoundments and land farms in a variety of meteorological conditions, and will allow for characterization of facilities utilizing different water and solid waste treatments. This study does not include characterization of emissions from produced water storage tanks. First results from this work are expected in mid-2015.

5.4 UDAQ Emissions Inventory Development

In June, 2014 UDAQ implemented a permitting process known as the General Approval Order for permitting new oil and gas wells when the permits meet certain requirements. In conjunction with this process UDAQ is creating an emissions inventory database that will use information about well site equipment that is required to be submitted as part of the permit approval process.

UDAQ currently has a permit database, however, the emissions that are associated with these sites are "allowable" rather than "actual" emissions; in other words, these are estimates of the maximum amount of emissions that these sites are allowed to produce each year. As a general rule allowable emissions are greater than the actual emissions on an annual or seasonal basis. For this reason UDAQ's inventory database will create a system for collecting an actual emissions inventory on an annual basis. It will also be created as an online system to make the process of collecting and compiling the inventory more efficient for the regulated community. The initial implementation of the UDAQ emissions inventory database will be operational by January, 2015.

Jurisdictional authority in the Basin is complex mixture of Tribal, State, and Federal laws and regulations. The state of Utah has regulatory authority on some oil and gas producing lands but not on those classified as "Indian Country". Since this database will only cover permitted sources on state-regulated lands, sources in the Basin operating on Indian Country as well as the many production sites whose emissions are less than the permitting threshold (de minimis) will still need to be accounted for. It is the intention of UDAQ to work with all of the stakeholders in the Basin to facilitate building a new and updated oil and gas inventory during calendar year 2015. While the intent of this project will be to develop a "SIP" (State Implementation Plan) quality inventory, the Basin-wide inventory will not be a UDAQ inventory since it will involve lands administered by the Tribe, BLM, EPA and the state of Utah.

5.4.1 An Updated Inventory for State, Tribal, and Federal Jurisdictions

From UDAQ's perspective an oil and gas inventory in the Basin should fulfill at least three objectives: 1) Provide a baseline inventory with enough resolution in specific sources of emissions that targeted regulations can be evaluated for their potential effectiveness. 2) As emission reductions are accomplished, the baseline inventory can be used to account for

credits applied against future emission reduction requirements. 3) A high degree of spatial resolution coupled with an improved understanding of speciated VOC in the inventory will improve one important aspect of uncertainty in the air quality model which is the uncertainty in the emission inputs.

To the degree that the inventory is based on individual equipment on site, which is the basis for UDAQ's new database of permitted sources, emission factors that reflect current practices will be important. Emission factors for specific production activities will be paramount since onsite equipment will be accounted for through the permitting system. Questions to be considered for the initial implementation relate to creating a set of default emission factors. Would emission factors applied to the entire basin lack the resolution necessary to reflect different gas compositions within the Basin? If so, would it be practical to create default emission factors that vary by individual well field? Figure 5-9 shows a subset of the production fields in the Uinta Basin.

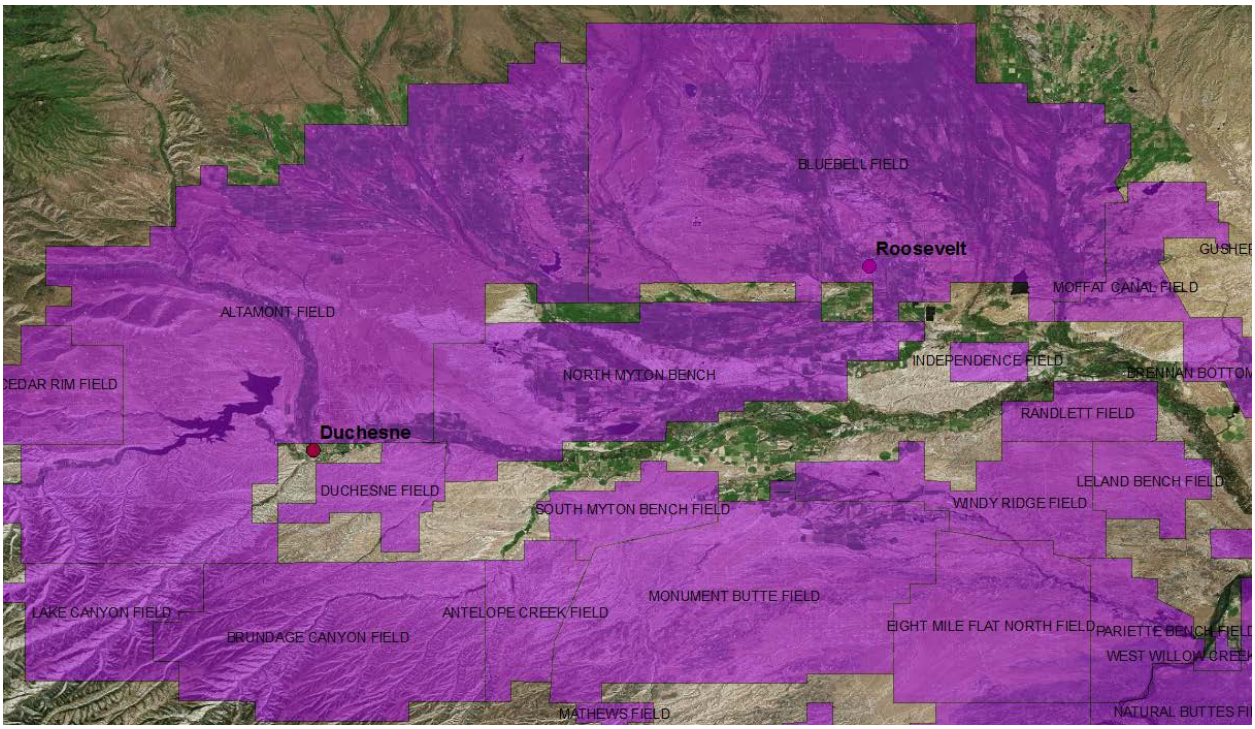

Figure 5-9. Subset of well fields in Duchesne County.

The UDAQ database is designed specifically for permitted sources whose emissions are greater than five tons per year of any one pollutant and will only cover those sites under state jurisdiction. There are three other components of a complete-basin inventory that must also be estimated: Drilling activity, which is a transient source; production on state lands by individual sources whose emissions are less than five tons per year; and all sources of activity on Indian Country which would include drilling, minor and major source permit holders, and all sites that fall under the permit limits. Once these other sources of emissions are estimated, the

process of distributing these emissions throughout the Basin for air quality modeling analyses is relatively straightforward through GIS processing.

5.5 Summary

The importance of a more highly refined emissions inventory for oil and gas has been brought into focus by photochemical modeling work that was completed during 2014. Modeling groups from NOAA, UDAQ, EPA, AECOM, and the Bingham Research Center have undertaken modeling studies that have focused on various inputs to the air quality model including meteorology, emissions, and chemistry parameters.

Aspects of the emissions inventory that require further analysis include the relative proportions of NOx and VOC; speciation of the VOC to reflect gas composition of the different production processes; and the spatial distribution of emissions throughout the oil and gas producing areas. The NOAA top-down inventory has provided the first constraint on the inventory tied to field measurements. Suggestions for potential refinement of calculations for a top-down inventory outlined in section 5.2 provide a means to further test newly developed inventories that will be created throughout 2015. These refinements, along with improvements to other parts of the modeling system, will continue to reduce the uncertainty inherent modeling such a complex system.

---

[i] 2009. WRAP O&G Emissions Workgroup: Phase III Inventory. http://wrapair2.org/PhaseIII.aspx

[ii] http://www.blm.gov/pgdata/etc/medialib/blm/ut/natural_resources/airQuality.Par.34346.File.dat/UTSO_EmissionsTSD121913.pdf

[iii] 2014. WRAP. WESTJUMP Air Quality Modeling Study. http://wrapair2.org/WestJumpAQMS.aspx

[iv] 2013. Harper, K. *UDAQ Updated Oil and Gas Inventory for the Uinta Basin*. http://www.deq.utah.gov/locations/U/uintahbasin/docs/2013/02Feb/uboilandgasinventory.pdf

[v] Ahmadov, R., S. McKeen, M. Trainer, R. Banta, A. Brewer, S. Brown, P. M. Edwards, J. A. de Gouw, G. J. Frost, J. Gilman, D. Helmig, B. Johnson, A. Karion, A. Koss, A. Langford, B. Lerner, J. Olson, S. Oltmans, J. Peischl, G. Pétron, Y. Pichugina, J. M. Roberts, T. Ryerson, R. Schnell, C. Senff, C. Sweeney, C. Thompson, P. Veres, C. Warneke, R. Wild, E. J. Williams, B. Yuan, and R. Zamora, 2014, Understanding high wintertime ozone pollution events in an oil and natural gas producing region of the western U.S., *Atmos. Chem. Phys. Discuss*., 14, 20295-20343, doi:10.5194/acpd-14-20295-2014.

[vi] Karion, A., C. Sweeney, G. Pétron, G. Frost, R.M. Hardesty, J. Kofler, B.R. Miller, T. Newberger, S. Wolter, R. Banta, A. Brewer, E. Dlugokencky, P. Lang, S.A. Montzka, R. Schnell, P. Tans, M. Trainer, R. Zamora, and S. Conley, 2013, Methane emissions estimate from airborne

measurements over a western United States natural gas field, *Geophys. Res. Lett*., 40, 4393–4397, doi:10.1002/grl.50811.

[vii] Helmig, D., C.R. Thompson, J. Evans, P. Boylan, J. Hueber, and J.H. Park, 2014, Highly Elevated Atmospheric Levels of Volatile Organic Compounds in the Uintah Basin, Utah, *Environ. Sci. Technol*., 48, 4707-4715, 10.1021/es405046r.

[viii] Koss, A.R., J. de Gouw, C. Warneke, J.B. Gilman, B.M. Lerner, M. Graus, B. Yuan, P. Edwards, S. Brown, R. Wild, J.M. Roberts, T.S. Bates, P.K. Quinn, 2015, Photochemical aging of volatile organic compounds associated with oil and natural gas extraction in the Uintah Basin, UT, during a wintertime ozone formation event, Atmos. Chem. Phys. Discuss. (in press).

[ix] Edwards, P.M., S. Brown, J. Roberts, R. Ahmadov, R. Banta, J. de Gouw, W. Dubé, R. Field, J. Flynn, J. Gilman, M. Graus, D. Helmig, A. Koss, A. Langford, B. Lefer, B. Lerner, R. Li, S. Li, S. McKeen, S. Murphy, D. Parrish, C. Senff, J. Soltis, J. Stutz, C. Sweeney, C. Thompson, M. Trainer, C. Tsai, P. Veres, R. Washenfelder, C. Warneke, R. Wild, C. Young, B. Yuan, and R. Zamora, 2014, High winter ozone generated by carbonyl photolysis in a shale gas and oil producing region, *Nature*, accepted for publication 8/6/14.

[x] http://oilgas.ogm.utah.gov/Maps/OG_Maps.htm

[xi] Warneke, C., F. Geiger, P. M. Edwards, W. Dube, G. Pétron, J. Kofler, A. Zahn, S. S. Brown, M. Graus, J. Gilman, B. Lerner, J. Peischl, T. B. Ryerson, J. A. de Gouw, and J. M. Roberts, 2014, Volatile organic compound emissions from the oil and natural gas industry in the Uinta Basin, Utah: point sources compared to ambient air composition, *Atmos. Chem. Phys. Discuss*., 14, 11895-11927, doi:10.5194/acpd-14-11895-2014.

[xii] Oltmans, S.J. , A. Karion, R.C. Schnell, G. Pétron, C. Sweeney, S. Wolter, D. Neff, S.A. Montzka, B.R. Miller, D. Helmig, B.J. Johnson, and J. Hueber, 2014, A high ozone episode in winter 2013 in the Uinta Basin oil and gas region characterized by aircraft measurements, *Atmos. Chem. Phys. Discuss.*, 14, 20117-20157, doi:10.5194/acpd-14-20117-2014.

[xiii] J. Tollefson: Methane leaks erode green credentials of natural gas, Nature, 493, doi:10.1038/493012a, 2013.

[xiv] G. Petron, G. Frost, B. Miller, A. Hirsch, S. Montzka, et al.: Hydrocarbon emissions characterization in the Colorado Front Range: a pilot study, Journal of Geophysical Research D: Atmospheres, 117, D04304, 2012.

[xv] B.J. Stolp, A.L. Burr, K.K. Johnson: Methane gas concentration in soils and ground water, Carbon and Emery Counties, Utah, 1995-2003, U.S. Geological Survey, Salt Lake City, Utah, Scientific Investigations Report 2006-5227, 2006.

[xvi] B. Eklund: Practical guidance for flux chamber measurements of fugitive volatile organic emission rates, Journal of the Air and Waste Management Association 42, 1583-1591, 1992.

[xvii] R. Beusse, C. Dunlap, K. Good, E. Hauck, R. McGhee-Lenart, J. Narimatsu: EPA needs to improve air emissions data for the oil and natural gas production sector, Office of Inspector General, U.S. Environmental Protection Agency, Washington, D.C., Report Number 13-P-0160, 2013. Available at www.epa.gov/oig/reports/2013/20130220-13-P-0161.pdf.

[xviii] A. Bar-Ilan, R. Friesen, R. Parikh, J. Grant, A.K. Pollack, D. Henderer, D. Pring, K. Sgamma: Development of 2012 oil and gas emissions projections for the Uinta Basin, Environ, Novato, California, 2009. Available at wrapair.org/forums/ogwg/documents/2009-03_12_Projection_Emissions_Uinta_Basin _Technical_Memo_03-25.pdf.

[xix] S. Lyman, M. Mansfield, H. Shorthill, R. Anderson, J. Evans, C. Mangum, T. Shorthill: Wintertime emissions of hydrocarbons from produced water evaporation facilities, in Final Report: 2013 Uintah Basin Winter Ozone Study, T. Stoeckenius and D. McNalley (Eds.), Environ, Novato, California, 2014.

6.0 AIR QUALITY MODELING STUDIES OF WINTER OZONE

Authors
Gail Tonnesen[8], Lance Avery[9], Marc Mansfield[10], Huy Tran[3], Trang Tran[3], Ravan Ahmadov[11], Stuart McKeen[4], Peter Edwards[12], Erik Crosman[13], John Horel[6] , Courtney Taylor[14]

Measurement studies of ozone and its precursors in the Uinta Basin from 2011 to 2014 have provided valuable information on the emissions sources that contribute to ozone formation and the meteorological and photochemical processes that allow high ozone levels to build and persist in the basin. However, measurements are limited in their spatial coverage, and measurements alone cannot be used to predict how ozone will respond to changes in the emissions of the VOC and NOx precursors. Moreover, measurements cannot be used to determine the amount of emissions reductions required nor the optimal combination of VOC or NOx emissions reductions needed to attain the National Ambient Air Quality Standard (NAAQS) for ozone. Air quality models are a valuable complement to measurement studies because models can be used to predict the response of ozone to emissions changes across the basin, to provide information on the most effective emissions reductions strategies for attaining the NAAQS, and to evaluate the effects of uncertainty in the emissions inventory and other model input data on ozone attainment strategies.

While models are a valuable tool for air quality planning, models also have uncertainty, and a model that performs poorly may incorrectly predict the response of ozone to changes in emissions. A comprehensive evaluation of a model is required to assess its usefulness for predicting how ozone is formed and how it will respond to changes in emissions. A model performance evaluation (MPE) uses comparisons of model predictions to observations to assess how well the model represents the processes that control ozone formation. These processes are complex and uncertain, and therefore the MPE should be tailored to assess how accurately the model represents each of the following processes:

- Emissions inventories of VOC and NOx, including the spatial and temporal distribution of emissions and the speciation or reactivity of the VOC mixture.
- Meteorological conditions that affect ozone dispersion and chemistry including the intensity and persistence of the stable inversion layer; wind speed and direction and the effect of winds on mixing and transport; snow cover and snow albedo, cloud cover, fog and precipitation that affect photolysis rates; and the deposition of ozone and other chemical species to surfaces.

[8] U.S. Environmental Protection Agency, Region 8, Denver, Colorado
[9] Utah Department of Environmental Quality, Salt Lake City, Utah
[10] Bingham Research Center, Utah State University
[11] Cooperative Institute for Research in Environmental Sciences, University of Colorado at Boulder.
[12] Department of Chemistry, University of York
[13] Department of Atmospheric Sciences, University of Utah
[14] AECOM Corporation, Fort Collins, CO

- Indicators of chemical reactions that form ozone, including measurements of the secondary products of those reactions and ratios of products that can be used to assess if ozone is formed in a VOC-sensitive or NOx-sensitive chemical regime.

Measurements collected during the Uinta Basin field studies provides an extensive set of data that can be used in the MPE to assess how well the model represents each of these processes. This chapter describes the air quality modeling efforts that are currently in progress, including a description of the types of models being used, and summarizes preliminary results from these modeling studies.

6.1 Box Model Studies

Photochemical air quality models range in complexity from relatively simple "box models" that simulate ozone chemistry at a single point, to more complex and physically realistic "grid models" that simulate the transport of pollutants over a large spatial domain. Edwards et al. (2013, 2014) describe the results of a box model study in which the precursor species are constrained by measured concentrations at the Horsepool research site. Carter and Seinfeld (2012) also performed a box model study of winter ozone conditions using measured concentrations of precursors at monitoring sites in southwest Wyoming. The value of box model studies is that they can provide insights into the chemical processes that affect ozone formation at the site where the measurements are made. While box models can provide valuable insights into photochemical processes, they do not take into account spatial variations in emissions and the transport and mixing of emissions from different sources, and thus box models cannot be used to evaluate the expected impact of basin-wide VOC or NOx emission reductions. Instead, more physically realistic and spatially detailed photochemical grid models are used to evaluate regulatory attainment strategies for ozone across the entire basin. A benefit of grid models is that they explicitly represent the dispersion and transport of pollutants and the spatial variability in emissions and ambient concentrations of precursors and ozone. Thus, box models are generally not useful for evaluating and designing precursor control strategies; a more physically realistic grid model is needed for this purpose. Nevertheless, the box model provides valuable information on chemical processes at the site where measurements are available. This information can be used to assess whether grid model simulations accurately represent the chemistry and thus represents an important contribution to the overall model evaluation.

Carter and Seinfeld (2012) performed a box model study of the reactivity of VOC emissions using speciated VOC measurements at two monitoring sites carried out in field studies in the Upper Green Basin in southwest Wyoming in February 2008 and in March 2011. They found significant differences in VOC speciation and sensitivities of ozone to VOC and NOx emissions, with one site modeled for the 2008 episode being highly NOx-sensitive and insensitive to VOC, whereas the other site modeled with 2008 data and both sites modeled with 2011 data exhibiting strong sensitivity of ozone to changes in VOC concentrations. Carter and Seinfeld (2012) also found that the major contributors to ozone formation in Wyoming were alkenes and aromatic VOC species, even though they constituted only a small fraction of the total VOC mass. They also found that the relative reactivity of VOC species in winter is similar to that

previously observed in summer, with formaldehyde and other aldehydes, alkenes and aromatics having the greatest reactivity, while alkanes have low reactivity. It should be noted that high concentrations of alkenes have not been observed in the Uinta Basin and that some researchers have suggested that alkenes analyzed in the limited number of canister samples collected in the Upper Green Basin may contain positive biases due to artefacts in the data. Formaldehyde, aldehydes and aromatics are the most reactive VOC species in the Uinta Basin; only limited measurements of aldehydes are available in the Upper Green Basin. Carter and Seinfeld concluded that the box model was useful for evaluating the VOC reactivity during winter ozone episodes but that photochemical grid models are required to assess ozone attainment strategies.

Edwards et al. (2014) performed box model simulations of ozone chemistry using data collected at the Horsepool research site during the 2013 field study and concluded that ozone formation at this location is sensitive to VOC reductions, i.e. VOC reductions would be expected to result in ozone reductions. Their results also suggest that NO_x reductions, either by themselves or in conjunction with VOC reductions, would also lead to ozone reductions at Horsepool.

Box model simulations were performed using the Dynamically Simple Model of Atmospheric Chemical Complexity (DSMACC). The model chemistry scheme is generated by the Master Chemical Mechanism (MCM) V3.2 and contains detailed inorganic chemistry and a near explicit degradation scheme for 32 of the observed VOCs and oxygenated VOCs (OVOCs), resulting in 2,754 species and 10,675 reactions. The MCM v3.2 chemistry scheme was updated to include temperature dependent yields for organic nitrates based on Carter and Atkinson (1989).

All primary VOC species in the model are introduced via a constant emission rate over the entire 6-day simulation period, tuned to best match the observed concentrations. Observed UBWOS 2012 VOC ratios were used to increase the VOC constraints for 2013, on the assumption that changes in VOC emission ratios between the two years is minimal. Reactive nitrogen is introduced into the model via a constant emission of NO. $ClNO_2$ was constrained to the observed diurnal profile, and the potential impacts of HONO were assessed using data and understanding gained from all 3 years of observations at Horsepool.

Physical loss of all species via mixing, and to a lesser extent deposition, is represented through a bimodal first order loss term. The rate and diurnal variation of this parameter is based on Lidar and tether sonde observations of planetary boundary layer (PBL) height and the concentration profile of long-lived species such as CH_4. The measured O_3 deposition velocity is included as a separate first order loss for O_3 for the sake of completeness, although this term is negligible compared with the mixing term. Simulations were constrained to the observed average diurnal temperature profile, and observed photolysis frequencies were used to scale TUV calculated photolysis rates.

The model successfully reproduces observed ozone and OVOCs (PAN, PPN, acetone, acetaldehyde, MEK), providing confidence in model performance. Simulations find O_3 production photochemistry to be close to peak efficiency for the observed NOx and VOCs. This is due to a large radical source from the photolysis of carbonyl species produced during VOC

oxidation, and the overwhelming dominance of primary VOCs in the calculated OH reactivity budget.

6.2 Description of Photochemical Grid Models

Photochemical grid model simulations of winter ozone episodes are under development by the Utah Division of Air Quality (UDAQ), EPA, BLM, University of Utah, Utah State University and NOAA. A photochemical modeling system includes five basic components:

1. A prognostic meteorological model that provides 3-dimensionsal gridded meteorological data, including wind speed and direction, inversion layer height, solar radiation, temperature, humidity, precipitation, clouds and snow depth.
2. An emissions inventory and emissions processing system to prepare emissions data for input to the photochemical model.
3. Ancillary data and models for solar radiation, initial and boundary conditions, and land use types.
4. A photochemical model that simulates the emissions, transport, chemical processing, deposition and ambient concentrations of VOC and NOx precursors, intermediate products, and secondary pollutants including ozone and fine particulate matter.
5. Observational data to evaluate the performance of the modeling system

The most widely used meteorological model is the Weather Research Forecast (WRF) model. For winter ozone studies it is especially important that the WRF model be able to simulate the extremely stable and persistent cold air pool conditions that create strong, shallow inversion layers in the Uinta Basin. WRF must also be able to reproduce the snow cover conditions because snow albedo enhances the photochemical reactions that produce ozone, and snow cover plays an important role in strengthening the inversion conditions. Results of WRF model research and development for application to cold pool conditions are described by Neemann et al. (2014).

The two most widely use photochemical models for air quality management are the Comprehensive Air Quality model with extensions (CAMx; ENVIRON, 2013) and the Community Multiscale Air Quality (CMAQ) model (Byun and Schere, 2006). For both CAMx and CMAQ, the meteorological and air quality model simulations are performed separately, and a preprocessor is used to prepare WRF results for input to the air quality model. NOAA researchers are using the WRF-Chem model in which the air quality model is integrated with the WRF meteorological model, allowing for simulation of feedbacks which can occur between air quality conditions and meteorological parameters.

6.3 Meteorological Model Evaluation and Development

6.3.1 University of Utah WRF Modeling

University of Utah (UU) researchers performed WRF model simulations to investigate the meteorological characteristics of the 31 January–6 February 2013 cold-air pool in the Uinta Basin and the resulting high ozone concentrations (Neemann et al., 2014). Flow features

affecting cold-air pools and air quality in the Uinta Basin have been studied, including: penetration of clean air into the basin from across the surrounding mountains, elevated easterlies within the inversion layer, and thermally-driven slope and valley flows. The sensitivity of the boundary layer structure to snow cover variations and cloud microphysics were also examined. Snow cover increases boundary layer stability by enhancing the surface albedo, reducing the absorbed solar insolation at the surface, and lowering near-surface air temperatures. Snow cover also increases ozone levels by enhancing solar radiation available for photochemical reactions. Ice-dominant clouds are shown to enhance cold-air pool strength compared to liquid-dominant clouds by increasing nocturnal cooling and decreasing cloud forcing of the longwave radiation budget.

6.3.2 Utah State University WRF Modeling

Utah State University (USU) performed WRF sensitivity tests for the January 26-30 2013 episode to determine an optimal model configuration. Four WRF configurations were tested:

- Reference (REF) configuration: partially adapted from ARMS-BLM project with some changes that increase model resolution and were primarily tested to be more realistic in capturing snow depth evolution;
- UUMOD configuration: test case using the WRF configuration recommended by Neemann et al. (2014).
- SNODAS configuration: same as UUMOD but with substitute snow water equivalent and snow depth initial/boundary conditions (IC/BC) by Snow Data Assimilation System (SNODAS) 30 arc seconds resolution;
- SNODAS_d03 configuration: same as SNODAS but implements ARMS-BLM observational nudging approach for wind and temperature parameters for the 1.3-km domain.

The results of these four WRF sensitivity simulations were compared with observed temperature, surface wind-speed, snow depth and albedo data for monitoring sites within the Uinta Basin. The sensitivity tests indicated that:

- Fine resolution SNODAS data applied for snow field IC/BC improved model performance in simulating snow depth;
- Observational nudging corrected the averaged warm bias in temperature from 1^{o}C to lower bias value of 0.2^{o}C but had almost no effect on correcting the relatively large bias in surface wind speed (2m/s) produced in those simulations without nudging;
- Idealizing snow cover based on observational data to initialize snow field within Uinta Basin area (Neemann et al., 2014) notably improved model performance in simulating snow depth and albedo.

Therefore, a combination of UUMOD configurations, SNODAS data for snow IC/BC for areas outside Uinta Basin and ARMS-BLM nudging approach was chosen for the USU-WRF simulations. Evaluation of model results indicated that the combined configuration allowed the WRF model to capture very well surface temperature, snow depth and albedo, and the timing

of inversion events and their break up during the full January 6 to February 14 2013 simulation period.

6.3.3 Bureau of Land Management WRF Modeling

The Bureau of Land Management (BLM) WRF modeling, conducted by AECOM and Sonoma Technology Incorporated (STI), tested and evaluated multiple WRF configurations to optimize the performance for winter modeling in the Uinta Basin. Both qualitative and quantitative (statistical) analyses were used to examine the performance of the WRF simulations. Qualitative analyses of the meteorological model performance were conducted for two air quality episodes: January 8 to 23, 2010 and February 21 to March 8, 2010. The model results for these time periods were compared with:

- Observations of surface and upper-level pressure patterns;
- The spatial variability of observed precipitation, precipitation amounts, and snow cover; and
- The observed vertical profiles of wind speed, direction, temperature, and dew point.

In general, it was found that the WRF model was capable of reproducing the observed synoptic and precipitation patterns, including snow cover, during the events analyzed; however, the model tended to over-predict the extent of snow coverage during early fall and late spring. The model generally was able to simulate the vertical structure of the atmosphere, including vertical profiles of wind direction and speed, as well as the height of the planetary boundary layer. However, the model had difficulty replicating sharp vertical changes in the dew point temperature (located well above the boundary layer in the cases analyzed).

The quantitative assessment of the 2010 simulation compared model results to observations using various statistical measures. The statistical results were evaluated over different temporal and spatial extents to assess the WRF model's performance for accuracy, consistency, and reasonableness with respect to available observations. In general, the simulation performed well for all meteorological parameters evaluated in the Uinta Basin, including low temperatures during cold-pool stagnation events. During the winter, including during cold-pool events, the model wind speed tends to be biased slightly low (bias of -0.5 m\s) and the temperature biased slightly high (bias of +1 degree Kelvin). Altogether, the model's ability to reproduce important synoptic and vertical patterns as well as key meteorological parameters such as temperature and wind speed provided confidence in the model's ability to reproduce important physical processes during periods with elevated concentrations of air pollutants.

6.3.4 EPA WRF modeling

EPA performed WRF model simulations for several winter periods (2010-11, 2011-12, 2012-13) at 12 and 4km resolutions, with additional sensitivity tests performed for 2010-11 using multiple input datasets and physics parameterizations. The default WRF configuration did not accurately replicate snow cover in the basin. WRF sensitivity simulations were conducted using SNODAS snow cover data. WRF simulations using high-resolution snow cover data more accurately simulated snow cover, thus leading to more accurate albedo simulations. However,

the EPA WRF simulations still failed to capture the intensity and longevity of cold pools, either not simulating a strong enough inversion or eroding the cap too quickly. EPA is continuing to evaluate possible causes of poor WRF performance for vertical mixing during cold air pool inversion episodes.

6.3.5 NOAA WRF-Chem modeling over the Uinta Basin for January-February 2012 and 2013

The Weather Research and Forecasting model coupled to chemistry (WRF-Chem) is a state of the art coupled meteorology-chemistry model used in a wide range of studies such as dust, air quality and aerosol-radiation feedback. The WRF-Chem model (version 3.5.1) was used at NOAA/ESRL/CSD to simulate wintertime meteorology, methane distribution and photochemistry over the Uinta Basin (UB) for January-February, 2012 and 2013. Most of the results from the modeling study have been published in Ahmadov et al., (2015). Major findings from this study are highlighted below.

The WRF-Chem model ran on two nested domains with 12 and 4km resolution focusing on the UB. For the vertical grid 60 layers were selected, where 18 of them were located within lowest 500 m. The main settings of the model configuration were presented in Table S2 of the supplemental material in Ahmadov et al. (2015). It should be noted that in this configuration no data assimilation was used. Below we list major conclusions from the meteorological comparisons within the WRF/Chem simulations:

- The model can simulate meteorological fields in winter of 2012 quite well, when mostly snow free conditions and relatively warm weather were present.
- The WRF model is also able to capture cold pool like meteorological conditions during 2013 in the UB. This is crucial for air quality modeling in the region, as low wind and shallow vertical mixing layers trap the air pollutants within the UB.
- To capture the 2013 cold pool type stagnant meteorological conditions, a reasonable amount of snow cover in the UB should be present in the meteorological fields that are used to initialize WRF simulations, such as North American Mesoscale analysis fields (www.emc.ncep.noaa.gov).
- The daytime mixing layer heights during stagnant meteorological conditions were mostly in the range of 50-200 m over the UB as determined from the tethersonde measurements conducted by NOAA researchers in the winter of 2013. The model can capture the range of the observed very shallow daytime boundary layers, but cannot accurately simulate the spatiotemporal variability of the shallow boundary layers. It is possible that further refinement of the WRF grid resolution and improvement of the physics parameterizations and using various data assimilation methods (e.g. observation nudging) could improve the complex structure of the weekly unstable boundary layers observed over the UB during daytime.

6.4 Photochemical Air Quality Modeling

6.4.1 Photochemical Air Quality Modeling at NOAA/ESRL/CSD

Researchers at NOAA performed a WRF-Chem modeling study primarily focused on photochemistry. Multiple sensitivity simulations were performed to quantify contribution of different factors driving high ozone events in the UB. Two anthropogenic emissions inventory datasets were used to simulate methane and photochemistry in the UB. These emission datasets are described in Section 5.2 within the "Emission Inventory Development Activities" section of this report. Below are the major findings from NOAA's WRF-Chem model study as described by Ahmadov et al. (2015):

- Evaluations of the model results for winter of 2012 and 2013 show greater underestimates of CH_4 and other volatile organic compounds (VOCs) using the NEI-2011 inventory compared to the case when the observationally based, top-down emission scenario was used. Model comparisons with continuous CH_4 measurements suggest the CH_4 flux estimate (55,000 kg/hour) derived by Karion et al. (2013) for the eastern part of the UB provides a low end estimate for the UB, where the major source of CH_4 is the oil and natural gas (NG) industry.
- Unlike VOCs, the NEI-2011 inventory significantly overestimates the emissions of nitrogen oxides (NO_x) in the UB, while the top-down emission scenario results in a moderate negative bias.
- As Figure 6-1 shows, the WRF-Chem simulations using the top-down emission case capture the high O_3 episodes in 2013 quite well. In contrast, simulations using the bottom-up inventory are not able to reproduce any of the observed high O_3 events in the UB.
- Temporal patterns of O_3 within the UB during the snow free winter of 2012 are simulated well by WRF/Chem using either emission inventory since local ozone formation is minimal. Thus meteorological conditions play a key role in the occurrence of the high UB O_3 events within the model (and observations). Moreover, the same WRF-Chem model configuration together with the top-down emission estimates can be successfully applied to the highly contrasting meteorological and photochemical conditions in the UB.
- For wintertime conditions air quality models need to consider increased photolysis rates and modified dry deposition velocities of chemical species due to snow cover on the ground. Without a high surface albedo, and reduced O_3 deposition velocity induced by the snow cover, the model fails to reproduce the high O_3 events observed in 2013.
- High O_3 concentrations are sensitive to reductions of VOC emissions, but not that of NO_x, suggesting that targeting VOC emissions would be an efficient way for O_3 abatement strategy in the UB.
- Emissions of aromatic VOCs contribute to high O_3 concentrations nearly as much as alkane species, despite the much lower fraction of aromatics relative to alkanes in the UB.

- Primary emissions of nitrous acid are not necessary to simulate high O_3 in the Basin. This is an important conclusion, as nitrous acid emissions from heterogeneous snow chemistry was previously considered as one of the potential drivers of high O_3 in the UB.
- Estimates of primary emissions of formaldehyde from the industrial processes associated with the oil and gas sector need to be improved. Primary formaldehyde emissions contribute noticeably to O_3 in the UB, however the model still predicts high O_3 levels without formaldehyde emissions.

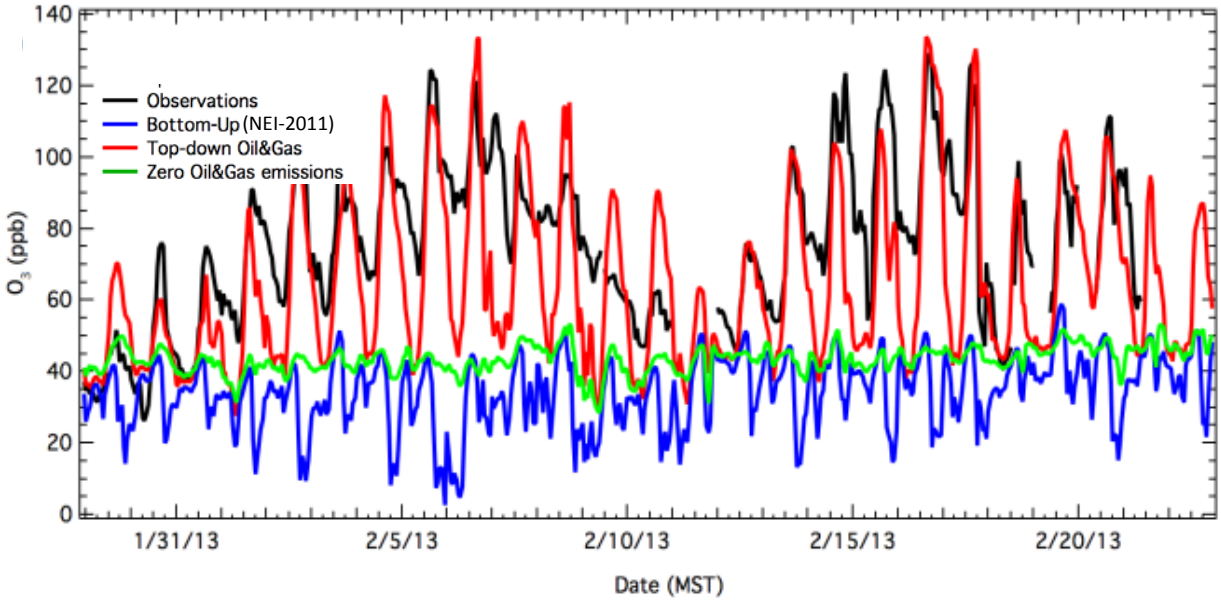

Figure 6-1. Time series of the measured and modeled by the NOAA WRF-Chem model hourly O_3 mixing ratios at Horsepool. Here three emission scenarios are used in the model. These emission datasets are 1) bottom-up (EPA NEI-2011), 2) top-down (built by using atmospheric in-situ measurements), and 3) the emission case where all the oil and natural gas emissions are set to zero in the model.

6.4.2 BLM ARMS Air Quality Modeling

The BLM ARMS study, conducted by AECOM and STI, investigated the performance of the CMAQ and CAMx photochemical grid models and found that both models produced enhanced ozone concentrations during the winter ozone episodes that occurred in early 2010. Based on a detailed inter-comparison of model performance, the study concluded that the CMAQ model was able to replicate wintertime ozone formation and timing in the Uinta Basin better than the CAMx model. Comparison of CMAQ ozone modeling results with 2010 ozone observations in the Uinta Basin showed the model was able to capture both episodic events and seasonal ozone trends.

The CMAQ model showed good agreement with periods of elevated winter ozone in the Uinta Basin, particularly relative to the Ouray monitor, which typically monitored the highest winter

ozone concentrations in the basin during 2010, but CMAQ tended to under-predict ozone peaks in winter by approximately 10-20 ppb. Some key differences between measured and modeled concentrations are that modeled daily peak ozone concentrations occur earlier in the day and decline more rapidly than measurements. Although limited measurement data are available for comparison with the 2010 model results, modeled vertical ozone concentrations and spatial extent of surface maximums are generally consistent with observations during other years.

6.4.3 USU Air Quality Modeling

USU researchers have begun photochemical model simulations using CMAQ v5.0.2 and CAMx v.6.1 for studying high ozone episode during the winter season in the Uinta basin. The Emission Inventory (EI) data for base year 2010, developed by AECOM for the ARMS-BLM project, served as the baseline EI for the USU model platforms. Spatial surrogates were developed to allocate emission data to a 1.3 km horizontal grid-spacing domain. Minor modifications have been made to the photolysis and dry deposition modules of CMAQ v5.0.2 to support the USGS 33 landuse category scheme that was used in the USU-WRF simulations. Initial model evaluation with respect to ozone performance showed that both CMAQ and CAMx had similar performance, and they both highly under-estimated ozone concentrations. Although various factors may have contributed to this poor performance, discrepancies in emission input data is apparently the main factor. Recent sensitivity tests comparing VOC profiles for oil and gas area emissions derived by AECOM in the ARMS-BLM project with default EPA VOC profiles showed that assigning formaldehyde-containing VOC speciation profiles for oil & gas source categories in Utah yielded significantly higher ozone concentrations in comparison with using non formaldehyde VOC speciation profiles. Therefore, selecting the appropriate VOC speciation profiles for oil and gas emission sectors is an important step in the preparation of accurate emissions for photochemical modeling studies. This is consistent with UDAQ's work in which they compared default EPA VOC profiles with the profiles derived for the 3 States Air Quality Study (Avey, 2014). More work is being carried out to investigate a suitable set of VOC speciation profiles and to improve the EI used with the model platforms.

The BLM emissions inventory developed by AECOM (AECOM, 2013) for base year 2010 is used in the photochemical model platforms being developed at USU's Bingham Research Center. The model domain has been configured at 1.3-km resolution with 285×309 grid cells and is centered on the Uinta Basin. Spatial surrogates at 1.3-km resolution were unavailable, so a set was developed with ArcGIS using the most recent data from the Census Bureau; the Federal Emergency Management Agency; the National Land-Cover Dataset; the Utah Division of Oil, Gas and Mining; and others. Default SMOKE temporal surrogates and temporal surrogates (AECOM, 2013) for oil and gas activities were adopted for the Uinta Basin model domain. Emissions from the oil and gas sector were projected from base year 2010 to model year 2013 using scale factors derived from well counts and oil and gas production growth rate data. Figure 6-2 displays some of the results. The emissions inventories will be updated with measurements being made by USU's Bingham Research Center.

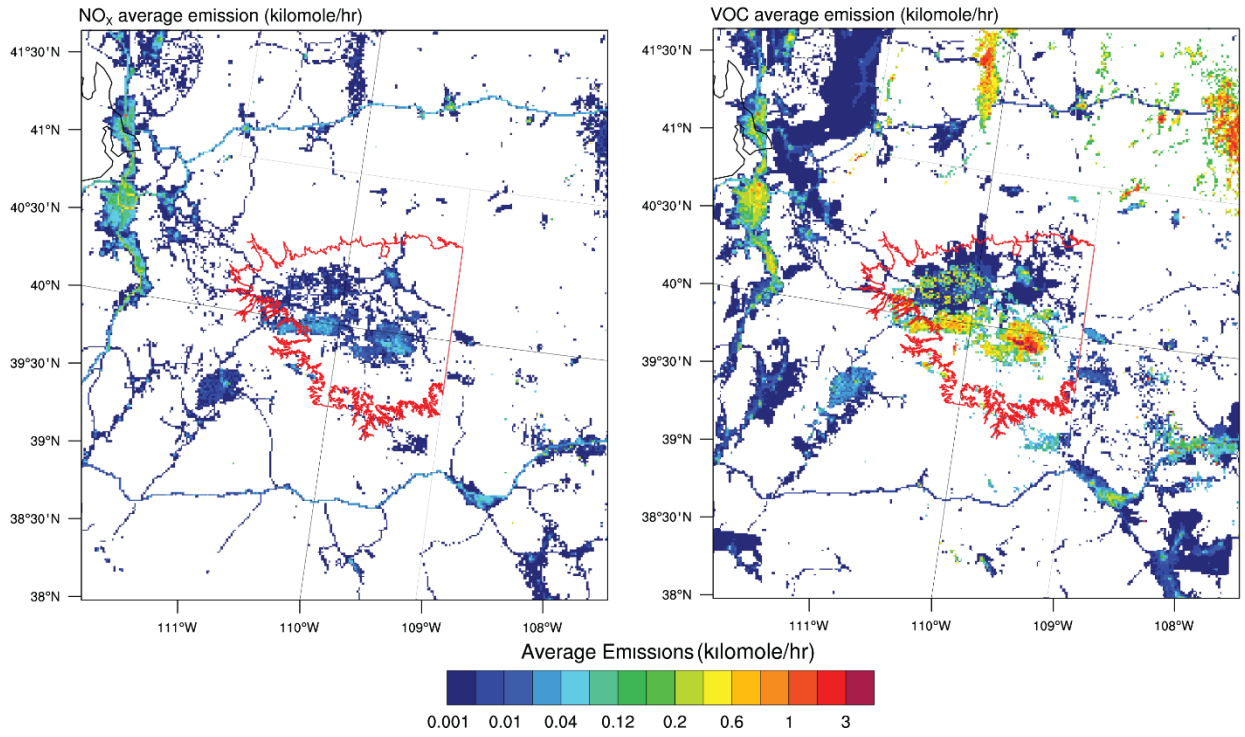

Figure 6-2. Average NOx (left) and VOC (right) emissions as processed by SMOKE. The red solid line depicts the Utah boundary of the Uinta Basin.

Sensitivity studies are also being performed to evaluate the effect of VOC speciation profiles, using a WRF-SMOKE-CAMx platform. Reference runs (REF) are being prepared in which SMOKE default profiles are applied for oil and gas emissions for comparison with test runs (ARMS) that are identical to REF except that profiles developed by AECOM under the BLM-ARMS project (AECOM, 2013) are used. The major difference in the two speciation profiles is that the REF runs assume higher formaldehyde emissions in the Uinta Basin (see Table 6-1). Preliminary results show that when speciation profiles containing higher formaldehyde are used, estimated ozone concentrations are significantly higher (Figure 6-3).

Table 6-1. VOC speciation profiles for oil and gas emissions in the Uinta Basin as used in the REF and ARMS runs, respectively.

REF_spc	pro_code	ALDX	BENZENE	ETH	FORM	IOLE	OLE	PAR	TERP	TOL	UNR	XYL	CH4	ETHA
2310010200	2487	1.16E-04	0.007	0.0866	4.90E-07	0.007409	0.077	0.7444	2.82E-04	0.007572	0.0729	0.003627	-	-
2310020800	0051	-	-	-	0.2	-	-	0.15	-	-	0.15	-	0.2	0.3
2310024100	0051	-	-	-	0.2	-	-	0.15	-	-	0.15	-	0.2	0.3
2310025100	0051	-	-	-	0.2	-	-	0.15	-	-	0.15	-	0.2	0.3
2310025200	0051	-	-	-	0.2	-	-	0.15	-	-	0.15	-	0.2	0.3
2310025300	0051	-	-	-	0.2	-	-	0.15	-	-	0.15	-	0.2	0.3
ARMS_spc	pro_code	ALDX	BENZENE	ETH	FORM	IOLE	OLE	PAR	TERP	TOL	UNR	XYL	CH4	ETHA
2310010200	9001	-	-	-	-	-	-	0.922374	-	0.021862	0.033543	0.018973	0.000991	0.002256
2310020800	9003	-	-	-	-	-	-	0.1387	-	0.00326	0.047692	0.000625	0.681881	0.127842
2310024100	9003	-	-	-	-	-	-	0.1387	-	0.00326	0.047692	0.000625	0.681881	0.127842
2310025100	9003	-	-	-	-	-	-	0.1387	-	0.00326	0.047692	0.000625	0.681881	0.127842
2310025200	9003	-	-	-	-	-	-	0.1387	-	0.00326	0.047692	0.000625	0.681881	0.127842
2310025300	9003	-	-	-	-	-	-	0.1387	-	0.00326	0.047692	0.000625	0.681881	0.127842

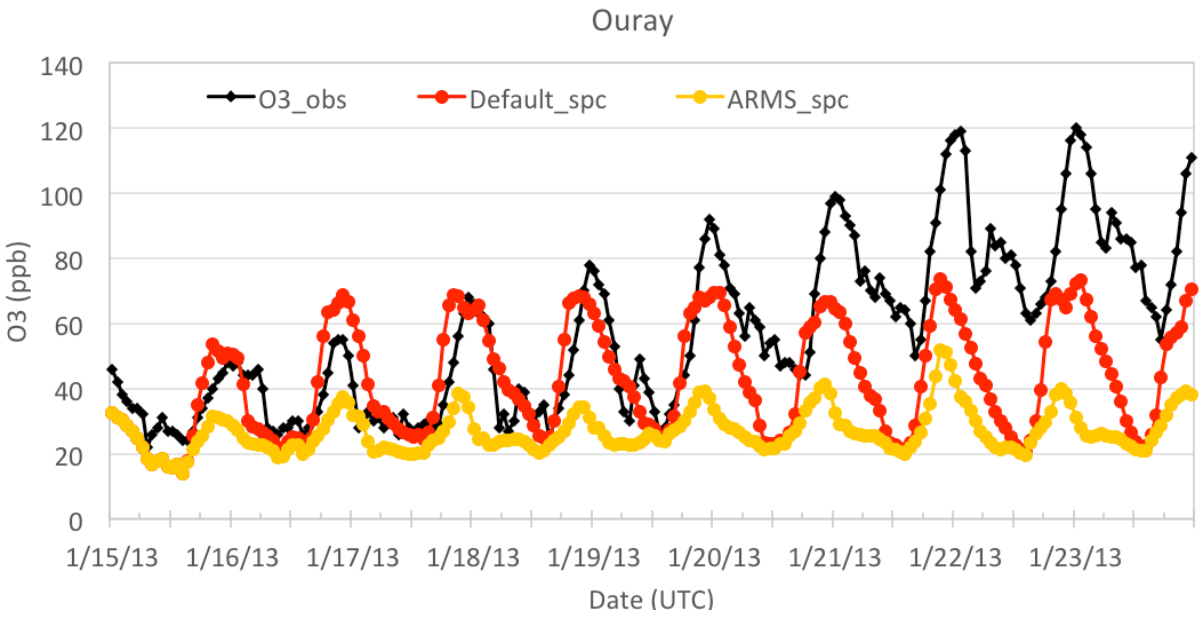

Figure 6-3. Temporal evolution of near-surface simulated (ARMS in yellow, REF in red) and observed (black) ozone concentration at Ouray.

VOC measurements (from USU Bingham Research Center and NOAA data) and other studies reported in the literature are being reviewed together with current VOC speciation profiles (including the SMOKE default, BLM-ARMS, WRAP-III, and Three-State Air Quality Study profiles) to develop the most representative and accurate model of the Uinta Basin.

Preliminary results also show that modeled nighttime ozone concentrations are much lower than observed values, especially during high ozone episodes (see Figure 6-4). One hypothesis for this behavior is that NOx is over estimated in the emissions inventories. Sensitivity simulations with reduced NOx emissions are being undertaken to test this hypothesis.

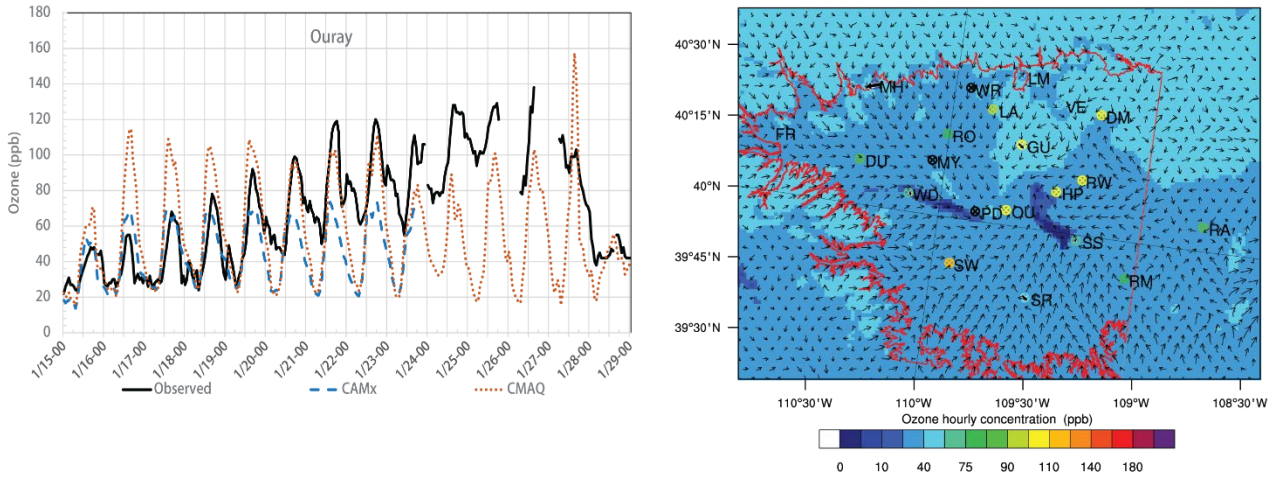

Figure 6-4. Nighttime ozone concentrations. Left: observed vs. modeled ozone concentrations at Ouray during 15-28 January 2013 episode. Right: horizontal distribution of modeled and observed ozone concentrations on 24 January 2013, 23:00 MST. The red line depicts the Utah Uinta Basin boundary. Crossed circles represent the magnitude of observed ozone concentrations and their locations. Thin and bold arrows depict wind speed and direction as simulated and observed, respectively.

6.4.4 Utah DAQ Air Quality Modeling

The Utah DAQ is performing CMAQ (version 5.0.2) simulations in the Uinta Basin for the high ozone event of February 01 -07, 2013. The meteorological data was provided by the University of Utah, with improvements focused on Uinta Basin specific WRF simulations which are described in Neemann et al. 2014). The bottom-up emission inventory used in the base case run is for 2011 and incorporates growth of oil & gas activities since 2006 (see Ch. 5). Utah DAQ also performed CMAQ sensitivity simulations to evaluate the effects of uncertainty in model input data. These include the following two model scenarios:

1. NODEP-TOPDOWN: The dry deposition velocity of ozone within CMAQ was set to 0 cm/s. The emission inventory was modified to approximately match the top-down inventory derived by Ahmadov et al., 2015. That is, input VOC emissions were doubled and input NOx emissions were reduced by 75%. However, in this case the VOC and NOx emissions were reduced across-the-board for all source categories whereas the top-down inventory derived by Ahmadov et al. is applied to just the oil and gas emission sources.

2. NODEP-FORM: The dry deposition velocity of ozone within CMAQ was set to 0 cm/s. A constant source of formaldehyde was added within the Uinta Basin to the bottom-up emission input files for CMAQ. This leads to formaldehyde concentrations in CMAQ between 2-10 ppb throughout the Basin. This added formaldehyde source was designed to approximately match the concentrations of measured formaldehyde at Horsepool.

Results at Horsepool and Ouray of the CMAQ base case and NODEP-TOPDOWN sensitivity runs for ozone during the Feb 01 - 07, 2013 timeframe are shown in Figures 6-5 and 6-6, respectively. The CMAQ Base simulation, which uses a bottom-up emissions inventory, is unable to produce sufficient ozone to match the observed concentrations. Ozone much more closely matching observed values is produced by the CMAQ NODEP-TOPDOWN sensitivity simulation with afternoon ozone peaks better simulated at Horsepool than at Ouray. Since at least some day-to-day nighttime ozone buildup is seen in the base case CMAQ run, it is not likely that setting the dry deposition to zero is the cause of the improved nighttime performance in the NODEP-TOPDOWN sensitivity simulation. This is also the case for the NODEP-FORM simulation described below (see Figures 6-8 and 6-9).

Time series of observed and simulated NOx at Horsepool and Roosevelt are shown in Figure 6-7. Observed NOx values shown in this figure are based on measurements using a photolytic NO_2 to NO converter which does not suffer from positive interferences from other reactive nitrogen species (NOz) characteristic of measurements made using a molybdenum converter. Results in Figure 6-7 indicate that the CMAQ NODEP-TOPDOWN simulation, in which the bottom-up NOx emission values are reduced by 75%, eliminates the large NOx over prediction bias seen in simulations based on the bottom-up inventory at Horsepool. However, the NODEP-TOPDOWN simulation results in under prediction of NOx at Roosevelt whereas the base case simulation is generally consistent with the observations apart from several short-term NOx spikes which may be associated with local fine-scale phenomena not well represented by the WRF and CMAQ gridded results. The result at Horsepool is consistent with the hypothesis that the bottom-up NOx emissions from sources impacting the Horsepool site are too high. The contrasting result at Roosevelt might be explained by the fact that the NODEP-TOPDOWN simulation is based on application of across-the-board NOx reductions in the DAQ top-down scenario (which would thus have impacted all NOx sources, including sources such as on-road vehicles which are concentrated in urban areas) as compared to just reducing oil and gas NOx emissions as is the case in the Ahmadov et al. top-down emissions scenario. However, further analysis will be needed to confirm this. It is interesting to note that NOy is actually under predicted by approximately 5 – 10 ppb at Horsepool (and even more under predicted at Roosevelt) in the NODEP-TOPDOWN simulation (Figure 6-8). This suggests that there remain significant biases in the nitrate budget in the UDAQ simulation that are not resolved by the reduction in NOx emissions.

"NOx" measurements at Ouray were only made using a molybdenum converter and thus cannot be directly compared with modeled NOx. However, an approximate comparison can be achieved by assuming the "NOx" measurements at Ouray can be represented by NOx* which is defined as the sum of NOx, reactive nitrate radical (RNO_3) and a fraction of PAN and HNO_3 as suggested by Lamsal et al., (2008):

$$NOx^* = NOx + RNO_3 + 0.95*PAN + 0.35*HNO_3$$

As shown in Figure 6-9, comparisons of observed and predicted NOx* at Horsepool and Roosevelt (where observed NOx* is the "NOx" measurement made by instruments using

molybdenum converters that were collocated with the photolytic NOx instruments) exhibit characteristics very similar to the NOy comparisons (Figure 6-8), consistent with the assumption that NOx* is a reasonable approximate of measurements made using a molybdenum converter. Comparison of observed and predicted NOx* at Ouray (Figure 6-10) indicate poor correlation between observed and predicted values, making it difficult to draw any conclusions about potential biases in the NOx inventory or the model nitrate budget. The poor correlation may be a result of problems with the WRF simulation as transport of pollutants is an important factor in determination of conditions at Ouray.

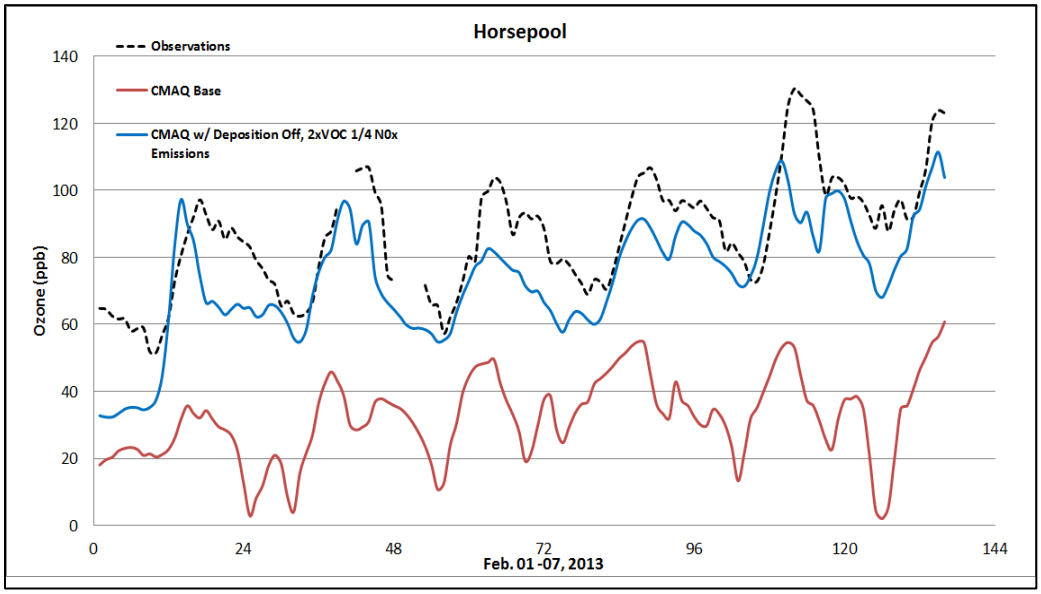

Figure 6-5. Ozone (ppb) time series at Horsepool for Observations (black dashed), CMAQ Base simulation (red), and CMAQ NODEP-TOPDOWN sensitivity (blue).

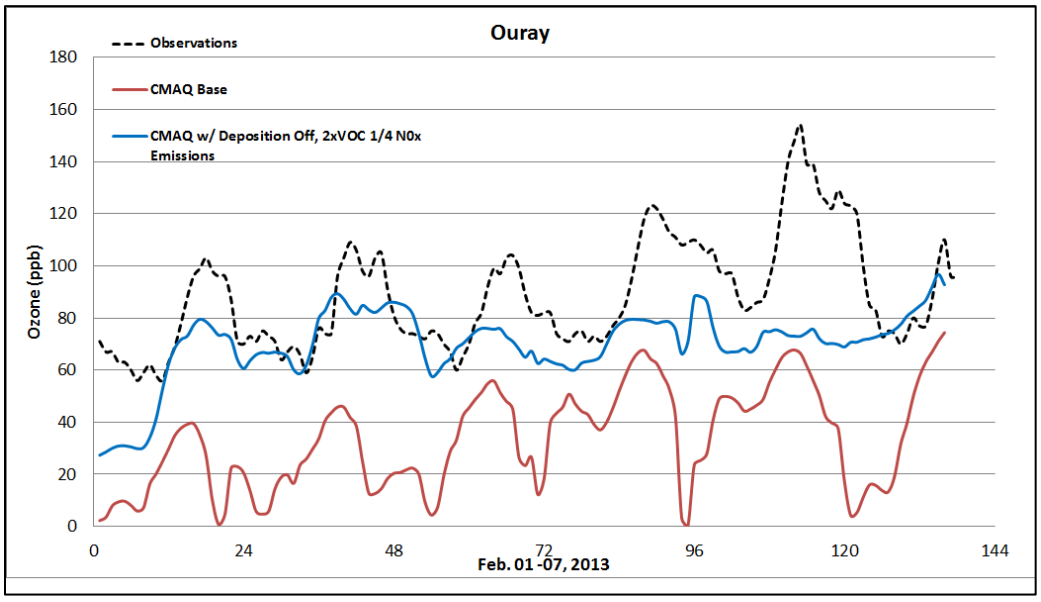

Figure 6-6. Ozone (ppb) time series at Ouray for Observations (black dashed), CMAQ Base simulation (red), and CMAQ NODEP-TOPDOWN sensitivity (blue).

Results of the CMAQ NODEP-FORM sensitivity for simulated ozone at Horsepool and Ouray are shown in Figures 6-11 and 6-12, respectively. Somewhat similar to the NODEP-TOPDOWN simulation, adding a constant source of formaldehyde to the bottom-up emission inventory leads to a large increase in modeled ozone when compared to the Base simulation. This constant formaldehyde source produces formaldehyde concentrations between 2 and 10 ppb at Horsepool that better match observed levels whereas concentrations are always less than 1 ppb in the Base simulation (Figure 6-13). The top-down emission inventory used in the NODEP-TOPDOWN sensitivity run gives better overall ozone model performance at the Horsepool location (Figure 6-5) than the NODEP-FORM sensitivity run (Figure 6-12). The opposite is true at Ouray, where the NODEP-FORM run (Figure 6-9) appears to simulate the afternoon ozone peaks better than the NODEP-TOPDOWN run (Figure 6-6).

In summary, the Utah DAQ base case CMAQ simulations using the bottom-up emissions inventory and no added formaldehyde do not produce the high observed ozone concentrations for the episode of Feb. 01 -07, 2013 whereas using either a top-down inventory with twice the VOC and one quarter of the NOx emissions of the bottom-up inventory or simply increasing emissions of formaldehyde in the bottom-up inventory leads to higher predicted ozone much more closely matching observed concentrations at Horsepool and Ouray. Comparisons of predicted and observed NOx at Horsepool show much better agreement under the reduced NOx emissions incorporated into the top-down inventory although additional analysis is needed to fully evaluate potential biases in the bottom-up NOx inventory. A positive finding of the Utah DAQ CMAQ simulations is the ability to simulate the nighttime day-to-day ozone buildup throughout the episode.

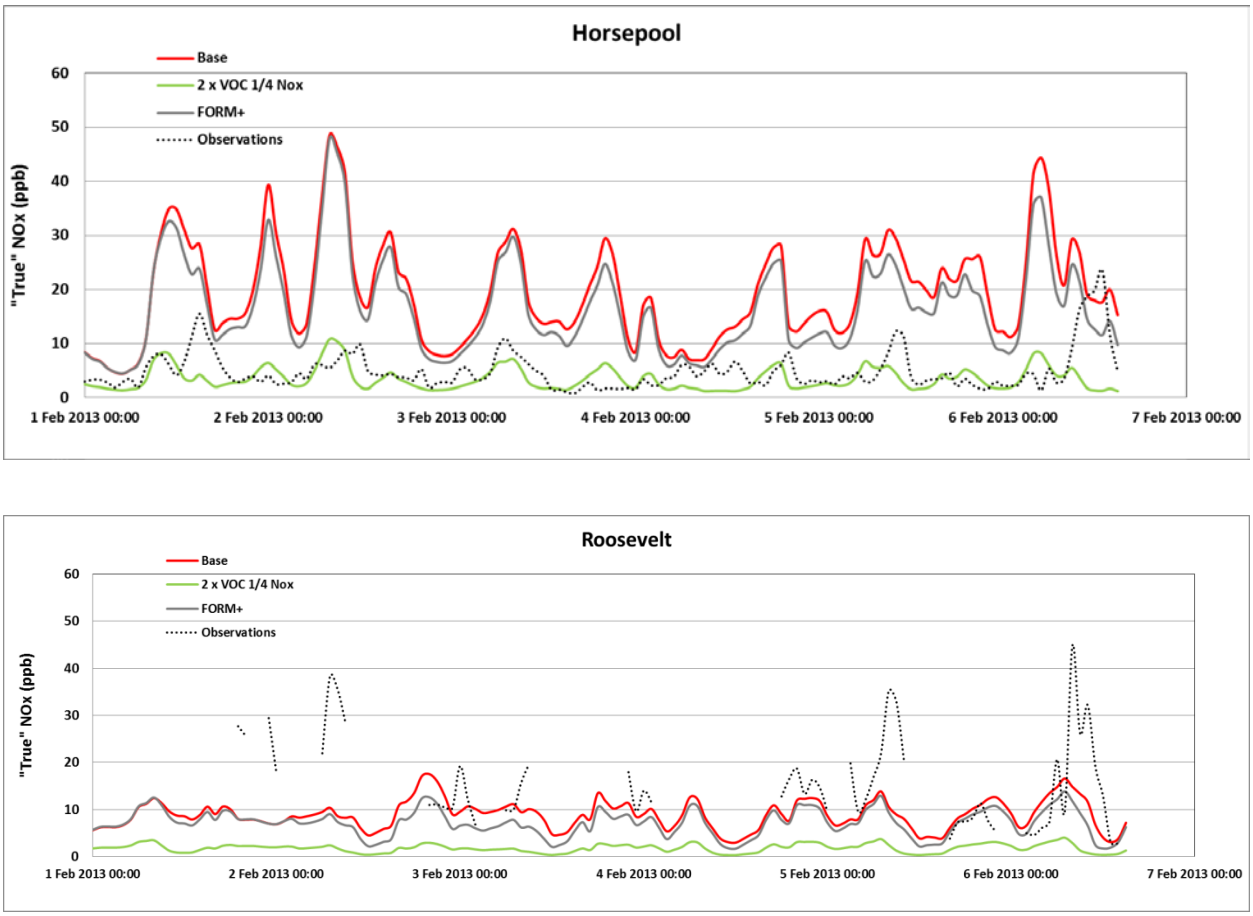

Figure 6-7. NOx time series at Horsepool (top) and Roosevelt (bottom) for observations (black dashed), CMAQ Base simulation (red), CMAQ NODEP-TOPDOWN sensitivity (green) and FORM+ sensitivity (gray). NOx measurements were made using a photolytic converter and thus represent the sum of NO and NO_2 only.

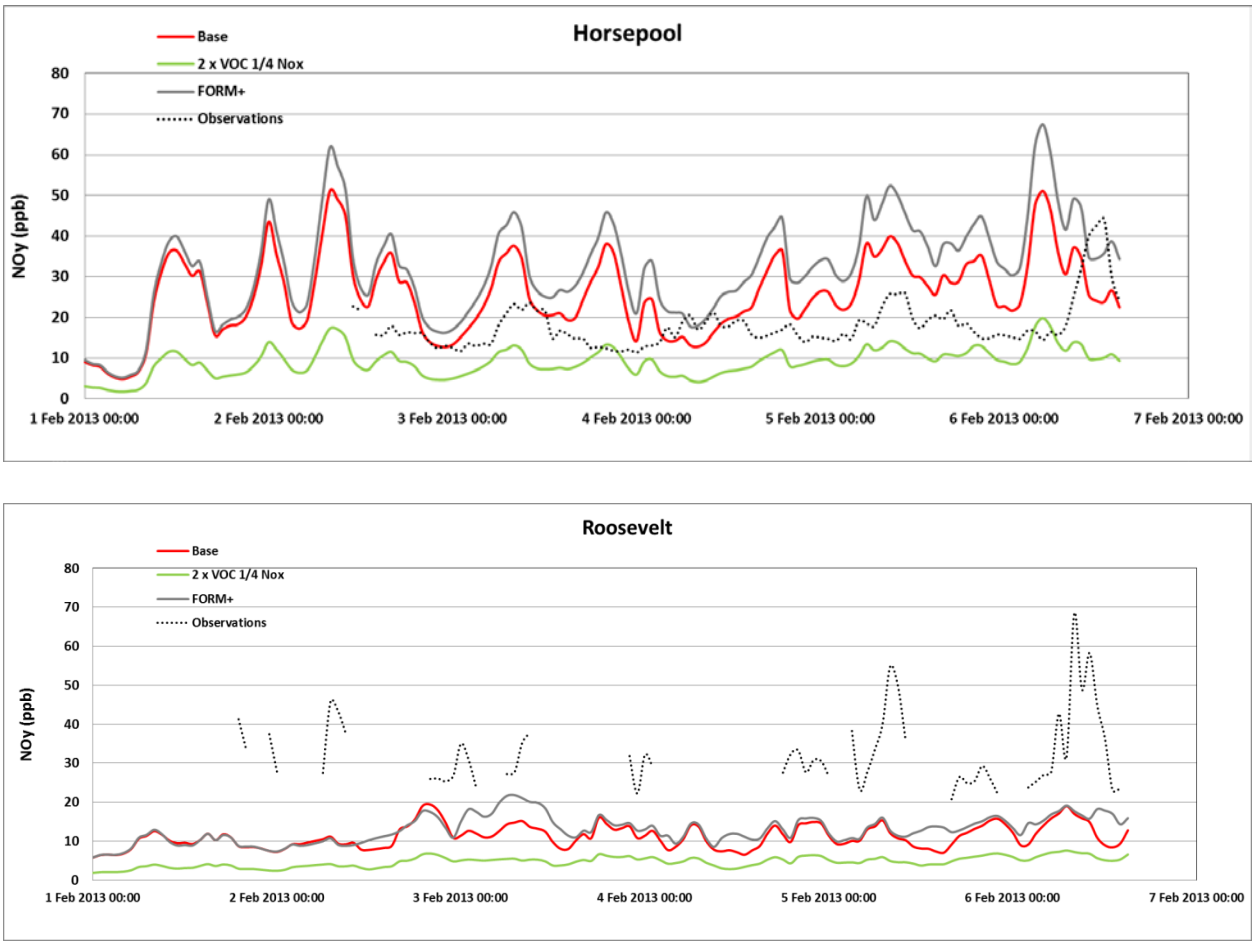

Figure 6-8. NOy time series at Horsepool (top) and Roosevelt (bottom) for observations (black dashed), CMAQ Base simulation (red), CMAQ NODEP-TOPDOWN sensitivity (green) and FORM+ sensitivity (gray).

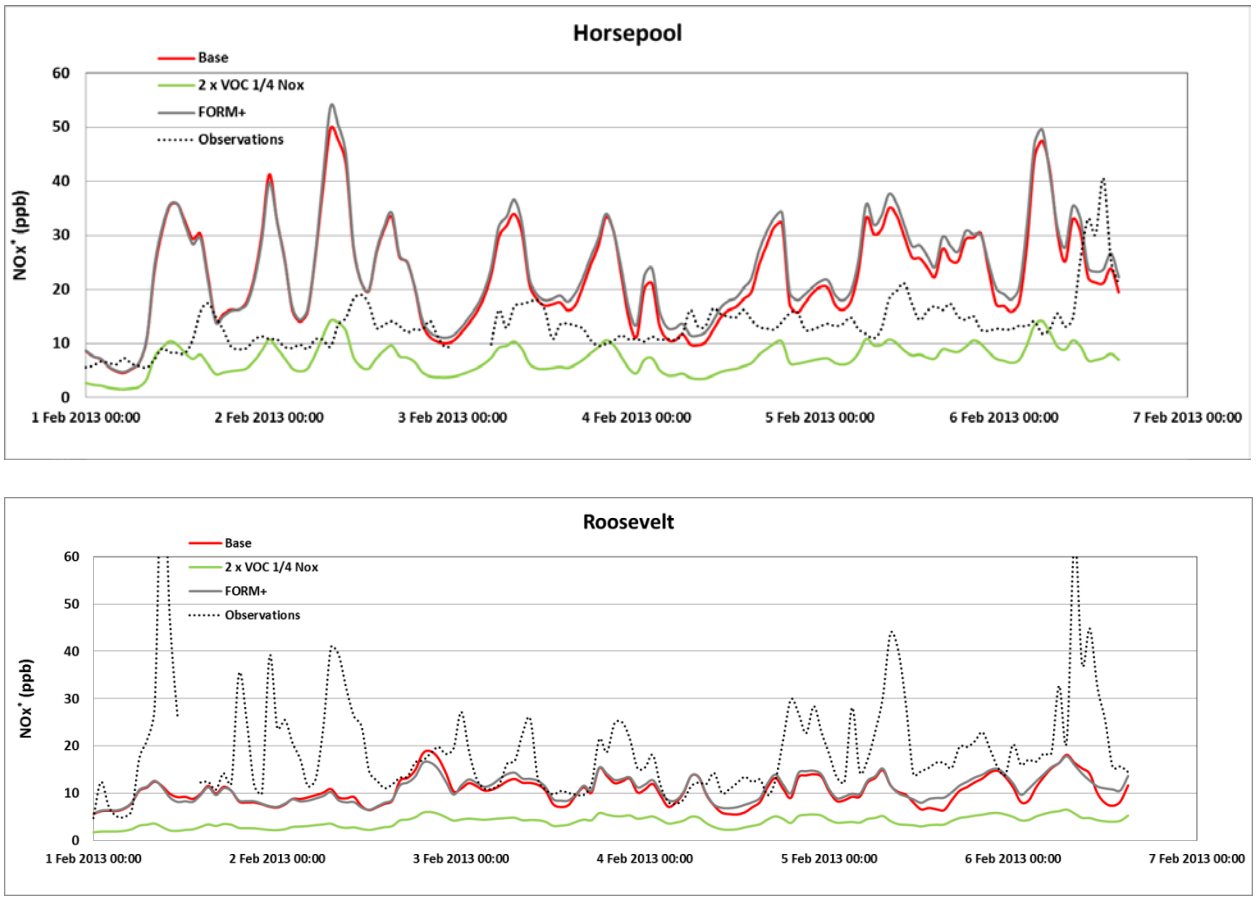

Figure 6-9. NOx* time series at Horsepool (top) and Roosevelt (bottom) for observations (black dashed), CMAQ Base simulation (red), CMAQ NODEP-TOPDOWN sensitivity (green) and FORM+ sensitivity (gray) where NOx* is as defined in the text.

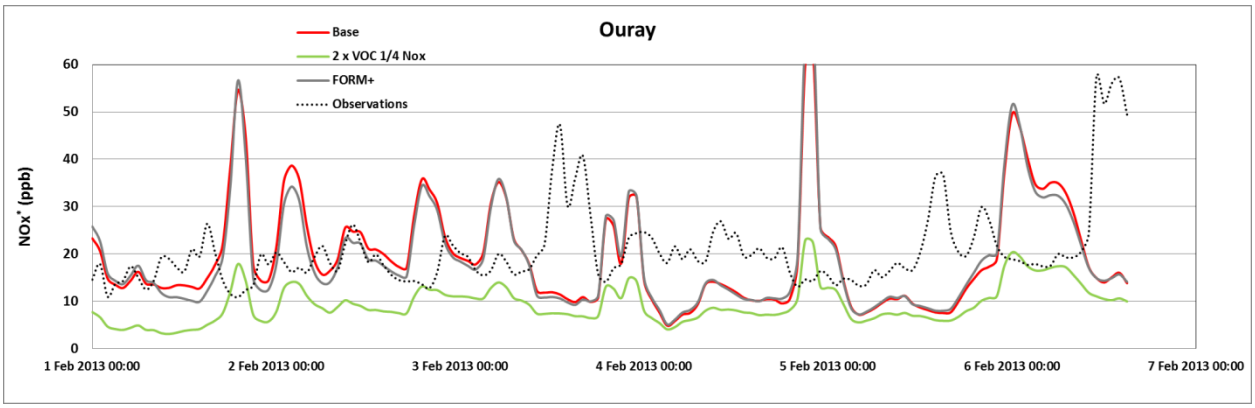

Figure 6-10. NOx* time series at Ouray for observations (black dashed), CMAQ Base simulation (red), CMAQ NODEP-TOPDOWN sensitivity (green) and FORM+ sensitivity (gray) where NOx* is as defined in the text.

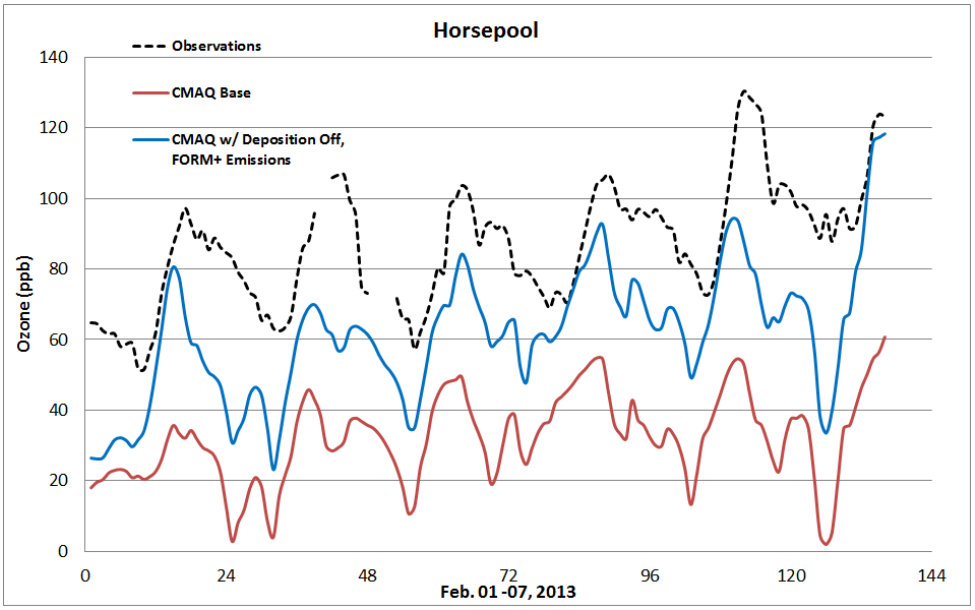

Figure 6-11. Ozone (ppb) time series at Horsepool for Observations (black dashed), CMAQ Base simulation (red), and CMAQ NODEP-FORM+ sensitivity (blue).

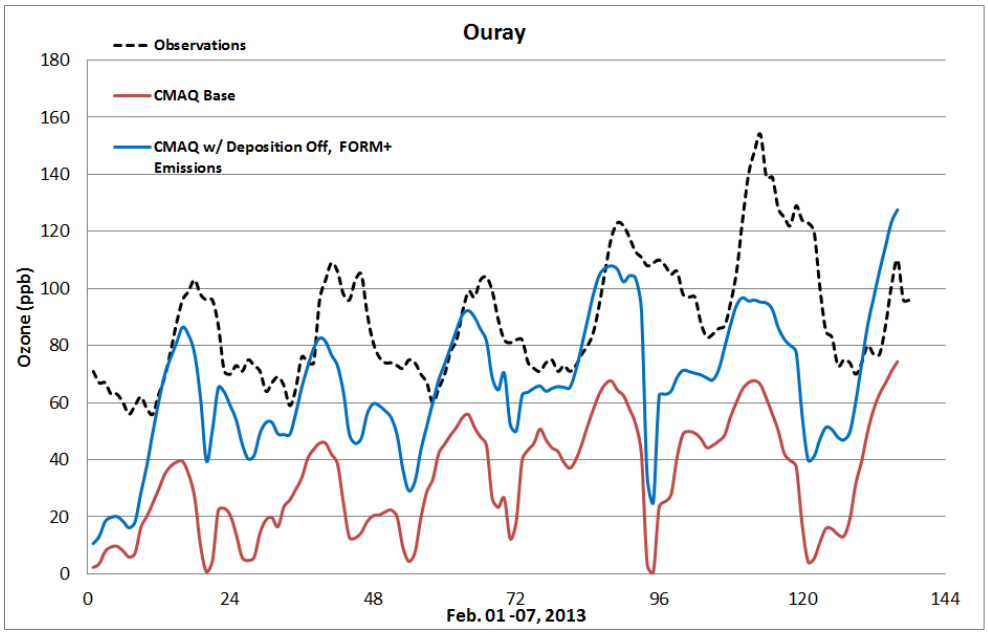

Figure 6-12. Ozone (ppb) time series at Ouray for Observations (black dashed), CMAQ Base simulation (red), and CMAQ NODEP-FORM+ sensitivity (blue).

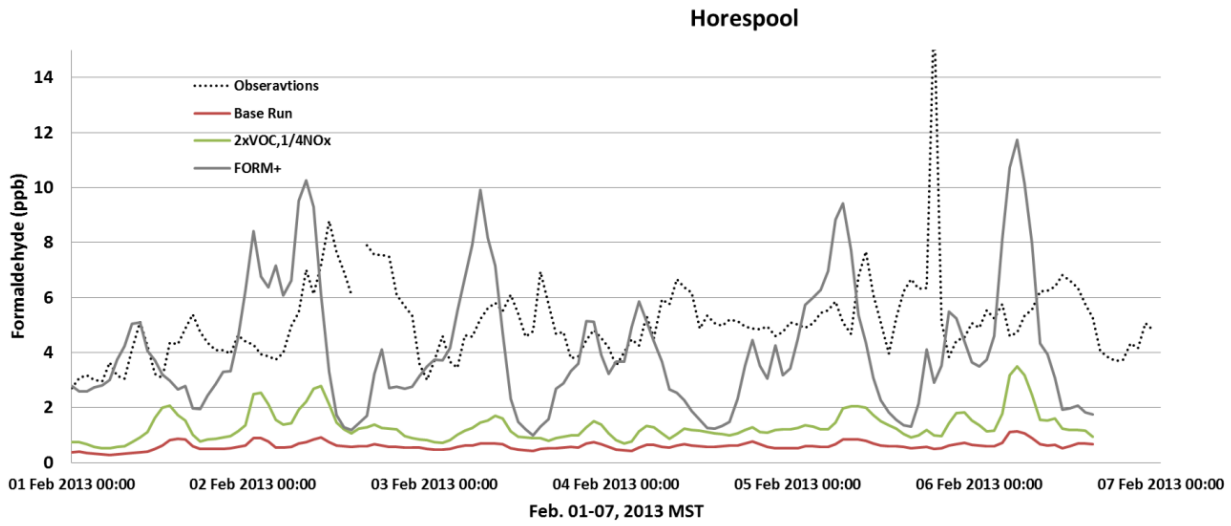

Figure 6-13. Formaldehyde (ppb) time series at Horsepool for observations (black dashed), CMAQ Basecase simulation (red), NODEP-TOPDOWN (green), and NODEP-FORM+ sensitivity simulations (grey).

6.4.5 EPA Air Quality Modeling

EPA has performed CMAQ simulations for January to March, 2011 and January to March 2013 using a 4 km grid resolution for a model domain that includes northern Utah, western Wyoming and western Colorado. The 2011 modeling used CMAQ version 5.0.1, and EPA found that the default CMAQ landuse treatment for snow albedo performed poorly for areas with generally flat terrain with light vegetation. This caused CMAQ to underestimate surface albedo and photolysis rates in the Uinta Basin and in the Upper Green Basin in Wyoming. Results of model sensitivity simulations with increased snow albedo resulted in enhanced ozone production. However, the model was still biased low for both ozone and VOC (Tonnesen et al., 2013). CMAQ version 5.0.2 includes an updated treatment of snow albedo for landuse characteristics found in the Uinta and Upper Green basins. As a result, CMAQ version 5.0.2 should more accurately represent snow albedo within the Uinta Basin, however, snow albedo is a critical factor that affects model performance and it should be carefully evaluated for model applications in other geographic areas. The version of CAMx used did not have a landuse specific snow albedo treatment, and as a result, CAMx underestimated snow albedo in the Uinta Basin. However, Utah DAQ is currently supporting work to update the CAMx model to provide a more accurate treatment of snow albedo. The EPA CMAQ modeling also showed a large negative bias for VOC in the Upper Green Basin in 2011, consistent with results of photochemical modeling performed by contractors for the Wyoming Department of Environmental Quality (Rodrigues et al., 2014). The EPA 2013 CMAQ modeling in the Uinta Basin also shows large negative bias for both VOC and ozone, and positive bias for NOx, consistent with results of the NOAA WRF-Chem base case modeling. EPA is continuing to perform WRF and CMAQ sensitivity and diagnostic studies to identify the causes of poor performance in CMAQ.

6.5 Summary and Recommendations for Future Work

Photochemical air quality models are needed in the Uinta Basin for several purposes including development of optimal emissions control strategies to reduce ozone and evaluation and disclosure of environmental impacts of energy production on federal lands. While the Uinta Basin is not currently designated non-attainment for ozone, it is likely that it will be designated nonattainment in the future if past trends in winter ozone continue. At that time, the state will be required to develop a state implementation plan (SIP) and the tribe or EPA will be required to develop a tribal or federal implementation plan (TIP of FIP) that adopts sufficient emissions control measures to bring the basin into compliance with the ozone NAAQS. Photochemical modeling studies will be useful for identifying the optimal VOC and/or NOx emissions control strategy for attaining the NAAQS. While it may be several years before modeling is needed as part of a SIP, TIP or FIP, modeling results can also be useful now for identifying priorities for emissions reductions that could reduce exposure to ozone in the near term and possibly prevent a future non-attainment designation, or result in a less severe category of non-attainment. Additionally, planning is in progress for development of oil and gas resources on federal lands/minerals in the Uinta Basin The National Environmental Policy Act (NEPA) requires that an Environmental Impact Statement (EIS) be completed for each project with the potential to significantly impact the environment that involves federal lands/minerals or federal permitting authority (including development on tribal land). . Air quality model simulations are typically carried out as part of the EIS to assess and disclose possible impacts of development projects. Improvements in emissions inventories and air quality models are needed in the near term to support the EIS process for oil and gas projects on federal lands.

The air quality modeling studies described here have identified a number of areas in which model improvements are needed. High priorities include improved performance of the WRF model to reproduce the observed snow cover and the persistent cold air pool inversion conditions. Development of improved emissions inventory data is also a high priority for continued research. Model simulations that were performed using the NEI emissions inventory data generally underestimated observed VOC and ozone concentrations, and when VOC emissions were increased to be consistent with observed VOC levels, the model performance for ozone was improved. However, poor model performance for dispersion and inversion layer strength may also contribute to poor model performance for precursors and ozone. If problems in the meteorological data contribute to model errors in simulating observed precursor levels, arbitrarily changing the emissions to match observed precursor levels may introduce compensating errors in the model. Thus, it is important that additional research be completed to reconcile the bottom-up NEI emissions data with the top-down observational constraints.

The model sensitivity testing and model research and development efforts described above are continuing, with UU, USU, BLM, UDAQ, EPA and NOAA continuing to collaborate on model performance evaluations. The State of Utah has also committed $350,000 to develop improved emissions data and models to evaluate winter ozone control strategies. Results of these ongoing model development and evaluation studies will be shared at future public meetings and in peer reviewed scientific publications.

6.6 References

Ahmadov, R. et al., McKeen, S., Trainer, M., Banta, R., Brewer, A., Brown, S., Edwards, P. M., de Gouw, J. A., Frost, G. J., Gilman, J., Helmig, D., Johnson, B., Karion, A., Koss, A., Langford, A., Lerner, B., Olson, J., Oltmans, S., Peischl, J., Pétron, G., Pichugina, Y., Roberts, J. M., Ryerson, T., Schnell, R., Senff, C., Sweeney, C., Thompson, C., Veres, P., Warneke, C., Wild, R., Williams, E. J., Yuan, B., and Zamora, R., (2015), Understanding high wintertime ozone pollution events in an oil- and natural gas-producing region of the western US, Atmos. Chem. Phys., 15, 411-429.

AECOM (2013) Emissions Inventory for Air Resource Management Strategy 2013, Utah State BLM Emissions Inventory Technical Support Document, November, 2013. Available at: http://www.blm.gov/ut/st/en/prog/more/air_quality/airprojs.html.

Avey, L., 2014. Uinta Basin Ozone Formation Sensitivity to Emissions, VOC Speciation and Meteorology. Presented at Uinta Basin Winter Ozone Study Science Meeting, 17-18 June, Vernal, UT.

Byun, D., Schere, K.L., 2006. Review of the governing equations, computational algorithms, and other components of the models-3 Community Multiscale Air Quality (CMAQ) modeling system. Applied Mechanics Reviews 59, 51-77.

Carter, W. P. L. and R. Atkinson (1989). A computer modeling study of incremental hydrocarbon reactivity. Environ. Sci. Technol., 23, 864.

Carter, W. P. L., and Seinfeld, J. H.: Winter ozone formation and VOC incremental reactivities 783 in the Upper Green River Basin of Wyoming, Atmos. Environ., 50, 255-266, 784 10.1016/j.atmosenv.2011.12.025, 2012.

Edwards, P. M., Young, C. J., Aikin, K., deGouw, J., Dubé, W.P., Geiger, F., Gilman, J., Helmig, D., Holloway, J. S., Kercher, J., Lerner, B., Martin, R., McLaren, R., Parrish, D. D., Peischl, J., Roberts, J. M., Ryerson, T. B., Thornton, J., Warneke, C., Williams, E. J., and Brown, S. S.: Ozone photochemistry in an oil and natural gas extraction region during winter: simulations of a snow-free season in the Uintah Basin, Utah, Atmos. Chem. Phys., 13, 8955–8971, doi:10.5194/acp-13-8955-2013, 2013.

Edwards, P. M., Brown, S., Roberts, J., Ahmadov, R., Banta, R., de Gouw, J., Dubé, W., Field, R., Flynn, J., Gilman, J., Graus, M., Helmig, D., Koss, A., Langford, A., Lefer, B., Lerner, B., Li, R., Li, S., McKeen, S., Murphy, S., Parrish, D., Senff, C., Soltis, J., Stutz, J., Sweeney, C., Thompson, C., Trainer, M., Tsai, C., Veres, P., Washenfelder, R., Warneke, C., Wild, R., Young, C., Yuan, B., Zamora, R.: High winter ozone pollution from carbonyl photolysis in an oil and gas, Nature, 514, 351–354, 2014.Karion, A., et al. (2013), Methane emissions estimates from airborne measurements over a western United States natural gas field, Geophys. Res. Lett., 40, 4393–4397, doi:10.1002/grl.50811

ENVIRON, 2013. User's Guide Comprehensive Air Quality Model with Extensions. ENVIRON International Corporation, Novato, California, www.camx.com.

Grell, G. A., Peckham, S. E., Schmitz, R., McKeen, S. A., Frost, G., Skamarock, W. C., and Eder, B., (2005), Fully coupled "online" chemistry within the WRF model, Atmos. Environ., 39, 6957-6975, 10.1016/j.atmosenv.2005.04.027.

Lamsal, L.N., R.V. Martin, A. van Donkelaar, M. Steinbacher, E.A. Celarier, E. Bucsela, E.J. Dunlea, and J.P. Pinto, (2008), Ground-level nitrogen dioxide concentrations inferred from the satellite-borne Ozone Monitoring Instrument, J. Geophys. Res., 113, D16308, doi:10.1029/2007JD009235.

Neemann, E. M., E. T. Crosman, J. D. Horel, and L. Avey, (2014), Simulations of a cold-air pool associated with elevated wintertime ozone in the Uintah Basin, Utah. Atmos. Chem. Phys. Discuss., 14, 15953-16000. www.atmos-chem-phys-discuss.net/14/15953/2014/

Rodrigues et al, (2014) Ozone Modeling Results and Analyses for Winter in Sublette County, Sweetwater County, and Lincoln County, Wyoming - Interim Report, April, 2014. Submitted to Wyoming DEQ, available at http://deq.wyoming.gov/aqd/winter-ozone/resources/technical-documents/.

Tonnesen, G., Baker, K., Sarwar, G., Rappenglueck, B., (2013), Winter Ozone Formation Sensitivity to Surface Albedo, Heterogeneous Chemistry and Precursor Emissions, 12th Annual CMAS Conference, October 28-30, 2013 Chapel Hill, NC. Available at: https://www.cmascenter.org/conference/2013/agenda.cfm.